Climate Impacts and Adaptation of US Maize

Jennifer Hsiao

A dissertation submitted in partial fulfillment of the
requirements for the degree of

Doctor of Philosophy

University of Washington

2022

Reading Committee:

Abigail L.S. Swann, Chair

Soo-Hyung Kim

Elizabeth Van Volkenburgh

Program Authorized to Offer Degree:
Department of Biology

University of Washington

Abstract

Climate Impacts and Adaptation of US Maize

Jennifer Hsiao

Chair of the Supervisory Committee:
Dr. Abigail L.S. Swann
Atmospheric Sciences and Biology

Over the next three decades rising population and changing dietary preferences are expected to increase food demand by 25–75%. At the same time, climate is also changing — with potentially drastic impacts on food production. Here, we take a modeling approach to disentangle and quantify climate impacts on maize yield in the U.S., investigate the underlying mechanisms that lead to yield changes under an idealized future climate scenario, and explore potential avenues for climate adaptation through identifying climate-smart plant traits and management strategies moving forward.

Temperatures over the next century are expected to rise. Warmer air has a higher capacity to hold water; thus warming the atmosphere without additional moisture input leads to drying through higher vapor pressure deficit (VPD). Increased temperatures and accompanied elevated VPD levels can both lead to negative impacts on crop yield. The independent importance of VPD, however, is often neglected or conflated with that of temperature. We show that increased temperatures and accompanied elevated VPD levels can both lead to negative impacts on crop yield. The negative impact of these two factors varied with precipitation levels and influenced yield through separate mechanisms. Warmer temperatures influenced yield by affecting phenological development – faster development under warmer temperatures led to overall shorter phenological stages and compromised time available for growth. Elevated VPD levels, on the other hand, increased water loss, triggering triggered several water stress responses such as reduced photosynthetic rates,

lowered leaf area development, and shortened growing season length. The rise in CO_2 levels only partially buffers yield loss, with the magnitude of impact greatest under drier conditions.

Next, we developed a data-model framework to standardize, track, and automate a large number of model simulations in order to explore crop performance within the vast trait (T) $\times$ management (M) $\times$ environment (E) landscape. We curated climate, soil, historic yield data, and cropping information into model-ready inputs to run simulations spanning a broad climate space. We then perturbed a number of key model parameters that spanned physiological, morphological, phenological, and management processes within the model to set up an ensemble of simulations within the perturbed trait-management space. Through this data-model framework, we identified phenology and morphology features key for crops to achieve high yield and low yield volatility, categorized several different strategies for crops to achieve high performance under current climate conditions, and quantified how crop performance could shift under future climate perturbation.

We envision findings from this work may complement the efforts of breeders, crop scientists, and agronomists, equipping them with localized cultivar and management targets and priorities to adapt to impending climate stressors.

TABLE OF CONTENTS

LIST OF FIGURES

Figure Number Page

LIST OF TABLES

ACKNOWLEDGMENTS

This dissertation would not have been possible without the support of many people. First and foremost, I want to thank my advisor, Dr. Abigail Swann, who has been my greatest advocate throughout the years. She is not only a great scientist but also a wonderful person. I have learned so much from her, both in and out of science, and I feel truly lucky to have been part of her group.

I also wish to thank my committee members, Dr. Soo-Hyung Kim, Dr. Elizabeth Van Volkenburgh, and Dr. Lauren Buckley for helping me develop, shape, and deliver my ideas, and my collaborators, Dr. Soo-Hyung Kim, Dr. Dennis Timlin, and Dr. Nathan Mueller, for the discussions, advice, and feedback that played a big part in forming this dissertation.

I want to thank past and present members of the EcoClimate lab and lab friends – Marlies Kovenock, Marysa Laguë, Gregory Quetin, Elizabeth Garcia, Claire Zarakas, Greta Shum, Amy Liu, Fiona Lo, Sam Pennypacker, Lucas Zeppetello, Jinhyuk Kim, Patrick Murphy, and Haynes Stephens. Thank you all for creating a supportive and lively environment for fun science conversations and a great many other things.

Thank you to the wonderful friends I've met and gotten to know and love throughout the years because of graduate school – Johanna Cantillo, Amber Hageman, Ana Bedoya, Melissa Lacey, Ryo Okubo, Will King, Fenix Garcia, Diego Alonso, Claire Rusch, Darshi Banan, and many others. I cherish the many memorable moments we've shared through both tough and fun times.

Finally, I want to thank my parents, Yuh-Ju Sun and Chwan-Deng Hsiao, for always believing in me. This dissertation and degree would not have been possible without their love and support.

DEDICATION

To my parents, Yuh-Ju Sun and Chwan-Deng Hsiao

Chapter 1

INTRODUCTION

Over the next decades population is expected to rise with a 24% increase by 2050 requiring 25–75% more food due to changing diets (Tilman et al., 2011; Hunter et al., 2017). At the same time, climate is also changing — with potentially drastic impacts on food production. This dissertation examines the impacts climate has on maize growth and yield in the US, and investigates how different adaptation strategies can mitigate potential yield losses associated with a changing climate.

Maize is the cereal crop with the largest global production, with planting areas spanning from temperate to tropical regions. The US is the largest single producer and grows up to 41% of the global total (Fischer et al., 2014), with most of its production centered in the corn belt states. Maize yield in the US has experienced a steady rise since the 1930s (Duvick, 2005). Large conversions from open-pollinated cultivars to hybrids contributed greatly to the earlier yield increases, while increases in fertilizer use and chemical weed control contributed to continuous yield gains following the green revolution since the 1960s. Persistent breeding exercises and associated changes in management practices (e.g. earlier planting dates for a longer growing season, higher planting densities) have also complemented the steady rise in yield (Sacks and Kucharik, 2011; Duvick, 2005; Duvick and Cassman, 1999).

As a C_4 crop, maize plants have higher photosynthetic efficiency, favor warmer climates, and show less sensitivity to changes in CO_2 concentrations when compared to their C_3 counterparts (e.g. wheat, rice). These characteristics make maize plants important crops when considering the future of global food security under a changing climate. Various studies, however, have shown that increasing temperatures can be harmful for maize growth, especially when temperature surpasses an optimal range (Schlenker and Roberts, 2009; Lobell et al., 2013). National-level yield data have also shown greater year-to-year yield variation in the past 20 years (citation). Barker et al. (2005) speculated this resulting from

a variation in moisture stress imposed on the high and increasing mean yield. Lobell (2014) observed greater sensitivity to drought in recent years over the time period of 1995 to 2012 of the field-level yield data analyzed within the study; in particular, sensitivity to vapor pressure deficit (VPD) has increased over the past two decades for their study period. The authors noted that some of this increased sensitivity may be associated with the continuous increase in planting densities and VPD effects on water stress and overall growth in plants. This raises the question of whether maize production can be sustained under a warming future, especially as water limitation regimes change (Harrison et al., 2014).

Adaptations of crop characteristics and management practices have the potential to mitigate some of the decrease in yield, but substantial knowledge gaps still remain for which adaptation techniques are likely to be most effective at any point in time, the mechanisms through which they can mitigate yield loss, and the relative effectiveness of different approaches. Many scientists recognize that mechanistic, process-based crop simulation models can be a powerful tool to synthesize cropping information, set breeding targets, and develop adaptation strategies for sustaining food production, yet thorough evaluation and application of crop models for developing specific climate-adaptation options (e.g., designing adaptive phenotypes for specific soil-climate combinations) for US agriculture remains scarce.

The remainder of this chapter will provide background information on climate impacts on US maize, adaptation strategies targeted for climate mitigation and adaptation, and further discusses the tools we used to study climate impact and adaptation for maize in the US.

1.1 Climate impacts on maize

1.1.1 Temperature and VPD

Over the coming decades the US maize system will increasingly be placed under stress in the face of expected changes in climate. In particular, temperatures are expected to rise, accompanied by increases in water demand by the atmosphere (Swann et al., 2016) and a reduction in humidity over land (Collins et al., 2013; Fu and Feng, 2014), both of which can

lead to a rise in VPD levels.

VPD is an indicator for the dryness of the air, defined as the difference between the amount of moisture in the air and how much moisture the air can hold when it is saturated. Warmer air has a higher capacity to hold water, thus warming the atmosphere without additional moisture input also leads to drying and higher VPD. VPD is a key environmental factor that affects plant growth and crop yield through different mechanisms than temperature (Fig. 1.1) (Sanginés de Cárcer et al., 2018; Breshears et al., 2013; Day, 2000; Ray et al., 2002; Shirke and Pathre, 2004). Failing to disentangle the impact of VPD from that of rising temperature prevents a true mechanistic understanding of the climate impacts of warming on crop growth and yield.

Several studies projected declines in yield due to future warming (Lobell et al., 2011a,b; Schlenker and Roberts, 2009). However, commonly used statistical approaches are derived from yield observations and climate records over the past few decades, and typically cannot disentangle the inherent correlation between temperature and VPD. Temperature impacts on crop yield analyzed through these methods, therefore, include embedded VPD impacts as well. Changes in CO_2 levels and water availability further complicate this interaction and add uncertainty to future crop yield projections.

The tight correlation between temperature and VPD makes it difficult to empirically tease apart the independent physiological response due to each factor (Barron-Gafford et al., 2007). For this reason, predictions of crop yields derived from observed responses of yield over the past few decades rarely account for the indirect effects from VPD which are thus implicitly embedded in the response of yield to temperature. Without disentangling the temperature and VPD yield response, these projections are unable to account for how each piece responds differently under increasing concentrations of CO_2, with potentially large implications under future climate conditions.

1.1.2 CO_2 and water availability

Changes in precipitation under future climate are also possible, but our confidence in the magnitude and even the sign of the change in precipitation is much lower than for expected

changes in temperature and humidity (Allan et al., 2020).

Elevated CO_2 levels have the potential to alleviate part of the stresses associated with hot and dry (i.e. high VPD or low soil moisture) conditions either through a biochemical response or a stomatal response (cite). Increased concentrations of CO_2 in the atmosphere can directly increase the CO_2 levels in the leaf inter-cellular air space, boosting photosynthesis through a biochemical response. Stomatal closure under elevated CO_2 concentrations can also reduce water loss and conserve soil moisture (Fig 1.1) (Leakey et al., 2009). This is especially critical for plants that face increased transpiration rates under high VPD environments (Fig. 1.1). Due to the nature of C_4 plants, benefits from higher CO_2 concentrations are often only observed under water stressed conditions for maize plants (Ghannoum, 2009), with the yield boost from elevated CO_2 under such conditions have been documented to be up to 40% (Manderscheid et al., 2014).

The magnitude of CO_2 effect on the stomatal and biochemical pathway can potentially shift how much of the vegetation response to warming is carried out through direct temperature effects versus through indirect effects of higher VPD associated with higher temperature, and hence shifting the overall response to warming. Decomposing the influence of the indirect effects of VPD associated with higher temperature from the direct effects of higher temperature is therefore an essential first step to quantify the response of crops under a changing climate.

1.2 Adaptation under a changing climate

As the climate warms, many aspects of agricultural systems can be adjusted to minimize yield loss. Specifically, here we use the term adaptation to refer to changes in crop choice and management practices that either mitigate negative impacts or take advantage of beneficial opportunities (IPCC Working Group II 2014). The capacity for adaptation contributes substantially to the direction of future crop yield projections and their associated uncertainty (Osborne et al., 2013).

Adaptation strategies such as progress towards breeding new cultivar traits, shifting planting dates and planting regions have been shown to have great potential in mitigating heat and VPD-caused yield loss (Butler and Huybers, 2013; Olesen et al., 2011), yet studies

that thoroughly evaluate different aspects of adaptation on a geospatial context are scarce.

In a broad scale meta-analysis of climate change and adaptation in agricultural crops, Challinor et al. (2014) suggested a 7-15% difference in projected yield when adaptation methods were incorporated. However, the effectiveness differed greatly amongst crops and growing regions; in particular, adaptation impacts in temperate maize remained highly uncertain, and the effectiveness was lower than for wheat and rice. Butler and Huybers (2013) examined maize in the US and empirically estimated that by moving locally adapted cultivars from one part of the country to another as the climate warmed (i.e. by moving cultivars from the South to the North) that overall projected yield losses could be mitigated.

Methods for adaptation considered in Challinor et al. (2014) included management practices such as shifting cultivars, optimizing irrigation and fertilization, and adjusting planting time (Butler et al., 2018; Deryng et al., 2011). Larger scale and more drastic adjustments are also proposed in other studies, such as migration in planting areas (Sloat et al., 2020), or breeding for climate-resilient phenotypes with desirable characteristics to cope with the changing climate (McCouch et al., 2013; Redden, 2013; Mickelbart et al., 2015; Abberton et al., 2016). A systematic examination of the effectiveness of different adaptation strategies and the mechanisms through which they alleviate yield loss is needed to better understand the potential importance of adaptation strategies for temperate maize in the US.

1.3 Climate resilient cultivars and management practices

Breeding has consistently played a critical role in the progress of continuous yield gain and was estimated to account for up to 50-60% of the total on-farm yield gain in the past several decades (Duvick, 2005). These gains through genetic improvements are complemented by changes in management practices, such as an increase in fertilizer use, chemical weed control, higher planting densities, and earlier planting dates (Kucharik, 2008; Cardwell, 1982). Recently, however, practices such as nitrogen application and weed control are nearly fully exploited in the US corn belt; simple adjustments in management strategies alone are likely insufficient to sustain an increasing yield trend. Additional yield gains would need to rely further on genetic improvements in new cultivars, as well as management changes that accompany climate-resilient characteristics to fully leverage the interactions between genetics,

environment, and management ($G \times E \times M$; Fischer and Edmeades, 2010; Hatfield and Walthall, 2015)

Progress towards breeding for climate adaptation has been demonstrated in several studies (Reynolds and Langridge, 2016; Fita et al., 2015; Ceccarelli, 2010). However, common breeding methods that either select for higher yield or eliminate defect traits do not allow for a clear understanding of the mechanisms in which favorable traits contribute to greater performance and yield. While selection for yield provides short-term advantages, it inevitably faces long-term limitations since it cannot account for potential trait trade-offs, and effective combinations of plant traits, if not actively sought for based on a mechanistic understanding of crop growth and yield, could only occur by chance (Donald, 1968). The process of identifying and selecting for optimal phenotypes can involve exploring the hills and valleys of a performance landscape (Messina et al., 2011), in which multiple strategies (e.g. different plant traits or management practices) could lead to an "ideal" crop, and what is considered "ideal" may differ between locations and climate. Creating frameworks that can quantify such yield-trait-performance landscape can be extremely useful to help identify and target plant traits suitable under novel future climate conditions (Hammer et al., 2020).

Requirements for breeding, delivering, and adopting a desirable phenotype depends on many factors, and the whole process can take years to decades (Challinor et al., 2017). Continued development of new phenotypes better-suited for future climate is critical for sustaining current yield trends or to prevent yield loss (Ceccarelli, 2010; Challinor et al., 2017; Burke et al., 2009). For example, documented trait changes to date include increases in biotic and abiotic stress resistances (e.g. maize rootworm resistance and drought tolerance), changes in morphological traits (e.g. more erect plant form to facilitate higher planting densities, improved root system architecture that improved soil water access; Hammer et al. 2009), and increases in physiological traits (e.g. higher photosynthetic rates, or higher nitrogen use efficiency; Duvick 2005; Fischer and Edmeades 2010). Our ability to utilize the genetic diversity preserved in wild relatives, landrace species, and undomesticated wild species to develop new climate-ready phenotypes is increasingly important to achieve sustainable and intensified food production (McCouch et al., 2013; Godfray et al., 2010).

Effective phenotypes not only vary with different environmental conditions but also vary

via interactions with management, as clearly articulated in the $G \times E \times M$ paradigm (Hatfield and Walthall, 2015). Maize phenotype advances in the past have been accompanied by a range of changes in crop management practices, including notable shifts in planting density, nutrient supply (Duvick, 2005), and planting dates (Butler et al., 2018). Similarly, we expect optimal management to shift under future climate conditions and in combination with different phenotypic traits. Further, the efficacy of a phenotype often varies considerably across environmental gradients (e.g. Messina et al. 2015). Such interactions emphasize the need for a $G \times E \times M$ approach to examining yield-trait-performance landscapes (Messina et al., 2011).

1.4 Model-aided adaptation strategies and process-based models

Mechanistic modeling tools that integrate physiological, morphological, and phenological properties of a crop (G), their performance under different management options (M), and their interactions with the surrounding environment (E) on a whole-plant level can serve as useful tools for breeding practices through the quantification of a yield-trait-performance landscape (Messina et al., 2011). The structure of the model allows for testing effects of traits (e.g. leaf elongation rate, total leaf number) on more integrated outcomes such as yield. Models also have the advantage of testing individual or combinations of traits and management options across a wide range of environmental conditions that would not be feasible under actual experimental settings (Cooper et al., 2020; Hammer et al., 2020). This makes integrative models ideal tools to test and screen for potentially promising trait and management combinations before carrying out actual breeding practices (Messina et al., 2011; Andrivon et al., 2012).

Ramirez-Villegas et al. (2015) provided a few successful examples of model-aided phenotype development, such as the New Plant Type program developed by IRRI for rice crops, which further inspired the super rice program in China. The newly developed rice varieties produced yields 15-25% higher than common hybrid cultivars planted in other regions in China (Peng et al., 2008), demonstrating simulation-inspired breeding as an effective way to guide breeding direction under a changing climate.

Process-based crop simulation models are powerful tools to investigate how crops will fare

under a changing climate (Boote et al., 2013; Jones et al., 2017; Ewert et al., 2015). Through dynamically representing the physiological, phenological, and morphological aspects of plant growth, these models can shed light on the underlying mechanisms that may lead to yield changes under shifting climate conditions; they can also be used to estimate the capacity for mitigation and adaptation in our current agricultural system, providing quantitative insight on tasks such as identifying new crop phenotypic traits that are more resilient to future climate conditions, shifting where existing cultivars are grown, and modifying current management practices (e.g. planting date, irrigation, cultivar choice).

1.5 The MAIZSIM model

In this dissertation, we use a process-based crop simulation model – MAIZSIM, as our main tool to study climate impacts on maize growth and yield, and to explore potential climate adaptation strategies and quantify their impacts.

MAIZSIM is a crop model developed and calibrated for maize plants to represent key physiological and physical processes such as gas exchange, canopy radiative transfer, carbon partitioning, water relations, nitrogen dynamics and phenology (Kim et al., 2012) (Fig. 1.2). The soil model included in MAIZSIM (2DSOIL) links the crop model to a 2-dimensional soil layer that simulates a dynamic soil water and nutrient vertical profile (Timlin et al., 1996). The model has validated through comparison against observations for a number of maize growing regions in the US and across the globe (Kim et al., 2012; Yang et al., 2009b,a; Timlin et al., 2019; Bassu et al., 2014; Durand et al., 2018). MAIZSIM is driven by hourly meteorological information throughout the growing season and uses this information to represent plant physiological responses such as stomatal opening, photosynthetic rates, leaf elongation, and allocation of carbon to various parts of the plant including grain. The model calculates soil water availability to the roots through simulating water potential and tracks how much leaf area is present at any point in time throughout the growing season. This information is integrated over the growing season to represent the final yield.

We describe datasets used to set up and run specific modeling experiments in further detail in chapter 3.

1.6 Dissertation structure

In this dissertation, we disentangle and quantify the yield impact temperature and VPD have on maize yield in the US, and investigate how rising CO_2 levels and changing precipitation patterns shifts yield impacts from increased temperature and VPD levels (Chapter 2). Next, we develop a modeling framework to identify high performing plant trait and management practices suitable for different agro-climate regions within the US maize growing region (Chapter 3). Finally, we test how high performing plant trait and management combinations differ between agro-climate regions and investigate how they may shift under a changing climate (Chapter 4).

1.7 Future work

In this dissertation, we set up a framework to assess independent yield impacts from different climate factors and investigate their interacting effects and net effects on maize growth and productivity within different agro-climate regions. We also established a data-model infrastructure that allows for large-scale ensemble modeling experiments in which we use to identify key plant traits and management practices that contribute to high yield under different climate conditions, and the mechanisms behind them.

Our work provides a starting point to investigate climate impacts on crop production, understand the mechanisms behind those impacts, and further explore adaptation strategies available under a changing climate. There are many more potential avenues that should be tested and quantified. Findings from our work provides motivation for closer collaborations between crop modelers and crop breeders to advance adaptation for cropping systems under a changing climate.

1.8 Figures and tables

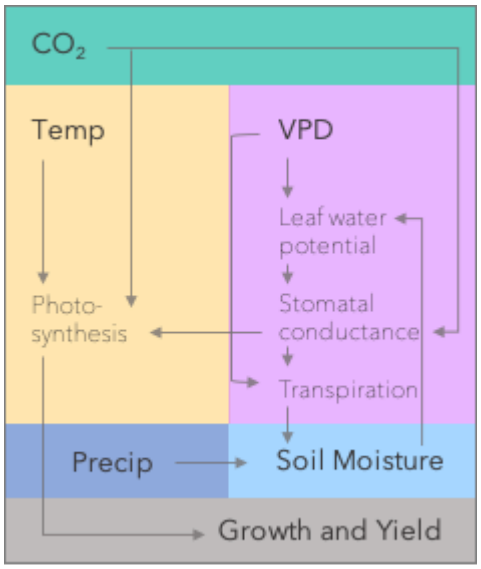

Figure 1.1: Physiological impacts of temperature (Temp.), vapor pressure deficit (VPD) on crop growth and yield and its interactions with CO_2 levels, precipitation, and soil moisture.

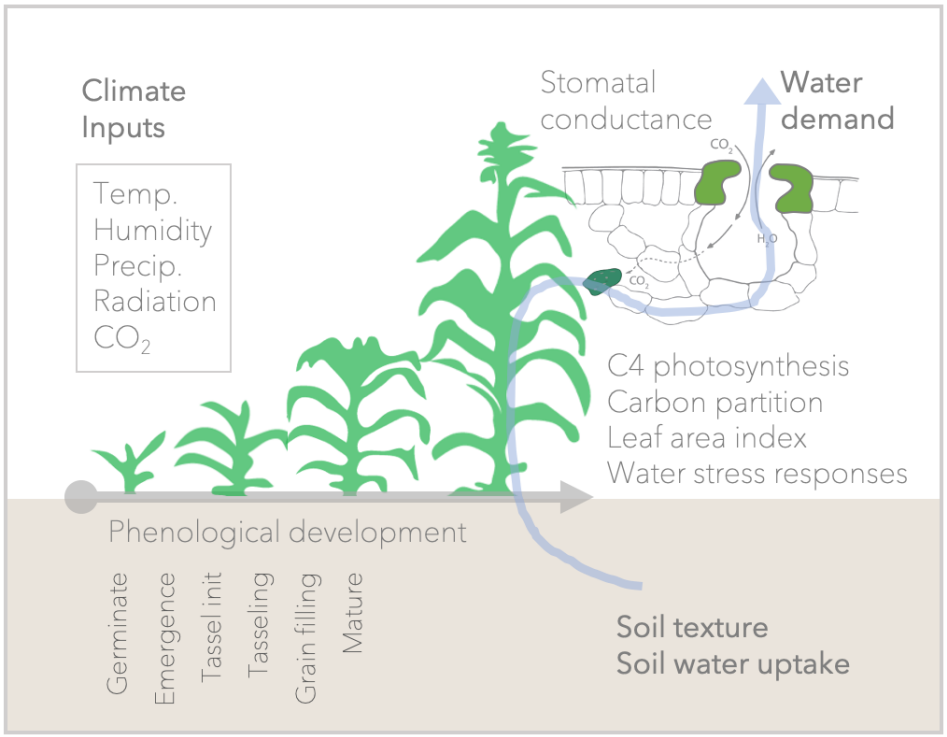

Figure 1.2: Diagram of the MAIZSIM model structure.

Chapter 2

MAIZE YIELD UNDER A CHANGING CLIMATE: THE HIDDEN ROLE OF VAPOR PRESSURE DEFICIT

Jennifer Hsiao[1], Abigail L.S. Swann[2,1], and Soo-Hyung Kim[3]

[1]Department of Biology, University of Washington, Seattle, WA; [2]Department of Atmospheric Sciences, University of Washington, WA; [3]School of Environmental and Forest Sciences, College of the Environment, University of Washington, Seattle, Washington

Citation: Hsiao, J., Swann, A. L. S., & Kim, S.-H. (2019). Maize yield under a changing climate: The hidden role of vapor pressure deficit. Agricultural and Forest Meteorology, 279, 107692. https://doi.org/10.1016/j.agrformet.2019.107692

Supporting Information referenced in this chapter can be found in Appendix A.

2.1 Abstract

Temperatures over the next century are expected to rise to levels detrimental to crop growth and yield. As the atmosphere warms without additional water vapor input, vapor pressure deficit (VPD) increases as well. Increased temperatures and accompanied elevated VPD levels can both lead to negative impacts on crop yield. The independent importance of VPD, however, is often neglected or conflated with that from temperature due to a tight correlation between the two climate factors. We used a coupled process-based crop (MAIZSIM) and soil (2DSOIL) model to gain a mechanistic understanding of the independent roles temperature and VPD play in crop yield projections, as well as their interactions with rising CO_2 levels and changing precipitation patterns. We found that by separating out the VPD effect from rising temperatures, VPD increases had a greater negative impact on yield (12.9 ±1.8%, increase in VPD associated with 2°C warming) compared to that from warming (8.5 ±1.4%,

the direct effect of 2°C warming). The negative impact of these two factors varied with precipitation levels and influenced yield through separate mechanisms. Warmer temperatures caused yield loss mainly through shortening the growing season, while elevated VPD increased water loss and triggered several water stress responses such as reduced photosynthetic rates, lowered leaf area development, and shortened growing season length. Elevated CO_2 concentrations partially alleviated yield loss under warming or increased VPD conditions through water savings, but the impact level varied with precipitation levels and was most pronounced under drier conditions. These results demonstrate the key role VPD plays in crop growth and yield, displaying a magnitude of impact comparative to temperature and CO_2. A mechanistic understanding of the function of VPD and its relation with other climate factors and management practices is critical to improving crop yield projections under a changing climate.

2.2 Introduction

Temperatures over the next century are expected to rise globally by 1.5 to 4°C (IPCC, 2013). Rising temperatures that exceed optimum for plant growth are considered detrimental for crop production (Sage and Kubien, 2007; Battisti and Naylor, 2009), leading many to question the sustainability of agriculture and food security under future warming (Lobell et al., 2013; Peng et al., 2004; Asseng et al., 2015). While much effort has been placed on understanding the negative yield impacts from temperature, the independent importance of vapor pressure deficit (VPD) is often neglected or conflated with temperature due to the tight correlation between the two climate factors.

VPD is an indicator for the dryness of the air, defined as the difference between the amount of moisture in the air and how much moisture the air can hold when it is saturated. Warmer air has a higher capacity to hold water, thus warming the atmosphere without additional moisture input leads to drying and higher VPD. VPD is not only an important atmospheric characteristic, but is also a key environmental factor that influences plant growth and development through mechanisms different from temperature (Eamus et al., 2013; Day, 2000; Shirke and Pathre, 2004; Ray et al., 2002; Sanginés de Cárcer et al., 2018). Both warmer temperatures and accompanied elevated VPD levels can lead to negative im-

pacts on crop yield, but through separate mechanisms. Warmer temperatures mainly affect plants through the temperature dependence of biochemical and developmental processes, influencing aspects of plant growth such as photosynthesis and developmental rate (Sage and Kubien, 2007; Craufurd and Wheeler, 2009). Elevated VPD, on the other hand, increases atmospheric water demand and plant water loss (Monteith, 1995). This can trigger stomatal closure (Day, 2000; Mott and Parkhurst, 1991; Arve et al., 2011) and several water stress responses such as lowered photosynthetic rates, reduced leaf area development, and an altered phenological timeline (Farooq et al., 2009; Salah and Tardieu, 1996; McMaster et al., 2005).

Several aspects of VPD may have led to this discrepancy between the focus on temperature versus VPD within the literature. It is technically difficult to control water vapor levels independent of temperature under larger-scale experimental settings. Often, chamber, greenhouse or field studies aimed towards understanding temperature effects on crop growth also include effects of elevated VPD that are embedded within increased temperatures. Limitations also exist within empirical modeling approaches that rely on statistical relationships derived from crop yield observations and climate records over the past few decades. As formulated, these approaches typically cannot disentangle the inherent correlation between temperature and VPD. Temperature impacts on crop yield analyzed through these methods therefore include embedded VPD impacts as well (Lobell et al., 2011b; Peng et al., 2004; Schlenker and Roberts, 2009).

A few empirical (Lobell, 2014; Zhang et al., 2017) and process-based modeling studies (Stöckle et al., 2003; Lobell et al., 2013) have recognized the importance of VPD effects on crop growth and yield, attributing mechanisms of yield loss under elevated VPD to decreased radiation use efficiency (Stockle and Kiniry, 1990) and increased water demand and drought stress (Ort and Long, 2014) in cropping systems. Studies have also shown VPD contributing to tree mortality in forested ecosystems (Breshears et al., 2013; Eamus et al., 2013) and altering water and carbon fluxes in various ecosystems (Novick et al., 2016). While temperature and VPD are tightly correlated at present day, we do not expect the relationship to remain constant. Even under conditions of constant relative humidity, increasing temperature leads to a non-linear increase in VPD. Further, projections of future climate

conditions suggest a decrease in relative humidity over land (Byrne and O'Gorman, 2016), implying even larger and more non-linear increases in VPD with warming. Understanding and quantifying the effects temperature and VPD independently have on crop yield is critical for future yield projections, especially when considering rising CO_2 concentrations.

Elevated CO_2 levels have the potential to alleviate part of the stress associated with hot and dry (elevated VPD) conditions either through a biochemical response in which more CO_2 boosts photosynthetic rate, or through a stomatal response in which stomatal closure under elevated CO_2 concentrations conserves water, improving plant water status and benefiting growth (Ghannoum et al., 2000). The complex interaction between CO_2, VPD, temperature stresses, and water availability, however, lead to uncertainties when quantifying the positive CO_2 response. This is particularly true for C_4 crops, which often show little to no CO_2 responses in the absence of water stress (Chun et al., 2011; Kim et al., 2006; Leakey et al., 2006; Manderscheid et al., 2014). A better mechanistic understanding of the underlying processes through which each factor affects growth and yield, and how the effects of individual factors interact with one another as well as with background climate conditions would allow us to reduce uncertainty in yield responses to future climate conditions.

In this study, we applied a process-based modeling approach to disentangle the independent effects temperature and VPD have on crop yields. We focused on maize (Zea mays), the C_4 cereal crop with the largest global production, by simulating yield through a coupled crop and soil modeling system developed and tested for maize (MAIZSIM-2DSOIL). Isolating the impacts from temperature and VPD allowed us to look into the interactions these two climate factors have with other aspects of a changing climate, such as rising CO_2 levels which benefit plant growth and changing precipitation patterns which could lead to water stress. We aim to 1) quantify the independent effects temperature and VPD have on maize yields, 2) gain a mechanistic understanding of the physiological processes that lead to their impacts on yield, and 3) identify their interaction with rising CO_2 levels and variation in precipitation patterns.

2.3 Materials and methods

2.3.1 Crop simulation model

We selected a coupled crop (MAIZSIM) and soil (2DSOIL) model to represent the detailed processes that exist within the soil-plant-atmosphere continuum (Kim et al., 2012; Yang et al., 2009b,a; Timlin et al., 1996). We briefly describe here several key model components that were critical for this study. In this coupled model system, the model simulates maize growth and development as a function of light, temperature, precipitation, humidity, CO_2 concentrations, soil water content, soil properties, and nutrient levels. The model tracks key phenological stages to dynamically capture growth and physiological processes that are coupled with the surrounding environment while accounting for the effects of water and nutrient stress.

During the vegetative stage, non-linear temperature functions simulate emergence, maturation and senescence of individual leaves, while a logistic equation scaled by a temperature function is used to describe leaf expansion (Kim et al., 2012). After transitioning into the reproductive stage, development is then determined by the ambient temperature and photoperiod (Kim et al., 2012). The model describes gas exchange properties of developed leaves by coupling a leaf energy balance equation, a biochemical C_4 photosynthesis model (von Caemmerer, 2000), and a stomatal conductance model (Ball et al., 1987). Modifications in the stomatal conductance scheme were made to account for stomatal sensitivity to soil and plant water status. Gas exchange is calculated through iteratively solving for these three components (Kim and Lieth, 2003), with carbon gained partitioned towards individual plant parts for growth, and water lost contributing to the overall water status within the soil and crop system.

The crop model is coupled with the 2DSOIL model that represents a two-dimensional soil domain capable of calculating heat and solute transportation (Timlin et al., 1996). The coupled model dynamically solves for plant growth and development on an hourly basis, incorporating the real-time changes in the driving weather data. In our work, we utilized the mechanistic structure of this model to analyze the independent and interacting effects of temperature, VPD and CO_2 on crop growth, development and final yield.

2.3.2 Model validation and application

The MAIZSIM model has been previously validated for its representation of gas exchange processes (Yang et al., 2009a), its leaf area simulation (Yang et al., 2009b) under various water regimes, as well as its temperature response of leaf growth, development and biomass (Kim et al., 2012). In addition to model validation with greenhouse datasets, MAIZSIM yield simulations have been tested against yield data collected from Free Air Carbon dioxide Enrichment experiments conducted at Thünen Institute in Braunschweig, Germany, to better understand yield simulations under elevated CO_2 conditions (Durand et al., 2018). Yield simulations have also been validated with actual yield data in selected locations in France, the US, Brazil and Tanzania, along with 22 other maize simulation models (Bassu et al., 2014), and applications of the model include estimating potential yield capacity in the U.S. Northeast Seaboard Region under current and projected future climate and land use scenarios (Resop et al., 2016). These different angles of model validation and applications showed that MAIZSIM is capable of representing maize growth and yield under a range of environmental conditions, and its consideration of various plant responses to changes in temperature, CO_2 concentrations and different water stress levels make it suitable for exploring yield responses under a changing climate.

In our study, we compared model simulations of final yield with county-level yield data from the USDA National Agricultural Statistics Service's annual survey to validate the model's performance in the selected simulations (Fig. A.1, USDA, NASS, `http://www.nass.usda.gov/Quick_Stats`). Since model simulations were not specifically calibrated for the cultivars, farming practices, and soil properties for each location, the main purpose of this comparison was not to evaluate whether the model accurately represented crop yield for each site, but rather to understand whether the model was able to pick up broad patterns of yield production. We up-scaled model yield outputs from single plant outputs (g/plant) to field-scaled units (tons/hectare) by assuming a uniformed planting density of 10 plants/m^2, and compared simulated model output of each site and year with actual yield data from the available yield data closest to each flux tower site (see site description below, Table A.1, Fig. A.2).

2.3.3 Location selection and weather data

The MAIZSIM model requires daily or hourly inputs of solar radiation, maximal air temperature, minimal air temperature, precipitation, relative humidity, and CO_2 concentrations for simulations. If a daily weather format is provided, the model runs an internal algorithm to interpolate the information into an hourly format. Detailed equations used for these estimations can be found in Timlin et al. (2002). We obtained all the information required for model simulation except for CO_2 concentrations through weather data archived within the AmeriFlux network (`http://ameriflux.lbl.gov/`). Based on availability of continuous daily weather data throughout the growing season, we selected four cropland flux tower sites in North America: Iowa (US-Br1, Prueger and Parkin), Nebraska (US-Ne1, irrigated, Suyker; US-Ne3, rain-fed, Suyker), Ohio (US-CRT, Chen), and Oklahoma (US-ARM, Biraud) (Fig. A.1). We set CO_2 concentrations to a constant 400 ppm as a representation for current CO_2 levels. Sites were chosen to span background climate conditions with a range of mean annual temperatures and precipitation. Detailed information on individual sites can be found in Table A.1. All available site data were used other than years with consecutive days of missing data (See below).

Ameriflux data are logged every 30 minutes, but gaps existed within the dataset. While MAIZSIM can also handle hourly and sub hourly weather input timesteps, we processed the 30-minute weather data into a daily input format to gap-fill short periods of missing weather data. To do so, we summed solar radiation over daylight hours, summed precipitation over a day, averaged relative humidity over a day, and selected daily maximal and minimal temperature. We defined a generic growing season starting from May until the end of October, and checked for missing meteorology data within this time frame. Missing data that were less than half the length of a day were simply removed and daily averages were calculated with the remaining data. When missing data length was longer than half a day, we removed data from that entire day and gap filled it by interpolating from the day prior and after. When data had consecutive days of missing data, we removed that year of data from the analysis. We listed the years with available weather data used for each simulation site in Table A.1.

2.3.4 Idealized climate treatment

We applied three main idealized climate treatments to the historical meteorological data to simulate the effect of 1) warming through a 2°C increase in temperature while holding VPD constant, 2) atmospheric drying through an increase in VPD associated with a 2°C warming while holding the temperatures constant, and 3) increasing CO_2 levels from 400 to 800 ppm. We tested these climate treatments independently as well as in combination (Table 2.1). These climate changes follow the general magnitude of temperature change expected to accompany a doubling of atmospheric CO_2 concentration from 400ppm to 800ppm for mid-latitudes (IPCC 2013a). In addition, we imposed a 30% rainfall cut for the drought treatment to extend the precipitation range of our weather data to investigate the role of water stress. We included the simulated kernel yield for each treatment within Table 2.1 as well to provide an overall picture on how the different climate factors influences final yield.

We applied each climate treatment independently to the historical meteorology time series collected from the Ameriflux network archive. We followed the Clausius-Clapeyron equation to carry out our temperature and VPD treatments. For our simulations, we assumed that atmospheric water content (i.e. specific humidity) remains constant throughout warming, which results in a VPD increase with warming. The MAIZSIM model requires RH as the humidity input, so we converted between VPD and RH within our calculations. For the warming treatment, we applied a 2°C temperature increase throughout the growing season, and increased RH to levels such that VPD would remain constant. Similarly, for the elevated VPD treatment, we calculated the increases in VPD that would have occurred under a 2°C warming and converted it into RH. We then applied the RH change to our weather data while holding temperature constant. Due to the non-linearity within the Clausius-Clapeyron equation, the magnitude of VPD change associated with a 2°C warming would vary with the temperature and humidity levels at each simulation site-year; the averaged increases in VPD across all simulations were 1.19 - 0.66 (kPa), with minimal increases as low as 0.17 and maximal increases up to 5.35 (kPa). Since these two treatments result from direct manipulation of historical meteorology data, they preserve the natural climate variability that existed within growing seasons and between planting years as well

as the correlations between variables other than the one being manipulated. We included the equations used for these calculations within our supplementary information.

The stomatal conductance model incorporated in MAIZSIM follows the original Ball-Woodrow-Berry model (BWB model) and simulates stomatal closure under low relative humidity within the atmosphere (Ball et al., 1987). While relative humidity and VPD both quantify water content in the atmosphere, they change at different rates as temperature increases, and plants respond more directly to VPD than to relative humidity (Mott and Parkhurst, 1991), presenting a possible limitation for our study. It is worth noting that a recent study from Franks et al. (2017) demonstrated that with appropriate calibration, the BWB model captured a similar stomatal response within a the range of 0.5-2 kPa when compared to a BWB model variant with modifications for tracking the stomatal response to VPD (Medlyn et al., 2011). The bulk of our meteorological conditions fall within this range.

2.3.5 Model setup and simulation protocol

We setup the model to represent a generic maize cultivar that requires 1600 growing degree days to reach maturity, and can develop a maximum of 15 juvenile leaves. We set a standard planting date of May-15 and planting density of 10 plants/m2, and supplied a total of 200 kg-ha-1 of Nitrogen throughout the simulation, with half supplied as base fertilizer prior to planting and the rest as top-dressing a month after planting. We divided the soil into four layers, and subscribed the top two soil layers to have a 0.65-0.28-0.06-0.01 sand-silt-clay-organic matter ratio, and the bottom two layers to have a 0.75-0.20-0.047-0.003 ratio.

We ran the model with the historical meteorology data for a control model simulation. We then forced the model with increased temperature, increased VPD, elevated CO_2, rainfall reduction treatments, and the combination of each to analyze the independent and interacting effects within and between each factor. Finally, we analyzed model outputs of growing season length, photosynthetic rate, total leaf area, predawn leaf water potential, stomatal conductance, and final yield.

2.3.6 Analysis of model responses

We calculated the percent impact each treatment (Temp, VPD and CO_2) and the combinations each had on yield (Table 2.1) by subtracting the simulated yield under climate treatments ($Yield_{treatment}$) from the simulated yield under the controlled climate ($Yield_{control}$), and further divided the output with $Yield_{control}$ (Eqn. 2.1):

$$YieldImpact = \frac{Yield_{treatment} - Yield_{control}}{Yield_{control}} \cdot 100\% \tag{2.1}$$

Next, we identified three main factors that could influence crop yield: growing season length which we defined as time from planting to maturity (days), mean photosynthetic rate during the grain-filling phenological stage (µmol m-2 s-1), and maximal total leaf area throughout development (cm2). We calculated the percent change in each of these growth factors when subjected to temperature, VPD, or CO_2 treatments as follows (Eqn. 2.2):

$$\Delta GrowthFactor = \frac{GrowthFactor_{treatment} - GrowthFactor_{control}}{GrowthFactor_{control}} \cdot 100\% \tag{2.2}$$

$GrowthFactor_{treatment}$ represents the simulated value of one of these factors of interest (growing season length, photosynthetic rate, or total leaf area) under climate treatments (i.e. Temp, VPD and CO_2). $GrowthFactor_{control}$ represents the simulated value of the same growth factor but under control climate conditions.

In addition, we averaged daily values of predawn leaf water potential (MPa) and stomatal conductance (mol $m^{-2}s^{-1}$) for each treatment throughout four developmental stages: emergence, tassel initiation, silking, and grain filling. Further, we utilized the natural precipitation variability within our meteorology data to analyze yield impacts (%) of temperature, VPD and CO_2 across precipitation levels. We classified growing season precipitation into four categories: high ($>$ 600 mm), medium (500-600 mm), low (400-500 mm), and very low ($<$ 400 mm) precipitation and calculated yield impacts (%) of each treatment within each precipitation bin. We calculated standard errors to represent variability between sites and years for all analyses.

2.4 Results

2.4.1 General agreement between simulated and actual yield

We compared crop yields simulated under the control weather input with actual county-level crop yield data collected from the years and proximate locations of which the weather data were collected (United Stated Department of Agriculture, National Agricultural Statistics Service, 2014). Figure A.2 shows the ability of the coupled model to simulate actual crop yield across the four simulation sites (map of site location shown in Fig. A.1). The model was able to represent yield variations across simulation sites and years due to the different weather inputs despite not being calibrated for specific cultivar and management practice for these sites. Model simulations represented a wider range of final yield values compared to observations, overestimating in locations and years with higher yields (Nebraska).

2.4.2 Yield responses to temperature, VPD, and CO_2

We summarized the simulated yield (g/plant) under different treatments across years and sites in Table 2.1. When compared to the control treatment, both warmer temperatures and higher VPD levels independently lowered yield by 8.5 ±1.4 % and 12.9 ±1.8 %, respectively, while imposing the two factors simultaneously lowered yield by 24.2 ±2.8 % (Fig. 2.1a). On the other hand, elevated CO_2 concentrations increased crop yield by 17.2 ±3.5 % (Fig. 2.1a). This boost in yield decreased when an elevated CO_2 level was accompanied by warmer temperatures or increased VPD, and the combination of all three climate effects (Temp, VPD, CO_2) partially canceled each other out, overall leading to a smaller reduction in yield by -4 ±3.4 % (Fig. 2.1a).

2.4.3 Mechanisms that contribute to changes in yield

Shortened growing season length (days), lowered photosynthetic rate (µmol $m^{-2}s^{-1}$), as well as a decreased leaf area (cm^2) can all negatively affect final yield (Fig. 2.1b). When compared to the control simulation, the main cause of the negative yield impact from increased temperature (Fig. 2.1a, High Temp) was a shortened growing season (-15.7 ±1.3 %, Fig. 2.1b), while effects from photosynthesis (1.0 ±1.6 %) and leaf area development

(0.6 ±0.4 %) were neutral. Warmer temperatures did not significantly influence predawn leaf water potential (Fig. 2.2a) or stomatal conductance (Fig. 2.2c); the temperature effects illustrated in Figure 2.1b were mainly carried out through temperature alone. Note that the magnitude of these values should not be directly compared against one another, since a 5% shortening of growing season length will not necessarily have the same yield impact of a 5% decrease in photosynthetic rate. However, comparing these values between treatments (Temp, VPD, CO_2) can provide an overall picture on what growth factors are affected more by our imposed climate treatments.

Compared to rising temperatures, increased VPD levels had a greater negative impact on final yield (Fig. 2.1a, Elevated VPD). This is because a shortened growing season (-10.0 ±1.9 %) was concurrent with lowered photosynthetic rates (-2.1 ±1.1 %) and a slight decrease in leaf area development rate (-0.8 ±0.5 %, Fig. 2.1b); these responses in photosynthetic rates and leaf area development to elevated VPD were in the opposite direction compared to the response under higher temperatures. Greater water loss under elevated VPD levels lowered predawn leaf water potential, leading to water stress signals that amplified later in the growing season (Fig. 2.2a). Changes in water relations therefore played a critical role in the direction and magnitude of plant responses under an elevated VPD treatment (Fig. 2.1b).

In contrast to temperature and VPD effects, higher CO_2 concentrations benefited yield (Fig. 2.1a, High CO_2). Stomatal closure under elevated CO_2 concentrations (Fig. 2.2c) conserved water for use later in the growing season and improved water relations (Fig. 2.2a). This change in plant water relations directly counteracted negative VPD effects that stemmed from water stress responses (Fig. 2.2b), and partially alleviated yield through an increase in photosynthetic rates (7.5 ±3.7 %), a prolonged growing season (6.4 ±1.2 %), and a slight boost in leaf area development (0.8 ±0.5 %, Fig. 2.1b).

2.4.4 The role of precipitation

For all treatments, the model generally simulated lower yield under lower precipitation. Over this natural range of precipitation variation present across the simulated sites and years,

the direction of yield impact from temperature, VPD and CO_2 remained consistent, but the magnitude of impact each factor had on yield varied with precipitation levels (Fig. 2.3). Warmer temperature and higher VPD showed a greater negative relative yield impact in years and sites with medium-to-low precipitation levels, while the positive relative impacts from elevated CO_2 levels were most pronounced under drier conditions (Fig. 2.3d). Changes in simulated yield (Fig. 2.3a-c) correspond with the calculated percent impact on yield (Fig. 2.3d). The overall effect of temperature, VPD and CO_2 treatments combined led to a net negative effect on yield (Fig. 2.4a), with the greatest percent impact present in the medium precipitation range (Fig. 2.4b).

A 30% precipitation cut amplified the negative temperature and VPD impacts on yield (Fig. A.3a & b) but diminished the positive CO_2 effects (Fig. A.3c). These responses were most pronounced under site-years with lowest precipitation levels, and led to further yield loss (Fig. 2.4b). The negative yield impacts from temperature were greater than that from VPD under higher precipitation levels, but vice versa under very low precipitation levels (Fig. A.3d).

2.5 Discussion

Both the 2 degrees of warming and VPD increase associated with that warming can independently lead to negative impacts on yield, with a larger yield decline due to the increased VPD than due to warming (Fig. 2.1a). Previous studies have largely focused on warming effects on yield loss (e.g., Lobell et al., 2013, 2011b, 2008; Peng et al., 2004; Asseng et al., 2015; Battisti and Naylor, 2009), but our results emphasize the importance of increased VPD levels that co-occur with warming. Elevated CO_2 levels, on the other hand, can partially alleviate yield loss from warming and increasing VPD, but at the levels we investigated (2 degrees warming, doubling of CO_2 from 400 to 800 ppm) the benefits from elevated CO_2 are not sufficient to completely compensate for the yield loss from warming and increased VPD.

2.5.1 Effects of elevated VPD

Under elevated VPD conditions, our simulation results showed lower photosynthetic rates, shortened growing season length, and a slight decrease in leaf area development (Fig. 2.1b). All of these factors contributed to a final loss in yield (Fig. 2.1a). These responses stemmed from increased water loss and water stress responses under a drier atmosphere (Fig. 2.2).

Various studies have demonstrated stomatal closure under dry atmospheric conditions in order to prevent excess water loss (Bunce, 2006; Mott, 2007; Monteith, 1995), but despite stomatal closure, transpiration often still increases under the greater water vapor gradient between the leaf and the drier surrounding air (Monteith, 1995). This phenomenon has also been demonstrated specifically in maize plants (Ray et al., 2002). Greater water loss can increase the water stress levels experienced by plants, further influencing plant growth and yield through stomatal closure, interruption or reduction in leaf elongation and expansion (Çakir, 2004; Nonami, 1998; Tanguilig et al., 1987; Salah and Tardieu, 1996), or shortened phenology (McMaster et al., 2005). We have accounted for these responses to water stress in our study, as the soil component within MAIZSIM tracks water status changes in the soil and the crop, quantifying it through soil and plant water potential (Fig. 2.2c). We find that predawn leaf water potential (and thus water status) continues to drop throughout the growing season under increased VPD (Fig. 2.2a) as stomatal closure is unable to fully compensate for drier air (Fig. 2.2b).Differences in the precipitation ranges experienced by individual site-years within treatment groups may have contributed to variations within simulated leaf water potential and stomatal conductance, but the overall pattern due to the climate treatments are still present.

The modified BWB model within MAIZSIM allows stomata to also respond to leaf water potential (Yang et al., 2009a), in which water-stressed plants with low leaf water potential show stomatal closure (Fig. 2.2). While carbon limitation through stomatal closure has less of an influence on C4 plants compared to C3 (Ghannoum, 2009), we still observed a lower photosynthetic rate (Fig. 2.1b) that accompanied stomatal closure under elevated VPD conditions (Fig. 2.2c), likely due to site-years under drier conditions. Lower leaf water potential in MAIZSIM also triggers a water stress response that reduces leaf expansion

(Timlin et al., 1996; Yang et al., 2009b) and alters whole-plant carbon allocation such that more carbon is partitioned towards roots instead of aboveground plant parts, causing the reduction in total leaf area simulated (Fig. 2.1b). While phenology in MAIZISM does not directly respond to soil or leaf water potential, the changes in leaf elongation rate indirectly affected developmental time in each phenological stage, shortening the overall growing season length (Fig. 2.1b).

2.5.2 Effects of elevated temperature

Temperature, when separated from VPD, had little effect on plant water status (Fig. 2.2). Instead, the yield effects of temperature were directly through the temperature dependence of various plant processes. This aspect can easily be confounded when temperature and VPD are considered together. In contrast to VPD effects, increasing temperature showed a combination of positive and negative effects on phenological (growing season length), morphological (total leaf area) and physiological (photosynthesis) processes important for growth (Fig. 2.1b), which partially compensated each other such that the negative impact caused by warming was slightly lower than that caused by increased VPD (Fig. 2.1a).

The cumulative effect of warmer temperatures throughout the growing season showed a pronounced impact in accelerating development (Fig. 2.1b), moving the plants through phenological stages more quickly, reaching the reproductive stage and maturity earlier (Kim et al., 2012), but the shortened developmental time also led to lower yield. Farming practices such as switching to more heat-tolerant cultivars and adjusting planting dates can modify the overall growing season length, mitigating yield loss under hot and high VPD conditions (Butler and Huybers, 2013; Sacks and Kucharik, 2011). We chose to set cultivar-related model parameters constant. This approach allowed us to look at yield impacts from temperature, VPD and CO_2 independent of other changing factors, but inevitably neglects the potential mitigating effects that can come from various farming and management practices.

Responses to warming in photosynthesis and leaf area development were lower in magnitude and varied in direction (Fig. 2.1b). Plants exhibit nonlinear temperature responses in various physiological processes including photosynthesis (Sage and Kubien, 2007) and leaf

growth (Kim et al., 2007). As a C4 crop, maize has a higher optimal temperature for many physiological processes compared to C3 plants, and are generally more adapted to warmer climates (Collatz et al., 1992). The direction and magnitude of temperature responses, therefore, depend greatly on whether the environmental temperature is greater or lower than the optimal temperature of each process (Kim et al., 2007). Due to this nonlinearity in temperature responses, the warming treatment we imposed did not consistently lead to negative impacts on photosynthesis and leaf area development, but instead varied with the range of baseline temperatures found at each simulation site (Table A.1). Cooler and wetter sites (i.e. Iowa, Nebraska) showed slightly positive temperature effects on photosynthetic rates (4.37 ±1.27, 4.49 ±2.91%, respectively). In contrary, the warmest and driest site (i.e. Oklahoma) showed negative effects (-3.53 ±2.46%).

2.5.3 Effects of elevated CO_2 and precipitation

Decreased stomatal conductance under our elevated CO_2 simulation (Fig. 2.2c) led to water savings and increased predawn leaf water potential later in the growing season (Fig. 2.2a). While improved plant water status benefited yield, the overall effects were not sufficient to outweigh the negative effects from temperature and VPD (Fig. 2.1a). The magnitude of positive CO_2 impact on yield varied systematically with total growing season precipitation, with dry years and locations showing a greater mitigating effect from elevated CO_2 levels and vice versa (Fig. 2.3d). This response is commonly documented for C_4 plants, in which benefits of elevated CO_2 on crop growth are often only pronounced under water stressed conditions (Ghannoum, 2009). Water savings have been more consistently documented in maize plants under elevated CO_2 conditions, either through lower evapotranspiration rates (Kim et al., 2006) or water use (Chun et al., 2011). On the other hand, CO_2 impacts on yield have been more variable and dependent on the level of water stress plants experience; chamber studies and Free-Air CO_2 Enrichment (FACE) experiments specific for maize showed little to no positive CO_2 effect on yield under well-watered conditions (Chun et al., 2011; Kim et al., 2006; Leakey et al., 2006), while yield boosts up to 40% were observed under droughted conditions (Manderscheid et al., 2014).

The magnitude of positive CO_2 impact within our simulations range approximately from 10-30% (Fig. 2.3d). These values are comparable with FACE site studies that observed large positive yield boosts from elevated CO_2 concentrations (Manderscheid et al., 2014). Durand et al. (2018) further tested how a collection of maize models represented the CO_2-water interacting effect demonstrated by Manderscheid et al. (2014) and revealed that despite a wide range of variability, models that specifically describe stomatal responses to CO_2 performed better in capturing the interacting effect between CO_2 and water status. MAIZSIM represents stomatal and photosynthetic response to CO_2, along with drought responses in leaf area development and carbon partitioning (Yang et al., 2009a,b). It is also coupled with a soil module that explicitly tracks the movement of water down the soil column, and represents water potential both in the soil and in the crop (Timlin et al., 1996), making it suitable to explore the interacting effect between CO_2 and water status. In addition, our choice of soil composition resembles a well-drained soil, which can potentially lead to water stress under rain-fed conditions. This can partially explain the positive CO_2 effects that were still present under site-years with higher precipitation levels (Fig. 2.3d). Precipitation patterns throughout the growing season may also contribute to the positive CO_2 effects, even under site-years with higher total growing season precipitation since a high total growing season precipitation does not always correspond to optimal precipitation for maize growth. When looking into the growing season precipitation patterns, we noticed that site-years with more consistent rainfall showed less of a positive CO_2 responses (Fig. 2.3c, small arrows), while years with lower or more variable rainfall events, especially earlier on in development or during the grain-filling stage, resulted in greater positive CO_2 effects on yield (Fig. 2.3c, big arrows). This is likely due to the shallower rooting profile in younger plants within the model that make plants more susceptible to early growing season drought, and water-stress impacts on carbon allocation during the grain-filling stage, respectively.

The greatest absolute (Fig. 2.3a & b) and percentage (Fig. 2.3d) yield loss from warmer temperatures and elevated VPD occur under a mid-range precipitation level. This pattern suggests that sufficient rainfall partially alleviated the negative impact from elevated temperature and VPD, while droughted conditions served as an additional stressor on top of warm temperatures and elevated VPD (Farooq et al., 2009), likely limiting the additional

contribution of elevated temperature and VPD to yield loss. The interaction that temperature, VPD, and CO_2 effects exhibit with varying precipitation levels demonstrated how the relative contribution of each factor on final yield, as well as their combined effects, can shift with plant water status (Fig. 2.3d & 4b).

Plant water stress can arise from high atmospheric water demand (VPD), low below-ground water supply (soil water potential), or a combination of the two (Novick et al., 2016). Both processes can independently limit crop growth through their effects on plant water status (Salah and Tardieu, 1996; Çakir, 2004). While precipitation level is a quick indicator for water supply and potential drought, several other factors such as soil properties, root development, and rooting depth together determine final water availability.

2.5.4 Future projections

As temperatures are projected to continue rising over the coming decades, so are VPD levels (IPCC 2013a). Projected increases in VPD mainly follow the patterns of warming, as warmer air has the capacity to hold more water vapor, and thus the deficit from saturation increases with temperature. Even if relative humidity remained constant as temperatures increased, VPD would still increase due to the non-linear nature of the Clausius-Clapeyron relation. However, projections suggest decreasing relative humidity over land under a warmer climate (Byrne and O'Gorman, 2016) which would lead to even larger increases in VPD. This poses a challenge in yield projection for models that do not consider temperature and VPD independently. Further, recent studies have also shown that stomatal closure under increasing CO_2 levels can limit water vapor input into the atmosphere, amplifying this trend of atmospheric drying due to vegetation and climate interactions (Berg et al., 2016; Swann et al., 2016). This decoupling between temperature and VPD is likely to lead to greater increases in VPD than predicted from temperature alone, which poses a challenge in yield projection for models that do not consider temperature and VPD independently, and emphasizes the importance of understanding the independent role of VPD in crop yield projections.

2.6 Conclusions

Our process-based modeling approach allowed us to quantify the direction and magnitude of the impact temperature, VPD and CO_2 independently had on final yield. While the absolute values shown in our results are specific to our model structure and setup, our results provided insight for the mechanisms behind these yield impacts: either through phenological (growing season length), morphological (leaf area development), or physiological (photosynthetic rate) processes. Our results illustrated that elevated VPD levels contributed greatly to the simulated yield loss under warming. This occurred through mechanisms linked to changes in water relations and were directly counteracted by water savings experienced under elevated CO_2 concentrations. These mechanisms were different from those that led to yield loss under warmer temperatures, which mainly acted through a shortened growing season. We also highlight the importance of water availability and its interaction with other climate properties (i.e. temperature, VPD, CO_2). While overall yield is reduced in lower precipitation years, the relative importance of each treatment factor on yield varies depending on the amount of precipitation. The relative yield boost from elevated CO_2 levels were larger in the lowest precipitation years and yield declines from warming and increased VPD were larger in the medium to low precipitation years. Such mechanistic and quantitative information on how different climate factors act independently and interactively to affect plant growth and yield can aid breeding programs for targeted breeding aimed towards climate change adaptation.

While climate plays a critical role for plant growth and production, management practices such as irrigation, fertilization, changes in planting dates or cultivars are also extremely important factors that affect the productivity within agricultural systems. Our work provides a starting point in examining the independent roles temperature and VPD play in crop yield projections, as well as their interactions with rising CO_2 concentrations and varying precipitation levels. Expanding this analysis to a broader geographic range with a wider representation of baseline climate conditions, while considering additional impacts from soil moisture, cultivar choices and farming practices, would provide further insight into the uncertainty in crop yield projections across agro-climate regions, and can provide guidance for

acclimation and adaptation strategies moving forward under a changing climate.

2.7 Acknowledgement

We thank Kyungdahm Yun for the technical support in setting up the MAIZSIM model. ALSS acknowledges support from NSF award AGS-1553715 to the University of Washington, and S-HK acknowledges support from a Specific Cooperative Agreement (58-8042-6-097) between USDA-ARS and the University of Washington. Finally, funding for AmeriFlux data resources was provided by the U.S. Department of Energy's Office of Science.

2.8 *Figures and tables*

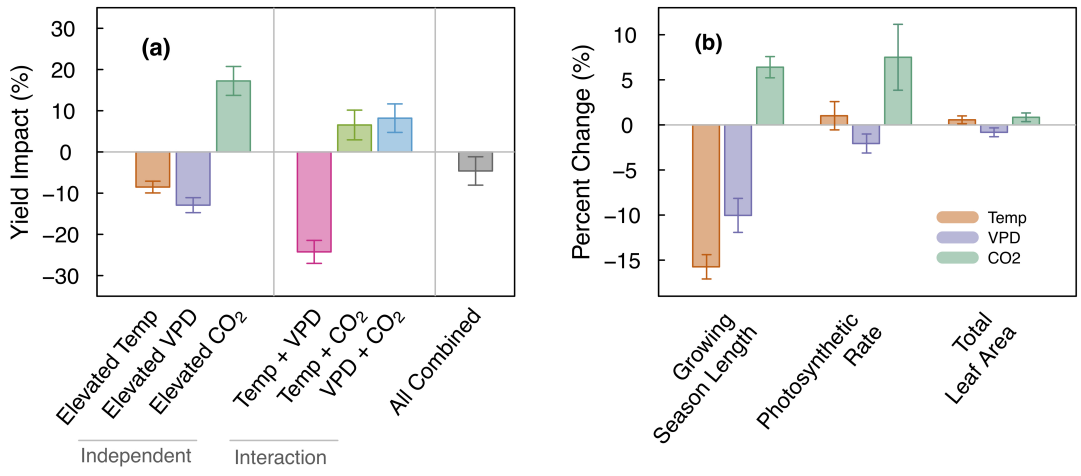

Figure 2.1: a) Percent yield impact from 2°C warming, increased VPD that accompanies 2°C warming, doubling of CO_2 levels from 400-800 ppm, and the combination of all three factors across all study locations and years. b) The percent change in growth factors (growing season length, photosynthetic rate, total leaf area) under temperature, VPD and CO_2 treatments. Error bards denote standard error calculated across simulation sites and years.

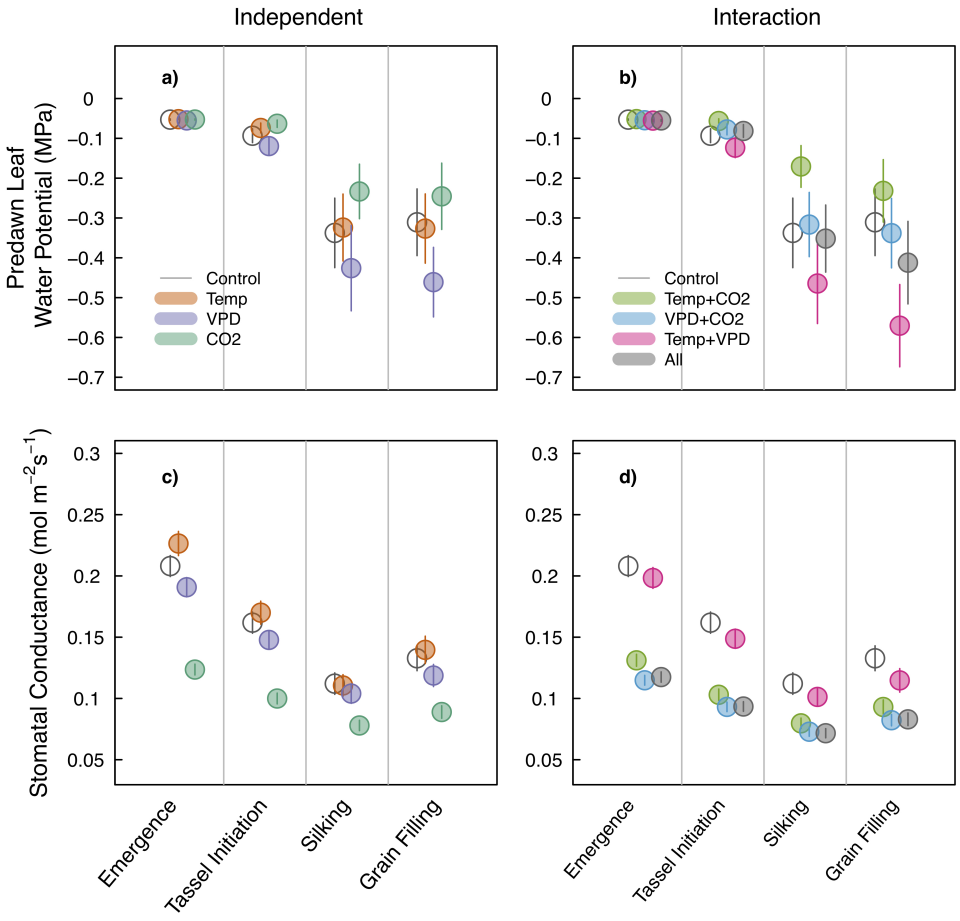

Figure 2.2: Average predawn leaf water potential (MPa) and stomatal conductance ($mol \cdot m^{-2} \cdot s^{-1}$) across developmental stages of emergence, tassel initiation, silking, and grain filling for single climate treatments (a, c) and climate treatment combinations (b, d). Single climate treatments include Control (open circle), Temp (orange), VPD (purple), CO_2 (green), while climate treatment combinations include Temp+CO_2 (light green), VPD+CO_2 (blue), Temp+VPD (pink), and All (grey). Error bars denote variability between site and years.

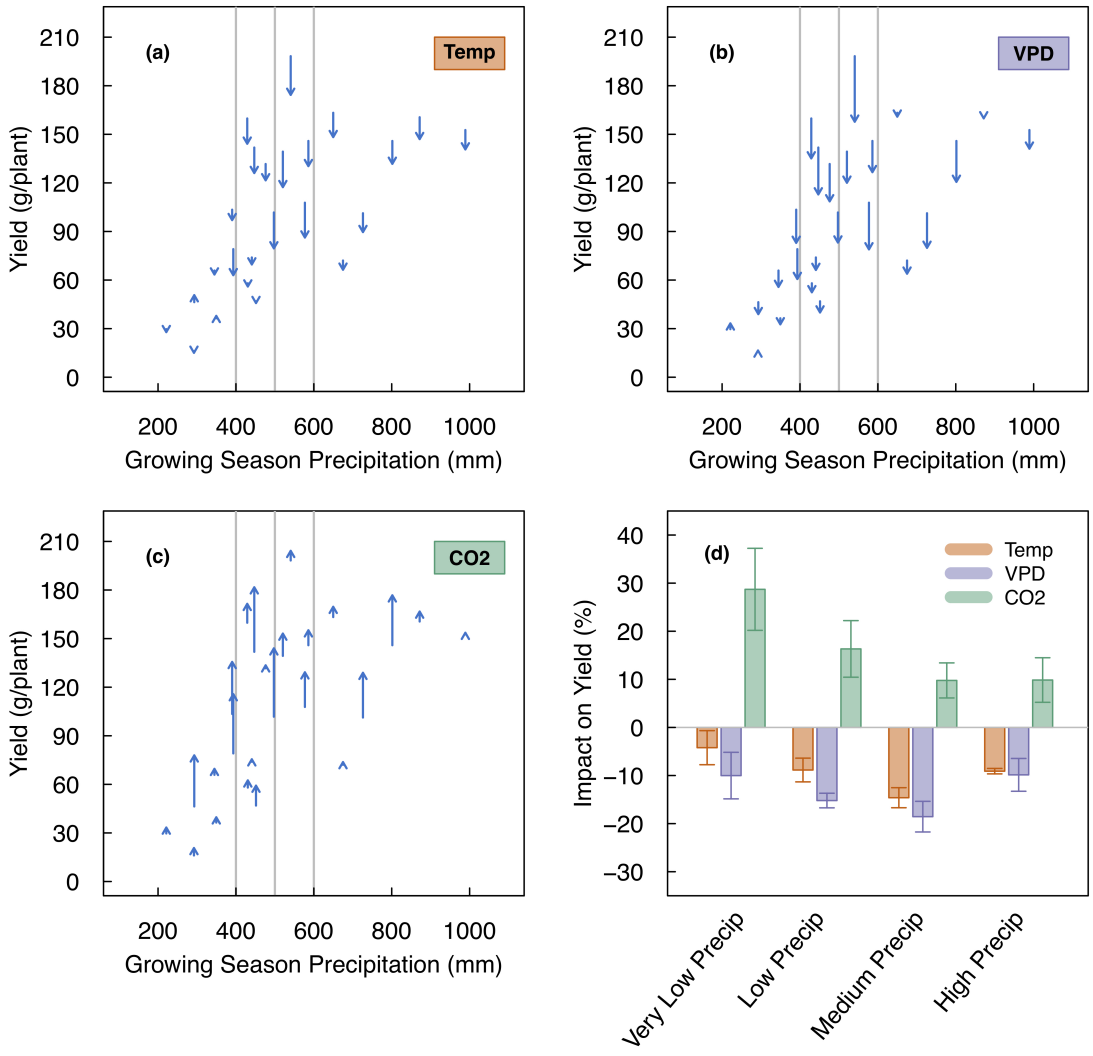

Figure 2.3: Direction and magnitude of yield change between treatment and control yield across precipitation range within simulated sites and years for a) temperature, b) VPD, and c) CO_2. The vertical grey lines categorize the precipitation range into very low (<400 mm growing season precipitation), low (400-500 mm), medium (500-600 mm), and high (>600 mm) precipitation levels. d) Percent yield impact from 2°C warming (orange), increased VPD that accompanies 2°C warming (purple), and doubling CO_2 levels from 400-800 ppm (green) under different precipitation ranges. Error bars denote standard error calculated across simulation sites and years.

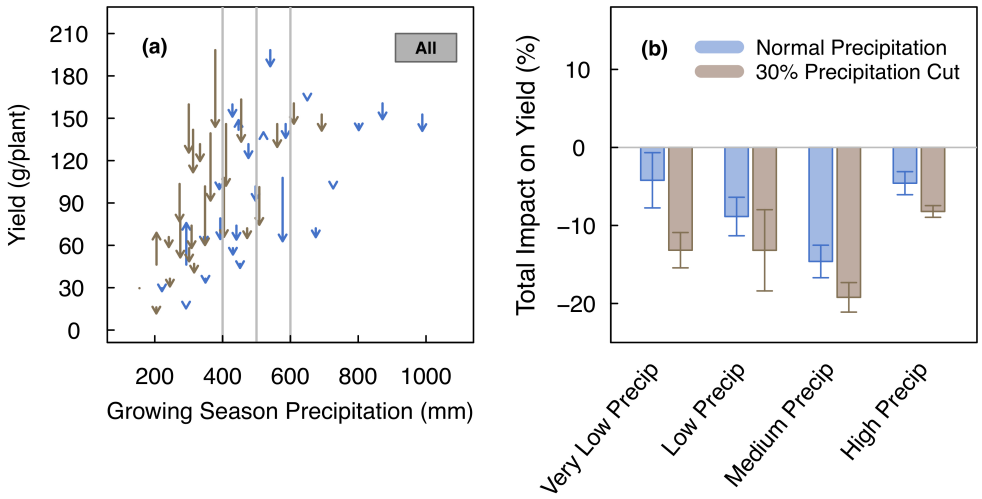

Figure 2.4: Direction and magnitude of yield change between the treatment (temperature, VPD and CO_2 combined) and controlled yield across precipitation range within simulated sites and years. The blue lines show results from the normal precipitation range, while the brown lines show results under a 30% rainfall cut. The vertical grey lines categorize the precipitation range into very low (<400 mm growing season precipitation), low (400-500 mm), medium (500-600 mm), and high (>600 mm) precipitation levels. b) Percent yield impact from temperature, VPD and CO_2 all combined across precipitation ranges for normal precipitation (blue) and 30% rainfall cut (brown).

Table 2.1: Treatment description and simulated kernel yield.

Treatment	Description	Simulated Yield (g/plant)
Control	Ameriflux weather data input.	103.24 ± 2.10
Elevated Temp	2°C warming with VPD held constant.	92.21 ± 1.84
Elevated VPD	VPD increases that occur under a 2°C warming, but with temperature held constant. Average VPD increases across all simulation site and years are 1.19 ± 0.66 (kPa).	88.71 ± 1.85
Elevated CO_2	Elevated CO_2 levels from 400 ppm to 800 ppm.	117.98 ± 2.22
Temp + VPD	2°C warming plus increased VPD.	77.33 ± 1.84
Temp + CO_2	2°C warming plus elevated CO_2.	106.15 ± 1.97
VPD + CO_2	Increased VPD plus elevated CO_2.	109.66 ± 2.20
All	2°C warming, increased VPD, and elevated CO_2 combined.	97.50 ± 2.04
Drought	30% rainfall cut.	86.18 ± 1.80

Chapter 3

CHAPTER 3 A FRAMEWORK FOR MODEL-ASSISTED T × M × E EXPLORATION IN MAIZE

Jennifer Hsiao[1], Soo-Hyung Kim[3], Dennis J. Timlin[4], Nathaniel D. Mueller[5], and Abigail L.S. Swann[2,1]

[1]Department of Biology, University of Washington, Seattle, WA; [2]Department of Atmospheric Sciences, University of Washington, WA; [3]School of Environmental and Forest Sciences, College of the Environment, University of Washington, Seattle, Washington; [4]USDA ARS Adaptive Cropping Systems Laboratory, Beltsville, MD, United States; [5]Colorado State University, Department of Soil and Crop Sciences, Fort Collins, CO, United States

3.1 Abstract

Breeding for new crop characteristics and adjusting management practices are critical avenues to mitigate yield loss and maintain yield stability under a changing climate. However, identifying high-performing plant traits and management options for different growing regions through traditional breeding practices and agronomic field trials is often time and resource-intensive. Mechanistic crop simulation models can serve as powerful tools to help synthesize cropping information, set breeding targets, and develop adaptation strategies to sustain food production. In this study, we develop a modeling framework for a mechanistic crop model (MAIZSIM) to run many simulations within a trait × environment × management landscape and demonstrate how such a modeling framework could be used to identify ideal trait-management combinations that maximize yield and yield stability for different agro-climate regions in the US.

3.2 Introduction

Food demand is increasing but our ability to sustain crop productivity will be impacted by a warming climate. Breeding has consistently played a critical role in the progress of continuous yield gain and was estimated to account for up to 50-60% of the total on-farm yield gain in the past several decades (Duvick, 2005). These gains through genetic improvements are complemented by changes in management practices, such as an increase in fertilizer use, chemical weed control, higher planting densities, and earlier planting dates (Kucharik, 2008; Cardwell, 1982). Recently, however, practices such as nitrogen application and weed control are nearly fully exploited in the US corn belt; simple adjustments in management strategies alone are likely insufficient to sustain an increasing yield trend. Additional yield gains would need to rely further on genetic improvements in new cultivars, as well as management changes that accompany climate-resilient characteristics to fully leverage the interactions among genetics, environment, and management (the G $\times$ E $\times$ M paradigm, Hatfield and Walthall (2015)).

Continued development of new cultivars better-suited for future climate is critical for sustaining current yield trends or to prevent yield loss (Challinor et al., 2017; Burke et al., 2009). Progress in breeding for climate adaptation has been demonstrated in several areas, including changes in morphological traits (e.g. improved root system architecture that improves soil water access; Hammer et al. (2009)), increases in drought and salinity tolerance (Fita et al., 2015; Messina et al., 2020a), improvements in physiological traits (e.g. greater nitrogen use efficiency; Fischer and Edmeades (2010)), and shifts in copping duration (Zhu et al., 2018), to name a few. Our ability to utilize the genetic diversity preserved in wild relatives, landrace species, and undomesticated wild species to develop new climate-ready cultivars is increasingly important to achieve sustainable and intensified food production (McCouch et al., 2013; Godfray et al., 2010).

Maize trait changes in the past few decades have also been accompanied by shifts in crop management practices, such as more erect plant forms that facilitated notable increases in planting densities (Duvick, 2005), shifts towards earlier planting dates by about 3 days per decade (Butler et al., 2018; Zhu et al., 2018), increases in nutrient supply (Duvick, 2005),

and increases in area irrigated (Mueller et al., 2016). In addition, the suitability of a cultivar often varies considerably across environmental gradients (e.g. Messina et al. (2015)), thus optimal plant traits and management options are usually identified within defined target environments (Cooper et al., 2016). This breeding strategy allows for designing different cultivars to perform favorably and withstand stresses in their target environments, and what is considered "ideal" may differ between locations and climate. We expect optimal management to shift under future climate conditions and in combination with different phenotypic traits, providing important means of adaptation in many systems (Deryng et al., 2011).

Mechanistic modeling tools that integrate physiological, morphological, and phenological properties of a crop (G), their performance under different management options (M), and their interactions with the surrounding environment (E) on a whole-plant level can serve as useful tools for breeding practices through the quantification of a yield-trait-performance landscape (Messina et al., 2011). The structure of such models allow for testing effects of traits (e.g. leaf elongation rate, total leaf number) on integrated outcomes such as yield. While mechanistic crop models may not specifically describe genetic-level properties, higher-level traits are often used as proxies to describe the underlying genotype. This makes models ideal tools to test and screen for potentially promising traits and management ($T \times M$) combinations under different climate and environmental conditions (E) as a first step before carrying out actual breeding practices (Andrivon et al., 2012; Messina et al., 2011), and on large scales that are often not feasible under actual experimental settings (Peng et al., 2020; Cooper et al., 2020; Hammer et al., 2020). Such information can further be used to synthesize cropping knowledge, set breeding targets, and develop climate-targeted adaptation strategies to sustain food production.

Despite broad recognition that mechanistic, process-based crop simulation models can be a powerful tool to synthesize cropping information, set breeding targets for developing climate-ready crops, and develop adaptation strategies for sustaining food production (Muller and Martre, 2019; Messina et al., 2020a), few comprehensive studies have been performed to produce climate-specific trait and management combinations for staple crops including maize in the US, a necessity given rapidly changing environmental conditions fac-

ing the US cropping systems. In this study, we construct a modeling framework to identify targeted plant traits and effective crop management to achieve maximum crop performance in both the current and future climates. Specifically, we addressed how an ensemble of plant traits (i.e. physiology, morphology, phenology) combined with realistic adjustments to management choices (i.e. shifting planting dates, planting density, and row spacing) can be used to build resilience and improve productivity under the stresses induced from a changing climate.

3.3 Material and methods

We set up a data-model framework to quantitatively identify high performing regions within a T × E × M landscape. The framework consists of three main components (Fig. 3.1): *1)* a process-based crop simulation model (section 3.3.1), *2)* model inputs to drive the model, including present-day climate information (section 3.3.2), idealized future climate information (section 4.3.4), simulation site soil information (section 3.3.4), and sampled trait and management options (section 4.3.3), and *3)* processed model outputs that identify performance within the T × E × M landscape (section 3.3.6 - 3.3.7), and summarized in-season growth outputs (section 3.3.8).

3.3.1 Process-based crop simulation model - MAIZSIM

MAIZSIM is a deterministic and dynamic model developed and calibrated for maize plants to represent key physiological and physical processes such as gas exchange, canopy radiative transfer, carbon partitioning, water relations, nitrogen dynamics and phenology (Kim et al., 2012). MAIZSIM interfaces with a 2-dimensional finite element model (2DSOIL) that simulates a dynamic soil water and nutrient vertical 2D profile (Timlin et al., 1996). The coupled model responds to daily or hourly meteorological information throughout the growing season that includes temperature, relative humidity, solar radiation, and CO_2 concentrations.

At the leaf-level, MAIZSIM captures gas exchange processes through a C4 photosynthesis model (von Caemmerer, 2000) coupled with a stomatal conductance model (Ball et al., 1987) and an energy balance equation (Collatz et al., 1992); leaf-level gas exchange processes are scaled to canopy-levels using a sunlit/shaded leaf framework (de Pury and Farquhar, 1997).

The model simulates crop development throughout the growing season following a nonlinear temperature response (Yin et al., 1995), and adopts a leaf area model developed by Lizaso et al. (2003) to describe the expansion and senescence of individual leaves. MAIZSIM dynamically simulates leaf water potential and uses it to trigger water stress responses such as reduced growth rate and hastened senescence when values drop below designated thresholds (Yang et al., 2009b).

The model has been validated at different scales – including physiological aspects such as gas exchange (Yang et al., 2009a), leaf development and biomass gain (Kim et al., 2012), leaf growth water stress responses (Yang et al., 2009b), as well as field-level validations in AgMIP projects (Bassu et al., 2014; Kimball et al., 2019) and FACE site studies (Durand et al., 2018) that tested for yield responses to different temperature and CO_2 conditions. The model has also recently been used to test the independent impacts of temperature versus VPD on growth and yield in maize growing regions in the US (Hsiao et al., 2019).

3.3.2 Present-day climate data

We assembled hourly data of temperature, relative humidity, precipitation, and solar radiation over years 1961-2005 for our simulation sites as weather data input for our model simulations. Specifically, we accessed hourly air temperature (T_{air}), dew point temperature (T_{dew}), and precipitation data from the NOAA National Center for Environmental Information Integrated Surface Hourly database (`https://www.ncdc.noaa.gov/isd`), and hourly solar radiation data from the National Solar Radiation Data Base (`https://nsrdb.nrel.gov/data-sets/archives.html`).

We followed the Clausius-Clapeyron equation (Eqn. 3.1-3.2) to back out atmospheric humidity information in the form of relative humidity (RH) from T_{air} and T_{dew}:

$$E_s = E_{sref} \cdot e^{\frac{L_v}{R_v} \cdot (\frac{1}{T_{ref}} - \frac{1}{T_{air}})} \tag{3.1}$$

$$E = E_{sref} \cdot e^{\frac{L_v}{R_v} \cdot (\frac{1}{T_{ref}} - \frac{1}{T_{dew}})} \tag{3.2}$$

The equation uses the saturation vapor pressure (E_{sref}, 6.11 mb) at a reference temperature (T_{ref}, 273.15 K), the vaporization latent heat (L_v, $2.5 \cdot 10^6$ J kg^{-1}), and the gas constant (R_v,

461 J $K^{-1}kg^{-1}$) to calculate the saturated water vapor pressure (E_s, mb) and the actual water vapor pressure (E, mb) at air temperature (T_{air}, K). We then use E and E_s to calculate RH (%) (Eqn. 3.3):

$$RH = \frac{E}{E_s} \tag{3.3}$$

We selected overlapping sites and years that had data available from both the Integrated Surface Hourly Data Base and the National Solar Radiation Data Base over years 1961-2005 and filtered for site-years that had less than two consecutive hours of missing data throughout the growing season (broadly defined to be between February 1st – November 30th) and retained at least two-thirds of the weather data (Fig. B.1). We then gap-filled any missing data by linearly interpolating the missing information with weather data of the hours prior and post the missing data point. Next, we linked valid weather stations with maize planting area and irrigation level data accessed through the United States Department of Agriculture – National Agriculture Statistics Service (USDA-NASS, `https://www.nass.usda.gov/Data_and_Statistics/index.php`). Specifically, we calculated the average maize planting area across our simulation period (1961-2005) in the continental US and accessed average irrigation level (%) for the same sites through four available census years (1997, 2002, 2007, 2012) (Fig. B.2). We used the planting area and irrigation level averaged across five USDA-NASS sites closest to each weather station (via Euclidean distance) to represent their cropping information, and to exclude sites that either had less than 10,000 acres of corn planted or had greater than 25 % of crop land irrigated. We excluded sites with less than 15 years of data to insure sufficient sampling to assess inter-annual climate variability (Soltani and Hoogenboom, 2003; Van Wart et al., 2013). Following this method, we were able to compile 1160 site-years of meteorology data for our simulations, which included a total of 60 sites, each site with available weather data ranging from 15-27 years (Fig. 3.2).

3.3.3 Idealized projected climate

We assembled idealized projected climate information at two future time points, 2050 and 2100, to analyze crop performance shifts under future climate (Table 3.1). Specifically,

we created monthly temperature and relative humidity anomaly maps under a substantial but not extreme greenhouse gas emissions scenario (SSP3-7.0, Riahi et al., 2017) from the latest Coupled Model Intercomparison Project version 6 (CMIP6) outputs; we used these anomaly maps to calculate location-specific warming and associated changes in relative humidity levels throughout the growing season for each simulation site (Fig. 3.3). This method preserves correlations between climate variables (i.e., between temperature, relative humidity, and solar radiation) on short timescales and limits known biases in modeled variability (Vargas Zeppetello et al., 2019; Donat et al., 2017). Since both magnitude and pattern of future precipitation projections are highly uncertain, we applied a general trend of precipitation reduction in accordance to the SSP3-7.0 scenario, and increased atmospheric concentrations of CO_2 to 550 ppm and 850 ppm for years 2050 and 2100, respectively (O'Neill et al., 2016).

Table 3.1: Description of idealized climate treatments with projected changes in temperature (T), relative humidity (RH), precipitation (precip.), and projected CO_2 concentrations by years 2050 and 2100 under the SSP3-7.0 emission scenario.

Year	Climate Scenario
2050	+ 1.4 °C mean T, -RH, -15% precip, 550 ppm
2100	+ 3.1 °C mean T, -RH, -30% precip, 850 ppm

3.3.4 Soil data

We used soil information from USDA-NASS locations nearby our simulation sites to curate site-specific soil files for each location. Soil properties are highly heterogeneous, and since our simulation sites are based on weather station locations that do not directly come from agricultural land, we use this method to broadly represent soil makeup of agricultural sites within the region without skewing towards any particular site. We queried soil information from the National Resources of Conservation Services (NRCS) SSURGO soil database (Soil Survey Staff) to identify soil properties for each NASS location with maize planting area greater than 10000 acres and irrigation levels less than 25%. For each site, we accessed soil

information at five depth categories (surface, 50, 100, 150, and 200 cm), which included sand–silt–clay–organic matter composition, soil bulk density (the oven dry weight of less than 2 mm soil material per unit volume of soil at a water tension of 1/3 bar), and the volumetric content of soil water retained at a tension of 1/3 bar (33 kPa, field capacity) and 15 bar (1500 kPa, wilting point) expressed as a percentage of the whole soil. With the sand–silt–clay composition, we categorized the queried soil data into 12 texture groups following the USDA Textural Soil Classification (Staff, 1999) and excluded sites classified as Sandy or Clay due to their lack of representation in agricultural fields. Next, we determined the soil class within each depth category for all our simulation sites by assigning it the most prevalent soil class from it's 11 nearest NASS sites calculated through Euclidean distance, and assigned it the mean soil conditions of that texture-depth class averaged across all NASS sites within that category. Finally, we estimated soil hydraulic properties of each soil type through a water release curve predicted by the van Genuchten equation (van Genuchten, 1980).

3.3.5 Sampling within the trait and management space

We selected several key model parameters that represent a range of maize traits and management options to investigate combinations that lead to high performance under present and future climate conditions. Since we do not have robust observation-based data on the natural distribution and boundaries of most parameters, we assumed a uniform distribution and set biologically reasonable boundaries around literature-based default values (Table 3.2). We assumed all parameters to be non-correlated and used a Latin hypercube sampling method (McKay et al., 1979) to create 100 different trait-management (T $\times$ M) combinations within the parameter space.

3.3.6 Performance within the $G \times E \times M$ landscape

We defined high crop performance as crops that achieve high yield (i.e. yield mean across years) and high yield stability (i.e. yield dispersion across years). We developed a cost function (Eqn. C.3) to quantify the performance of any T $\times$ M combination by calculating

Table 3.2: MAIZSIM parameters tested for yield optimization

Processes	Params	Description	Default (Range)	Citation
Physiology	g_1	Ball-Berry g_s model slope	4 (2∼6)	Miner et al. (2017); Shekoofa et al. (2016)
	V_{cmax}	Max RUBISCO capacity	65 (65∼80)	Kim et al. (2006); Wu et al. (2019)
	J_{max}	Max electron transport rate	350 (350∼420)	Kim et al. (2006); Wu et al. (2019)
	phyf	Reference leaf water potential (MPa) used to describe stomata sensitivity to leaf water potential	-1.9 (-3∼-1)	Tuzet et al. (2003); Yang et al. (2009a); Shekoofa et al. (2016)
Phenology	SG	Duration that leaves maintain active function (stay-green) after reaching maturity	3 (2∼6)	Zhang et al. (2019); Gregersen et al. (2013); Timlin et al. (2019)
	gleaf	Total leaf number	19 (11∼25)	Parent et al. (2018); Padilla and Otegui (2005)
	LTAR	Max leaf tip appearance rate (leaves/day)	0.5 (0.4∼0.8)	Kim et al. (2012); Padilla and Otegui (2005)
Morphology	LM	Leaf length of the longest leaf (cm)	115 (80∼120)	
	LAF	Leaf angle factor	1.37 (0.9∼1.4)	Campbell (1986); Dzievit et al. (2019)
Management	gdd	Growing degree days accumulated by sowing	100 (80∼160)	Sacks and Kucharik (2011); Timlin et al. (2019)
	pop	Density (plants/m^2)	8 (6∼10)	Timlin et al. (2019); Stone et al. (2000)

its distance to a theoretical best-performing combination within the yield and yield stability space (Eqn. C.3):

$$D_{score} = \sqrt{w_{yield} * (y_{mean} - y_{max})^2 + w_{disp} * (y_{disp} - d_{min})^2} \tag{3.4}$$

y_{mean} and y_{disp} represent mean yield and yield dispersion (variance/mean) across years for the target T × M combination at a specific simulation site, respectively. We standardized yield and dispersion to values between 0 and 1 to avoid skewed contribution due to difference in scale. y_{max} and d_{min} denote the standardized maximum mean yield (1) and minimum yield dispersion (i.e., maximum yield stability, 0) achieved within all T × M combinations at a specific simulation site. w_{yield} and w_{disp} are empirical coefficients between 0 and 1 that assign weighted importance to yield mean and yield dispersion, respectively.

We used the calculated D_{score} to rank the top 20 performing T × M combinations for each simulation site. We determined an overall ranking for each T × M combination based on their rankings across all simulation sites (Fig. 4.1a). With this method, T × M combinations with high rankings across a few sites versus combinations with medium ranking across several sites can all result in overall high performance. T × M combinations that do not rank within the top 20 performers at any site will not receive a ranking.

3.3.7 Regional difference in performance

We used a climate space approach to identify how the performance of G × M combinations differed with baseline climate conditions. We used a k-means clustering algorithm to cluster our sites based on mean growing season temperature and VPD, and total growing season precipitation, roughly dividing our simulation sites into four groups of climate spaces - cool and medium precip, mild, warm and wet, and warm and mild to dry (Fig. 3.6). We analyzed the performance of G × M combinations within each cluster of sites by calculating a standardized performance score (Eqn. 3.5):

$$P_{score} = \frac{\sum_{i=1}^{n} R_i}{R_{max} * n} \tag{3.5}$$

R_i denotes the performance ranking of a G × M combination at site i among a total of

n sites within each climate space, and R_{max} indicates the maximum performance ranking a G $\times$ M combination can achieve at a single site. In our workflow, we only considered the top 20 performing G $\times$ M combinations when ranking high performing combinations (see section 3.3.6), so R_{max} equals 20. The resulting standardized performance score ranges between 0 and 1, in which a G $\times$ M combination that ranks with highest in performance across all locations within the climate space would receive a P_{score} of 1.

3.3.8 In-season model outputs

MAIZSIM generates outputs of a number of plant growth outputs throughout the growing season on an hourly time step. We describe in Table 3.3 a select few outputs in more detail. We summarized these high time frequency outputs across four phenological stages (emerged, tassel initiation, tasseled and silked, and grain-filling) to facilitate analysis and interpretation. Specifically, we queried net photosynthetic rate (A_{n}), net carbon gain (P_{n}), and stomatal conductance (g_{s}) values from daylight hours, and averaged them within the designated phenological stages. We represented ear biomass, total biomass, and total leaf area ($ear\_biomass$, $total\_biomass$, LA) within each developmental stage with maximum values within each stage. Finally, we queried water supply, demand, and deficit (ET_supply, ET_demand, $water\_deficit$) values at noon and averaged all values within each phenological stage, and represented predawn leaf water potential (Ψ) with values queried at 5 am, and averaged the all values within each phenological stage.

3.3.9 Experiment setup and model simulation

We prescribed the sampled planting density (Table 4.1, *pop*) for each ensemble member and adjusted the planting date for each ensemble member and simulation site based on climate and growing degree days (GDD) requirements. We calculated GDD for each simulation site through accumulated heat units starting from February 1st with a base temperature of 8°C (Kim et al., 2012) and determined the planting date once GDD surpassed the sampled for each ensemble member (Table 4.1, *gdd*). This led to earlier planting dates in warmer regions and vice versa (Fig. 3.7), and created diversity in cropping cycle start time among T $\times$

Table 3.3: Key MAIZSIM outputs

Output	Description	Unit
A_n	Net photosynthetic rate	µmol CO_2 m^{-2} sec^{-1}
P_n	Net carbon gain	g /plant hour
g_s	Stomatal conductance	g H_2O m^{-2} sec^{-1}
ear_biomass	Total ear biomass	g/plant
total_biomass	Total plant biomass	g/plant
LA	Total leaf area	cm^2
phenostage	Phenological stage	-
ET_supply	Evapotranspiration (ET) supply	g H_2O
ET_demand	Evapotranspiration demand	g H_2O
$water\_deficit$	ET demand - ET supply	g H_2O
Ψ	Leaf water potential	MPa

M combinations, mimicking early versus late-planting cultivars (Fig. 3.13). To simulate well-fertilized conditions, we prescribed a total of 200 kg ha^{-1} of nitrogen throughout the growing season, applying half as base fertilizer prior to planting and the rest top-dressed one month post planting.

For each simulation site, we ran the MAIZSIM model with default parameters that represented a generic crop cultivar across all locations (see default values in Table 4.1). Next, we carried out a site-level ensemble of simulations in which we used past meteorology data (see section 3.3.2) to each of the 100 trait-management parameter combinations (see section 4.3.3) for each of our 1160 site–years (see section 3.3.6) and identified top performing (high yield and yield stability) trait-management combinations. Finally, we repeated the site-specific trait and management ensemble of simulations with idealized future climate (see section 4.3.4) to understand how high performing trait and management combinations under current climate conditions fared under future climate.

3.3.10 Model validation

We validated simulated yields with default parameter values (control phenotype, see Table 4.1) with historic yield data from the United States Department of Agriculture – National Agriculture Statistics Service (USDA- NASS, `https://www.nass.usda.gov/Data_and_Statistics/index.php`). We compared yield data from observation sites closest to our simulation sites calculated through a Euclidean distance (Fig. 3.8). We scaled our whole-plant level simulation outputs to field level by applying a planting density of 10 plants per m^2 and compared our simulated yield with averaged yield observations in between years 2005-2012, since our default parameter and management options resemble modern-day plant traits, planting density, and planting dates.

3.4 Results and discussion

3.4.1 Model validation

In general, simulated yields showed less spatial difference compared to observations (Fig. 3.8). The model captured historic yield observations well in the higher latitude Corn Belt regions but overestimated yield in various warmer sites in southern locations (Fig. 3.9). Southern locations experience much warmer temperatures, especially during later parts of the growing season (Fig. B.3, grain-fill). While MAIZSIM dynamically describes temperature and water stress throughout the growing season through impacts on gas exchange and leaf developmental processes, the model lacks direct depiction of climate stress responses on reproduction processes such as flowering, pollination, and grain-filling, which are likely reasons for the yield over-estimation in warmer regions.

Cultivar differences between crops planted in southern versus northern locations could also contribute to these discrepancies. Farmers in warmer southern locations choose cultivars that are both planted and harvested earlier in the growing season, leading to an overall shorter crop cycle duration compared to those planted in the north (USDA-NASS, Crop Progress and Conditions). While our simulation set up captures earlier planting in warmer regions (Fig. 3.7), it does not capture potential differences in cultivar and management choices that growers in the south have likely been opting for in order to avoid late season

heat and water stress. Finally, we note that by applying a universal soil depth (200 cm), we may be overestimating soil water availability. This could disproportionately affect warmer locations in south, in which late-season water availability could partially alleviate water stress later in the growing season and contribute to yield overestimation in those locations (Fig. 3.9).

3.4.2 Performance difference across climate spaces

In Hsiao et al. (2022b, submitted), we followed the framework described in this paper and identified several top-performing strategies among all T × M combinations under present-day and future climate conditions, categorized based on different combinations of phenological (grain-filling start time and duration) and morphological (total leaf area) features. Top-performing strategies under present-day climate conditions included T × M combinations that either reached reproductive stage early (*Early Starting*), were slow in aging (*Slow Aging*), stress averting (*Stress Averting*), or had large canopies and were high in yielding (*High Yielding*). More details are described in Hsiao et al. (2022b) and briefly summarized below.

Early Starting, *Slow Aging*, and *Stress Averting* strategies all have a smaller canopy size and relatively earlier transition times from vegetative to reproductive stages, but differ in grain-filling duration. *Slow Aging* strategies have long grain-filling durations that prolong cropping duration, while *Stress Averting* strategies display the shortest longevity, allowing plants with this strategy to complete their cropping cycle early and avoid late season stressors such as dry and hot conditions. On the other hand, *High Yielding* strategies have larger canopy sizes accompanied by delayed transition from vegetative to reproductive stages. While all categorized as top-performing under present-day climate, these strategies showcase a range of trade-offs between yield and yield stability, with performance differing across simulation sites (Fig. 4.1, 3.10) and climate spaces (Fig. 3.11a).

Under current climate conditions, T × M combinations with *Slow Aging* strategies tend to be generalists, showing high performance across all climate spaces. On the other hand, strategies such as *Early Starting* fared best in cool and wet regions, while *High Yielding*

strategies perform best under warm and wet conditions (Fig. 3.11a). Under future climate conditions, we observed an overall yield loss for all T × M combinations in most simulation sites (Fig. 3.12), including strategies that improved in performance ranking with climate change (Fig. 3.12a), such as *High Yielding* and *Large Canopy* (Fig. 3.11c). In general, warmer regions with low precipitation levels exhibited the greatest yield sensitivity (% yield loss per degree C of warming, Fig. 3.12); high-performing strategies under future climate partially buffered, but did not prevent yield loss.

High-performing strategies under present-day climate conditions shifted with climate change (Fig. 3.11b, c). T × M combinations with early starting strategies experienced the greatest drop in performance ranking overall, showing declines in most climate spaces (Fig. 3.11c, *Early Starting*). Slow aging strategies still remained one of the higher performers by the end of the century (Fig. 3.11b, *Slow Aging*), but showed clear performance ranking declines in warm climate spaces (Fig. 3.11c, *Slow Aging*), allowing several other strategies to compete for top performance in those climate spaces (Fig. 3.11c); T × M combinations with high yielding and compensating strategies progressed further in performance ranking (Fig. 3.11c, *High Yielding*), and new high-performing strategies with larger canopies and delayed transition timings into reproductive stages emerged (Fig. 3.11c, *Large Canopy*, *Compensating*, *Middle Ground*).

3.4.3 Mechanisms for performance improvement

We analyzed detailed in-season outputs of various phenological, physiological, and morphological outputs of the model (Table 3.3) and describe here some general trends observed in top-performing T × M combinations.

Phenology

Climatological differences between simulation sites and parameter differences among T × M combinations both lead to the range of phenology output we see in our simulation outputs (Fig. 3.7, 3.13). Phenology differs across simulation sites due to imposed planting date adjustments based on growing degree day requirements, allowing for an earlier planting

date in warmer regions (Fig. 3.7). Climatological differences throughout the growing season further shape the difference, especially during the grain-filling stage in which simulation sites in the south become substantially warmer than those in the north (Fig. B.3), leading to hastened development (Fig. B.5). On the other hand, phenology differs among T × M combinations due to differences in perturbed traits linked to phenology (e.g. planting time, developmental rate, leaf number, Fig. 3.13). High performing T × M combinations under present-day climate conditions tend to show earlier starts in reproductive stages with a longer duration (Fig. 3.13). Higher ranking T × M combinations tend to show a greater fraction of grain-filling length over total growing season length (Fig. B.4b) despite no clear trends in total growing season length (Fig. B.4a).

Physiology

Net photosynthetic rates are generally higher in top-performing T × M combinations during transition from vegetative into reproductive stages (Fig. B.6), but the differences in photosynthetic rates become dominated by climatological differences between simulation sites during the final grain-filling stage, with greater photosynthetic rates in warmer southern regions (Fig. B.6). In general, we see a linear relationship between temperature and photosynthetic rate during vegetative stages (Fig. 3.14). This relationship eventually plateaus around 28-30 °C later in the growing season, and starts to decline in a few warmest site-years (Fig. 3.14b). While warmer temperatures generally led to higher photosynthetic rates, hastened development and greater water deficit under warmer conditions also led to overall shorter grain-filing durations (Fig. B.7, B.5a), compensating one another, dampening the overall difference between northern versus southern sites in terms of net carbon gained throughout grain-filling (Fig. B.8) and final yield (Fig. B.9).

Morphology

Differences in simulated total leaf area was largely dominated by parameter make up within T × M combinations, showing much less difference in simulated yield across sites (Fig. B.10). Simulated plants approached full canopy sizes around tassel initiation, and top-performing

combinations showed mid to lower total leaf area under present-day climate conditions. This was consistent with most top-performers under present-day climate exhibiting early transitions into reproductive stage (e.g., *Slow Aging*, *Early Starting*, *Stress Averting*). These strategies partly achieved early reproductive start through short vegetative stages through fewer total number of leaves and hence smaller canopy size (i.e., lower total leaf area).

3.5 Discussion

Crop production is expected to suffer under future climate conditions as the climate warms. Adaptation of crop management practices, location of planting, as well as adaptation of the crops themselves all have the potential to limit expected yield loss and help to sustain agricultural productivity. However, we lack a systematic understanding of which adaptations are likely to have the biggest impact and why, both critical pieces of knowledge for agricultural planning. Mechanistic, process-based crop simulation models can be a powerful tool to synthesize cropping information, set breeding targets, and develop adaptation strategies for sustaining food production, yet have been underutilized for developing specific climate-adaptation options.

Breeding for and adopting new cultivars involve exploring and navigating the hills and valleys of the G $\times$ E $\times$ M landscape, in which optimal plant traits and management options are identified within defined target environments (Messina et al., 2011; Cooper et al., 2016). Requirements from breeding, delivering, and adopting a desirable cultivar depends on many factors, and the whole process can take from years to decades (Challinor et al., 2017). Recent developments in breeding practices have greatly expanded the efficiency in genotyping and phenotyping methods (Voss-Fels et al., 2019), yet the breeding pipeline is still time and resource intensive, limiting its ability to explore the full range of G $\times$ E $\times$ M combinations and interactions.

A typical breeding cycle starts out by exposing a large germplasm pool under extremely high selection pressure, filtering genotypes from the order of 10^6 individuals down to a few dozen promising candidates (Messina et al., 2020a; Cooper et al., 2014b). In the early stages of a breeding program, trait selection is often limited to those that can easily be identified through automated processes, and commonly based on plants in early developmental stages.

It is not until later in the breeding cycle that selection criteria shift from genotype to phenotype-based, and promising hybrids are evaluated on-farm at various locations with a range of background climate conditions (Gaffney et al., 2015). Management optimization also occurs around this time, in which field trials are set up to identify the best management practices for the final candidates prior to commercial release. Further, common breeding methods that either select for higher yield or eliminate defect traits do not allow for a clear understanding of the mechanisms in which favorable traits contribute to greater performance and yield, and effective combinations of plant traits, if not actively sought for based on a mechanistic understanding of crop growth and yield, could only occur by chance (Donald, 1968).

There is growing recognition that mechanistic crop simulation models can be a powerful tool to synthesize cropping information, set breeding targets, and develop adaptation strategies for sustaining food production. Such applications can complement current breeding efforts of developing new climate-resilient cultivars by facilitating broad exploration of the G $\times$ E $\times$ M landscape within a modeled setting as a first step (Muller and Martre, 2019; Rötter et al., 2015; Cooper et al., 2020; Messina et al., 2020b). The process-based nature of such models allow for mechanistic insight through which these adaptations influence yield and their sensitivity to different climate factors, providing a more complete assessment of the uncertainty associated with different possible climate conditions, including those that do not currently exist yet.

Ramirez-Villegas et al. (2015) provided a few successful examples of model-aided breeding projects, such as the New Plant Type program developed by IRRI for rice crops, in which process-based models were used to help make informed decisions to target breeding directions and resulted in new plant types that out-yielded conventional cultivars within two breeding cycles (Peng et al., 2008). This success further inspired the super rice program in China that led to newly developed rice varieties with 15-25% higher yield than common hybrid cultivars planted in other regions in China (Peng et al., 2008). While model-aided breeding practices are less commonly targeted towards a changing climate (Ramirez-Villegas et al., 2015), demonstrated success under current climate suggest it as a promising pathway to guide breeding direction for climate adaptation moving forward, and expanded experi-

ments evaluating a range of G × E × M conditions can enable production system responses to changing environmental conditions (Messina et al., 2020, Wang et al., 2019).

Regardless, thorough evaluation and application of crop models for developing specific climate-adaptation options (e.g., designing adaptive phenotypes for specific soil-climate combinations) for US agriculture remains scarce. We bridge this gap by constructing an integrated data-model framework set up to explore crop performance across a defined G × E × M landscape. With this framework, we identified high-performing plant trait and management combinations (G × M) best suited for current climate conditions, as well as targets and priorities to adapt to impending climate stressors (E). Heterogeneity in performance exists within the sampled climate space, which stemmed from underlying physiological, morphological, and phenological processes within the simulated crop. Model outputs on hourly time steps allowed us to compile detailed in-season outputs of various plant processes and summarize them according to associated phenological stages. This form of model output allows for more in-depth analysis that go beyond final yield and yield volatility, and investigation of mechanisms that contribute to high crop performance and the differences across climate spaces and under future climate projections.

We demonstrate how such a framework can be used to identify adaptation options with an emphasis on climate-resilient plant traits and effective management that will mitigate yield loss and optimize productivity both across space and through time in US corn growing regions under future climate conditions. Our modeling results demonstrate that application of mechanistic modeling holds substantial promise to inform breeding within the US maize production system.

3.6 Acknowledgements

We thank Lucas Vargas Zeppetello for providing CMIP6 temperature and relative humidity projection scaling patterns. JH acknowledges support from the AFRI NIFA Fellowships Grant Program: Predoctoral Fellowships [grant no. 2020-67034-31736] from the USDA National Institute of Food and Agriculture. ALSS acknowledges support from NSF AGS-1553715.

3.7 Figures and tables

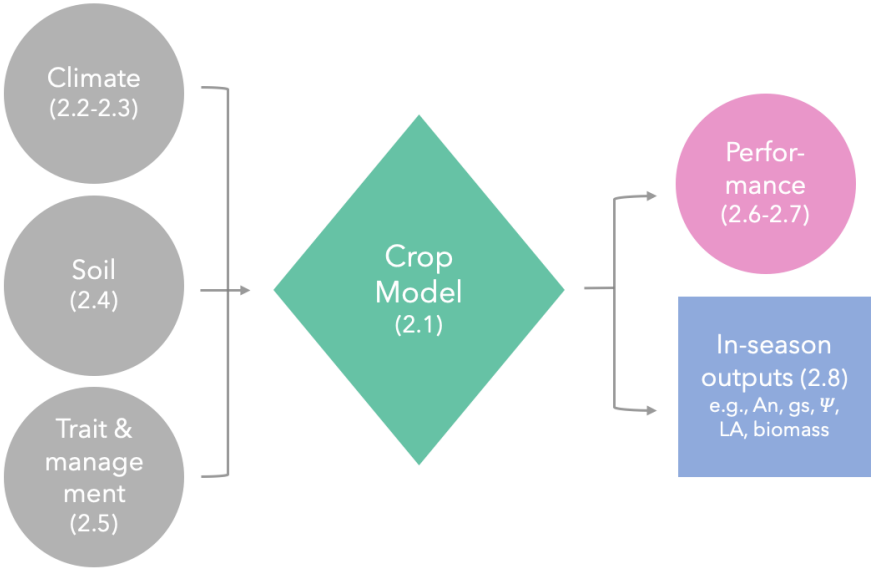

Figure 3.1: Diagram of the data-model framework.

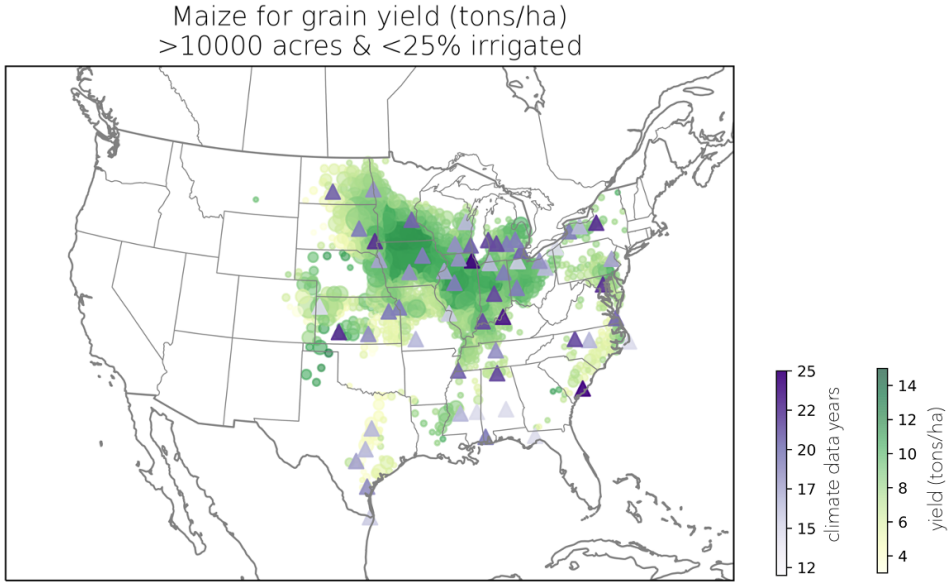

Figure 3.2: Simulation sites and number of years simulated (purple triangles), along with historic maize yield and planting area data (green circles). Colors indicate yield and circle size indicate planting area.

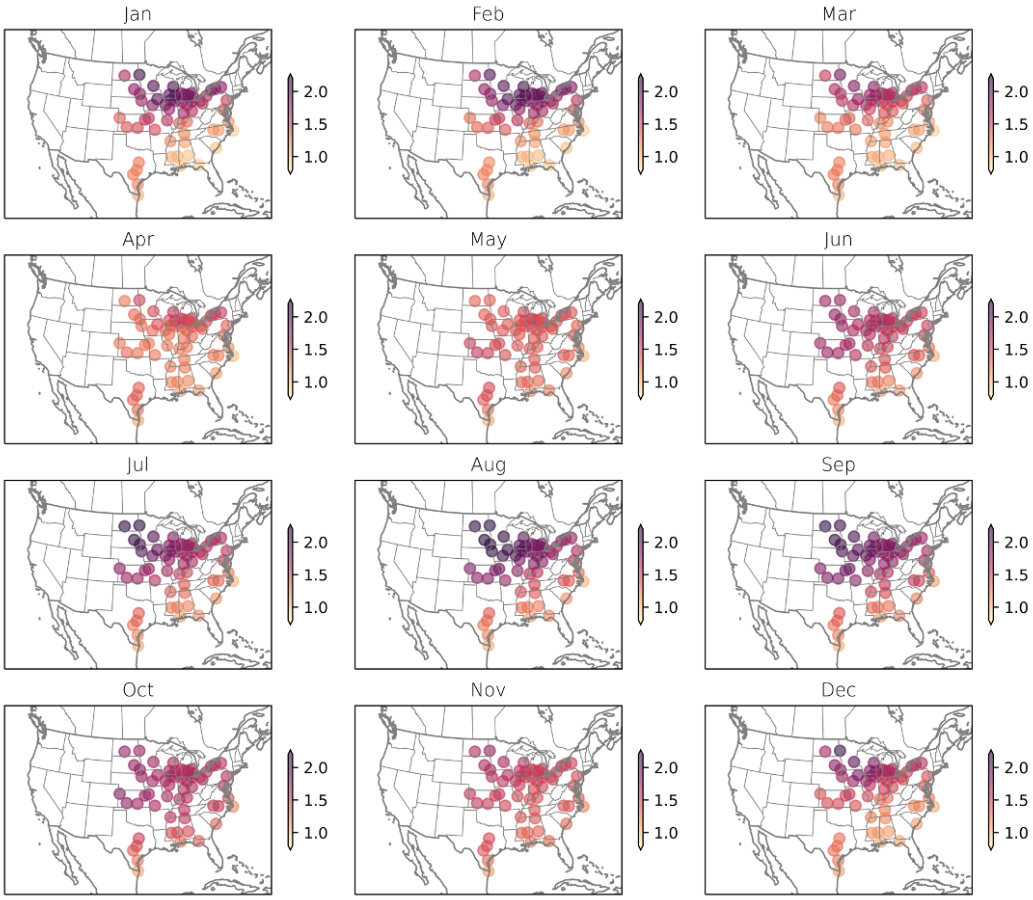

Figure 3.3: Monthly pattern of warming derived from CMIP6 multimodel means for our simulation sites. Numbers in color bar indicate temperature scaling values to multiply with global average climate sensitivity to calculate projected warming for each simulation site. For example, under our assumption of 3.1°C global average warming by 2100, a scaling value of 2 for a specific simulation site will equal a total warming of 6.2°C for that location.

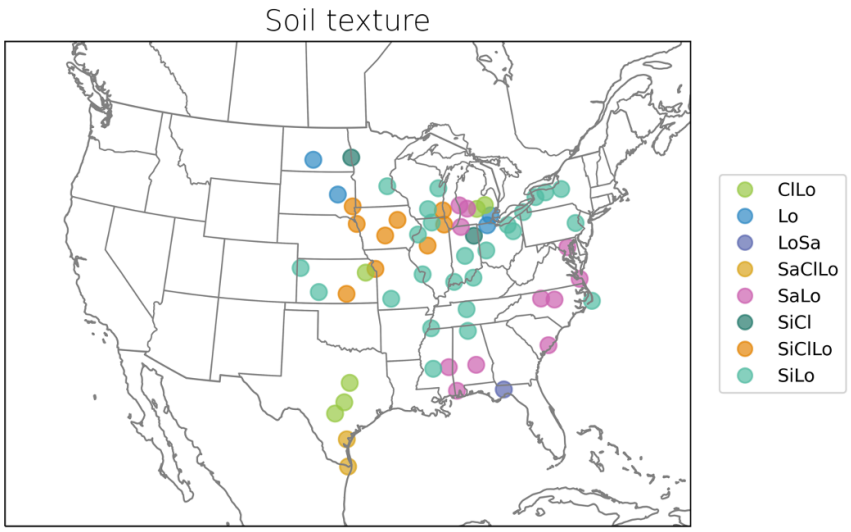

Figure 3.4: Soil texture across simulation sites. Soil texture categories include clay loam (ClLo), loam (Lo), loamy sand (LoSa), sandy clay loam (SaLoLo), sandy loam (SaLo), silty clay (SiCl), silty clay loam (SiClLo), and silty loam (SiLo).

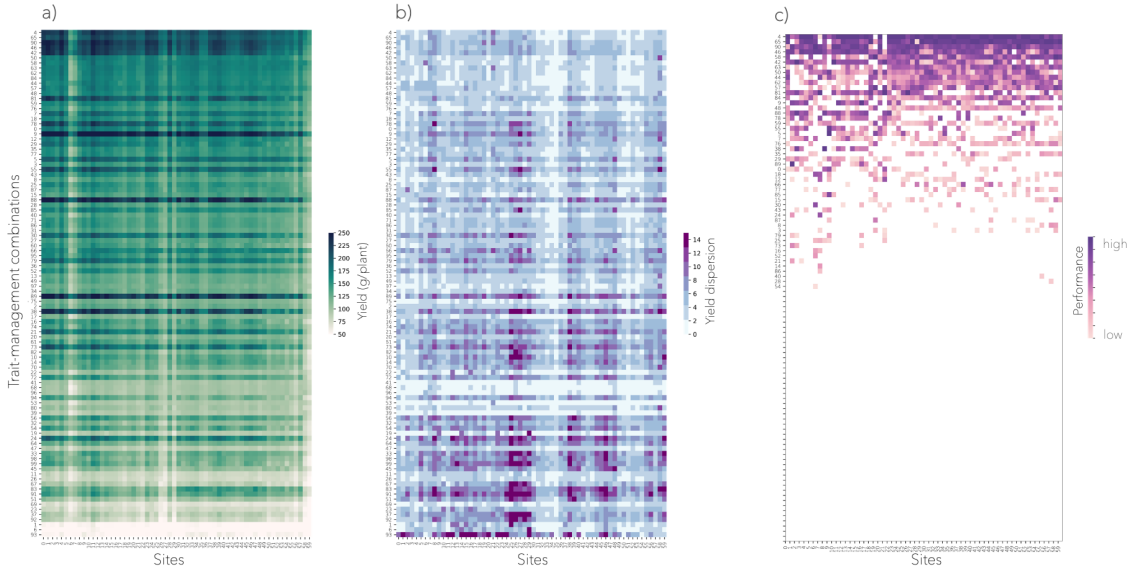

Figure 3.5: Simulated a) yield, b) yield dispersion, and c) performance ranking of across T × M combinations and locations. T × M combinations are ordered from top to bottom starting from the highest performance ranking. Sites are order from left to right from sites located in the south to the north.

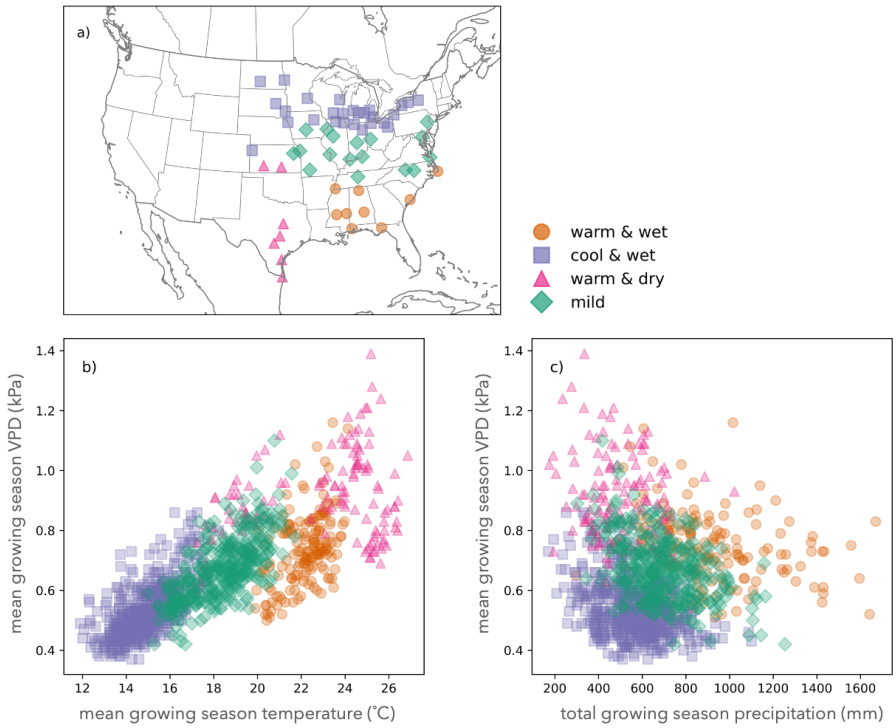

Figure 3.6: a) Map of simulation sites clustered based on mean growing season temperature (°C), mean growing season VPD (kPa), and total growing season precipitation (mm). Mean growing season temperature (°C), mean growing season VPD (kPa), and total growing season precipitation (mm) levels for all simulated site-years (b, c).

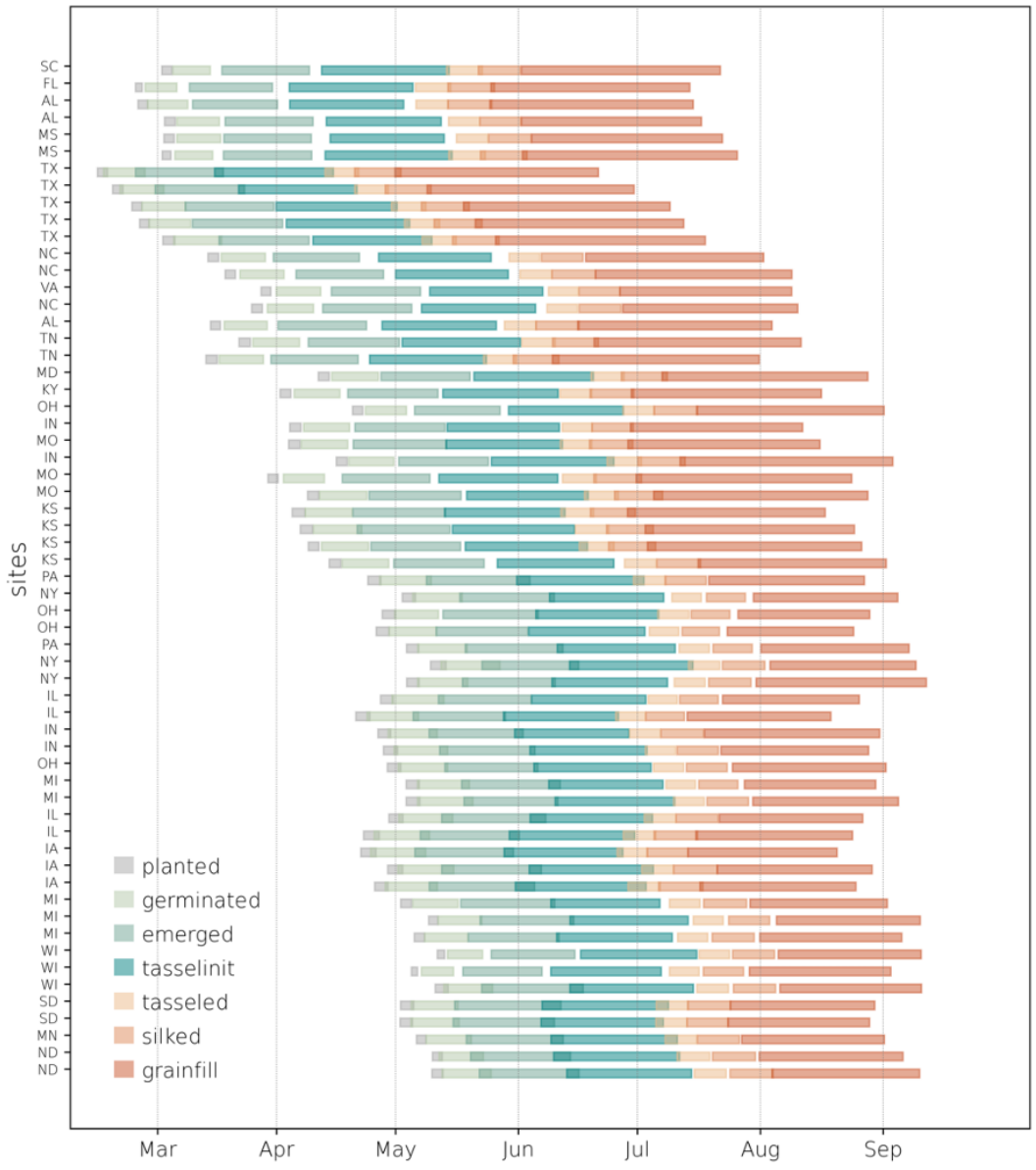

Figure 3.7: Start time and duration of each phenological stage across simulation sites, indicated by state abbreviations. Sites are roughly ranked by latitude, starting from southernmost sites towards the top.

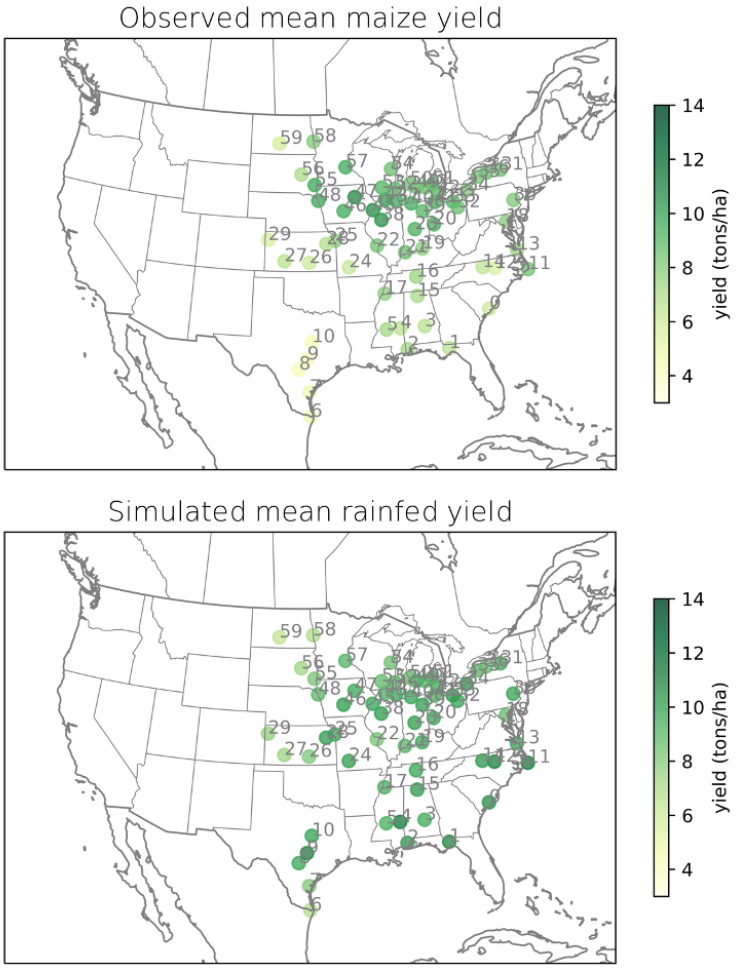

Figure 3.8: Observed (top) and simulated (bottom) yield (tons/ha) across simulated sites. Numbers indicate site numbers that correspond in Fig. 3.9.

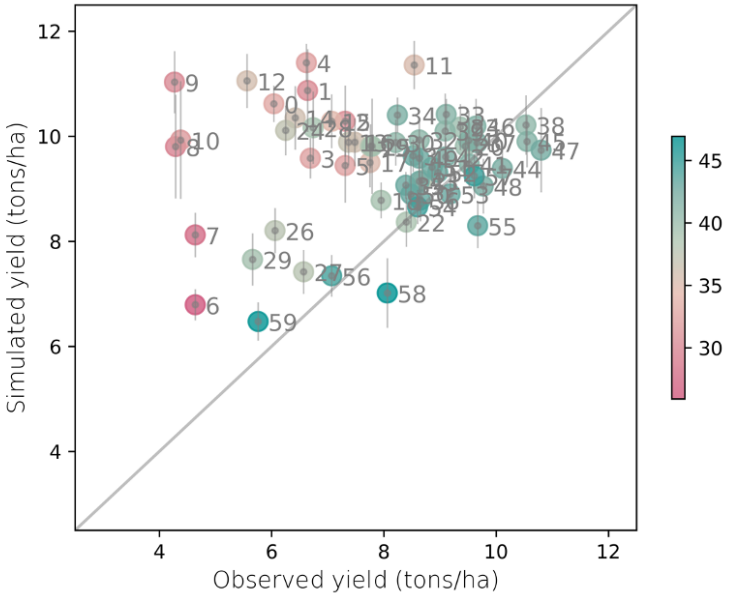

Figure 3.9: Observed versus simulated yield (tons/ha) across simulated sites. Colors indicate latitude of simulation site. Numbers correspond to site numbers shown in Fig. 3.8.

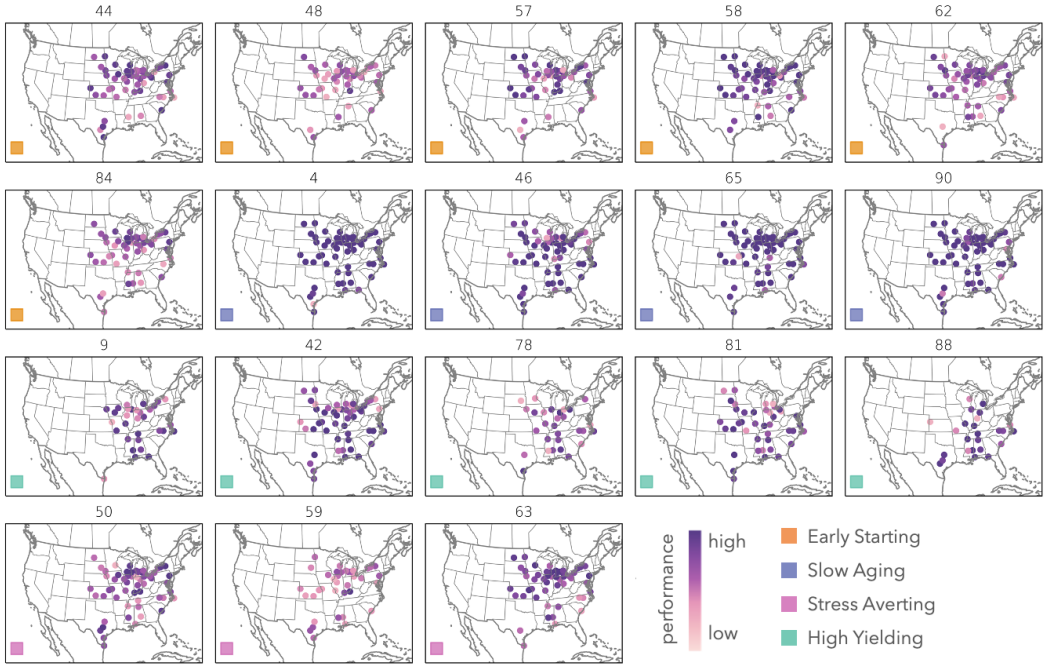

Figure 3.10: Performance ranking across simulation sites for T × M combinations of different top-performing strategies under present-day climate conditions.

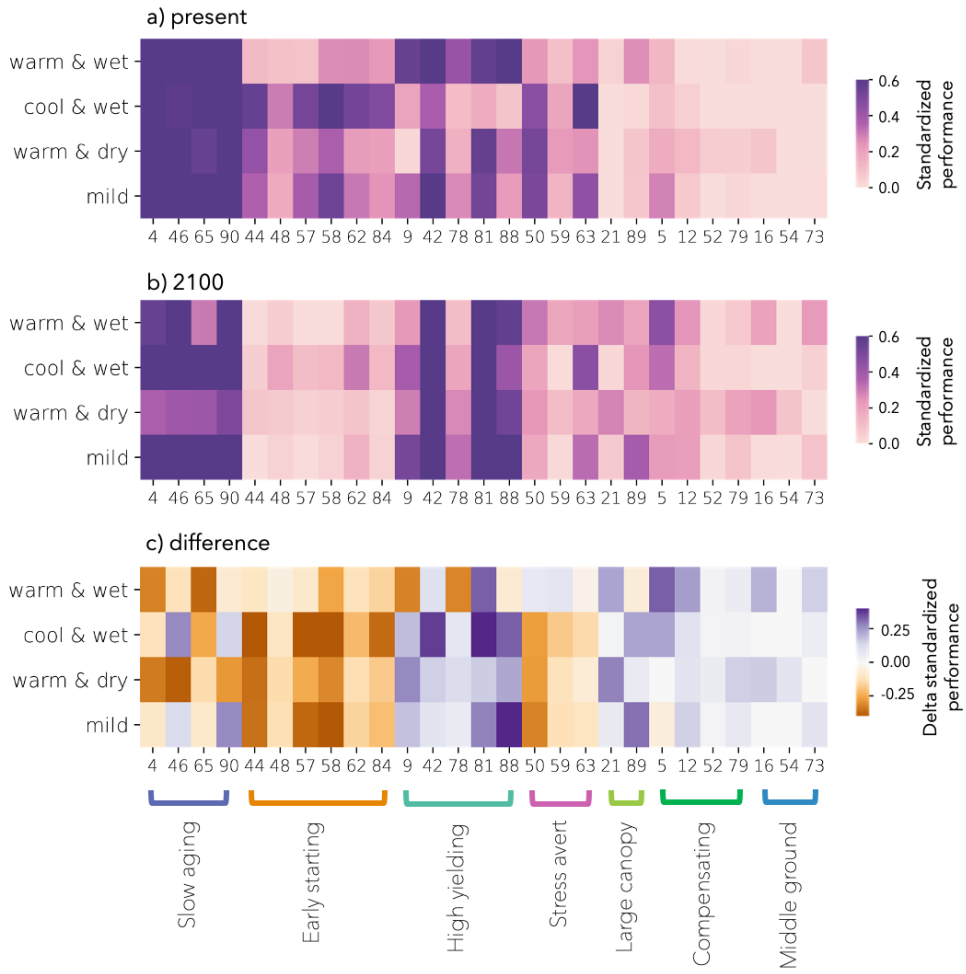

Figure 3.11: Standardized performance rankings of different strategies across climate spaces (see section 3.3.7) under a) current, b) future climate conditions, and c) the difference between the two.

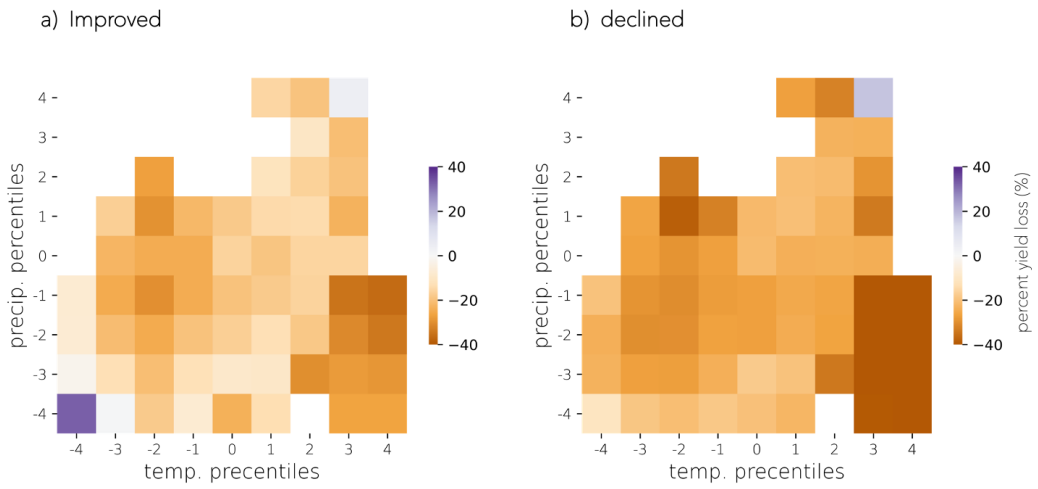

Figure 3.12: Percent yield loss within mean growing season temperature-precipitation climate space among T × M combinations that a) improved versus, b) declined in performance ranking under future climate conditions.

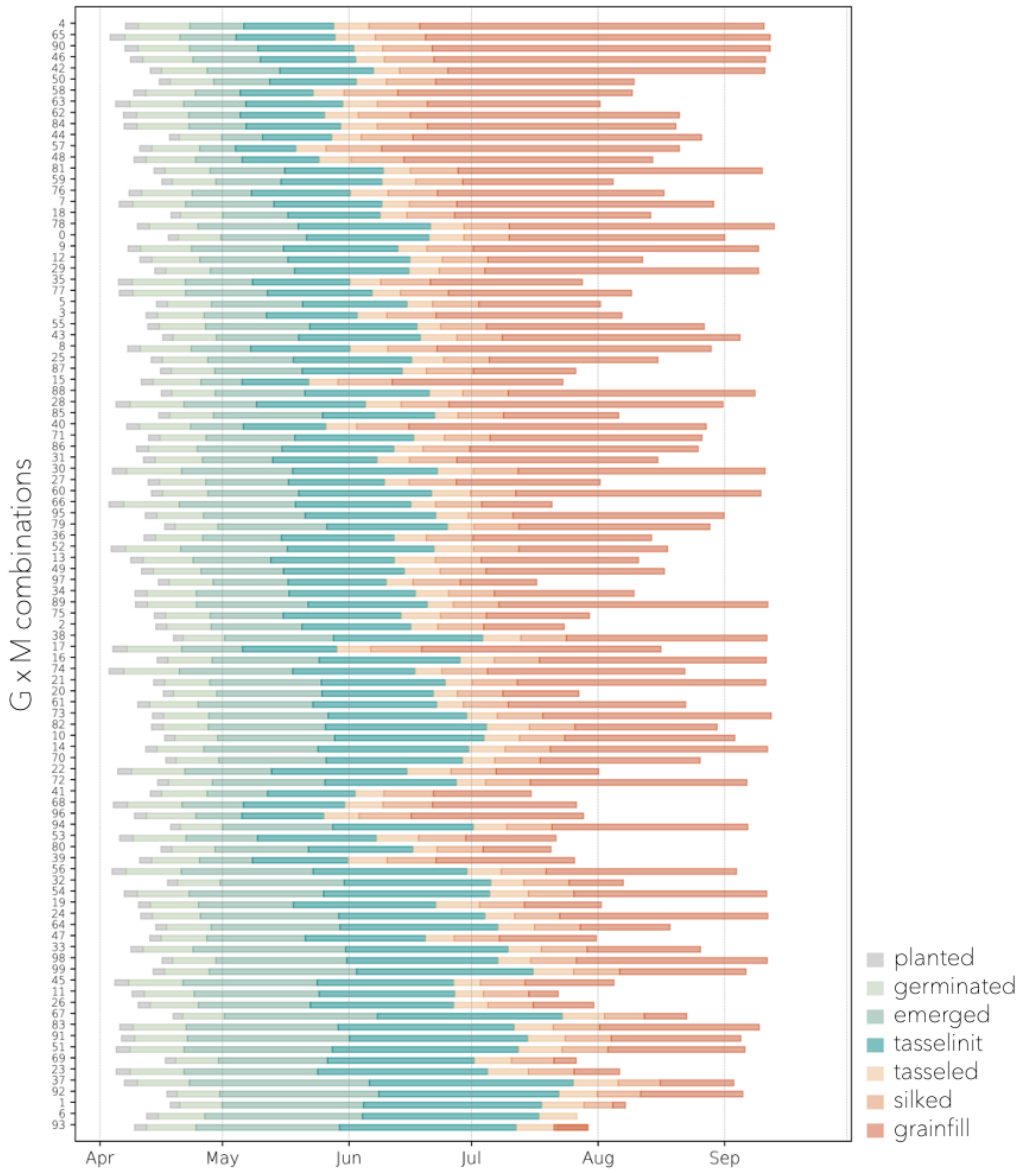

Figure 3.13: Start time and duration of each phenological stage across T × M combinations, averaged across all simulation sites, ranked by overall performance, with the highest performers listed towards the top.

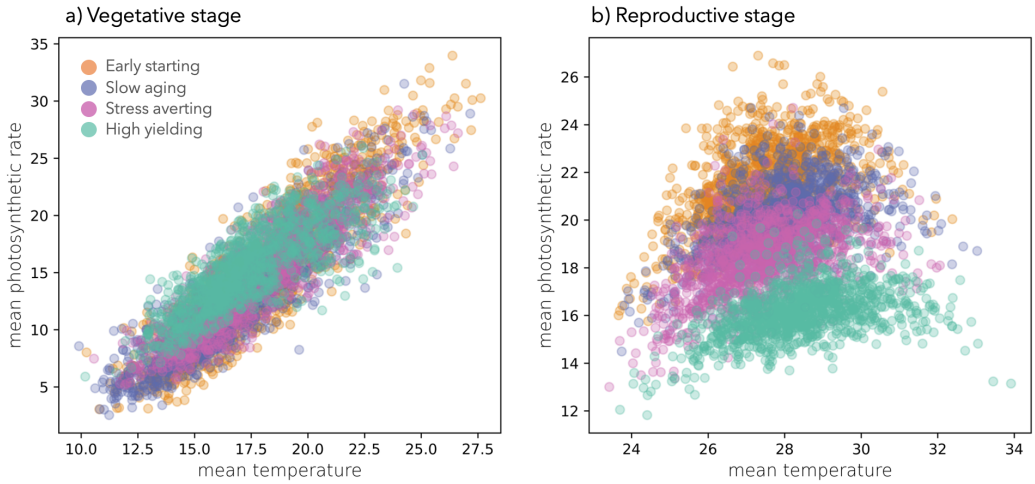

Figure 3.14: Relationship between mean temperature (°C) and mean photosynthetic rate (µmol CO_2 m^{-2} sec^{-1}) for all simulated site-years during a) vegetative versus b) reproductive stages for four representative T × M combinations within top-performing strategies.

Chapter 4

MODEL-AIDED CLIMATE ADAPTATION FOR FUTURE MAIZE IN THE U.S.

Jennifer Hsiao[1], Soo-Hyung Kim[3], Dennis J. Timlin[4], Nathaniel D. Mueller[5], and Abigail L.S. Swann[2,1]

[1]Department of Biology, University of Washington, Seattle, WA; [2]Department of Atmospheric Sciences, University of Washington, WA; [3]School of Environmental and Forest Sciences, College of the Environment, University of Washington, Seattle, Washington; [4]USDA ARS Adaptive Cropping Systems Laboratory, Beltsville, MD, United States; [5]Colorado State University, Department of Soil and Crop Sciences, Fort Collins, CO, United States ;

Citation: Hsiao, J., Swann, A. L. S., Kim, S.-H., Timlin, D. J., Mueller, D. (2022). Model-aided climate adaptation for future maize in the U.S. (submitted)

Supporting Information referenced in this chapter can be found in Appendix C.

4.1 Abstract

Over the next three decades rising population and changing dietary preferences are expected to increase food demand by 25–75%. At the same time climate is also changing — with potentially drastic impacts on food production. Breeding for new crop characteristics and adjusting management practices are critical avenues to mitigate yield loss and sustain yield stability under a changing climate. In this study, we use a mechanistic crop model (MAIZSIM) to identify high-performing trait and management combinations that maximize yield and yield stability for different agro-climate regions in the US under present and future climate conditions. We show that morphological traits such as total leaf area and phenological traits such as grain-filling start time and duration are key properties that impact

yield and yield stability; different combinations of these properties can lead to multiple high-performing strategies under present-day climate conditions, and a balanced compromise between yield and yield stability is critical to achieving high performance. We also demonstrate that high performance under present-day climate does not guarantee high performance under future climate. Weakened trade-offs between canopy size and reproductive start time under a warmer future climate led to shifts in high-performing strategies, allowing strategies with higher total leaf area and later grain-filling start time to better buffer yield loss and out-compete strategies with a smaller stature and earlier reproduction. These results demonstrate that focused effort is needed to breed plant varieties to buffer yield loss under future climate conditions as these varieties may not currently exist, and showcase how information from process-based models can complement breeding efforts and targeted management to increase agriculture resilience.

4.2 Introduction

Over the next decades, population is expected to rise, with a 24% increase by 2050, requiring 25-75% more food due to changing diets (Tilman et al., 2011; Hunter et al., 2017). Coincident with this increase in population, climate is also changing, with potentially drastic impacts on food production. A large body of previous work has projected decreases in crop yield under this changing climate — mainly due to increasing temperatures accompanied by higher vapor pressure deficit (VPD) and water stress (Lobell et al., 2013; Hsiao et al., 2019; Rigden et al., 2020). Climate adaptation through breeding for new crops and adjustments in management practices are critical avenues to sustain yield levels or partially mitigate yield loss (Challinor et al., 2014), leading to critical questions such as what crop traits and management are likely to be favorable and effective for adaptation at any point in time and space, the mechanisms through which they can mitigate yield loss, and the relative effectiveness of different approaches.

Maize yield in the US has experienced a steady rise since the 1930s (Duvick, 2005). Persistent breeding exercises were estimated to account for up to 60% of the total on-farm yield gain in the past several decades (Duvick, 2005; Fischer et al., 2014). These gains through genetic improvements (G) are further complemented by their interactions with

different environmental conditions (E), along with changes in management practices (M) such as earlier planting dates for a longer growing season, higher planting densities (Sacks and Kucharik, 2011; Duvick, 2005; Duvick and Cassman, 1999), as demonstrated in the G $\times$ E $\times$ M paradigm (Hatfield and Walthall, 2015). Continued development of new cultivars and adjustments in management practices better-suited for future climate is critical for sustaining current yield trends or to prevent yield loss (Ceccarelli, 2010; Challinor et al., 2017; Burke et al., 2009).

Plant breeders and agronomists have long leveraged conceptual models to identify and actively seek out breeding and management targets that contribute to productivity and yield. The concept of "ideotypes" (Donald, 1968) or "new plant types" (Jennings, 1964) date back to the 1960s, in which breeders would actively seek out or select for desirable traits to create cultivars of greater yield and/or quality, aiming towards constructs of idealized plants that were developed through physiological and morphological understandings of crops. This breeding method diverged from traditional approaches such as defect elimination or simply selecting for yield, providing an alternative method and way of thinking towards breeding. The genetic-centric concept of ideotype breeding has since been expanded to incorporate a modeling perspective, in which ideal combinations of traits (often represented through model parameters) are identified through simulation experiments (Martre et al., 2015; Andrivon et al., 2012). Many whole-plant level crop simulation models do not include specific genetic-level processes, and use physiological, morphological, and phenological traits as proxies to describe the underlying genotype. For this reason, we use the term trait (T) $\times$ E $\times$ M here instead to describe a concept similar to the G $\times$ E $\times$ M landscape.

Advances in mechanistic crop models in combination with available climate data and climate projections provide a unique opportunity to explore the vast T $\times$ E $\times$ M space. These tools can serve as a platform to apply and test the expanded modeling perspective of "ideotype breeding", allowing for better understanding of strategies and trade-offs within this landscape, and shed light on potential avenues for adaptation under different environments and with a changing climate (Peng et al., 2020). Previous studies have described such approaches with terminologies such as model-assisted ideotype design (Rötter et al., 2015; Martre et al., 2015; Semenov et al., 2014), predictive breeding (Washburn et al., 2020), and

yield-trait performance landscapes (Messina et al., 2011), to name a few. These concepts have been revisited and expanded over the years, facilitated by further understanding of plant processes and improved computing capacity (Hammer et al., 2006; Martre et al., 2015; Muller and Martre, 2019; Boote et al., 2021). Studies that use models to explore the hills and valleys within the T × E × M demonstrate how multiple pathways could lead to high performance; what is considered "ideal" may differ between locations and climate (Hammer et al., 2006; Messina et al., 2011), and under a changing climate (Semenov et al., 2014; Hammer et al., 2020).

In this work, we aim to identify broad climate adaptation strategies for maize in the US that can be achieved through breeding for new traits and adjusting management practices. Through a process-based crop simulation model (MAIZSIM), we *1)* set up ensembles of simulations to systematically explore a region within the T × E × M landscape, *2)* identify features that lead to high crop performance within the landscape that addresses both yield and yield stability, and *3)* quantify how these high-performing features shift under a changing climate.

4.3 Material and methods

Below we discuss our methods. Further detail on the framework and our methodological choices can be found in Hsiao et al. (2022a, preprint).

4.3.1 Crop simulation model

We used a process-based crop simulation model, MAIZSIM, to carry out our simulations across site-years in US maize growing regions. MAIZSIM represents key physiological and physical processes such as gas exchange, canopy radiative transfer, carbon partitioning, water relations, nitrogen dynamics, and phenological development (Kim et al., 2012). The soil model that interfaces with MAIZSIM (2DSOIL) links the crop model to a 2-dimensional finite element model that simulates a dynamic soil water and nutrient vertical profile (Timlin et al., 1996). MAIZSIM is driven by daily or hourly meteorological information (temperature, relative humidity, solar radiation, and CO_2 concentrations) throughout the growing season and uses this information to represent key plant physiological responses, such as

coupled stomatal and photosynthetic responses (Yang et al., 2009a), leaf development and elongation (Kim et al., 2012), and carbon partitioning and allocation (Kim et al., 2012). The model calculates soil water availability to the roots through simulating water potential and tracks how much leaf area is present at any point in time throughout the growing season (Yang et al., 2009b). All this information is integrated over the growing season to represent the final yield, and the model has been validated through comparison against observations for various maize growing regions in the US and across the globe (Yang et al., 2009a; Kim et al., 2012; Yang et al., 2009b; Bassu et al., 2014; Durand et al., 2018; Kimball et al., 2019; Hsiao et al., 2019).

4.3.2 Simulation sites and weather data

We assembled hourly inputs of temperature, relative humidity, solar radiation, and precipitation throughout the growing season (roughly defined between February 1st – November 30th) as meteorological drivers for our simulations. First, we used data from the United States Department of Agriculture – National Agriculture Statistics Service (USDA- NASS, `https://www.nass.usda.gov/Data_and_Statistics/index.php`) to select rain-fed (less than 25% irrigation) maize cultivation sites with greater than 10,000 acres of maize planted. Next, we identified weather stations near these maize cultivation sites with available hourly data from both the Integrated Surface Hourly Data Base and the National Solar Radiation Data Base over years 1961-2005. We excluded site-years with less than two consecutive hours of missing data and gap-filled any remaining missing data by linearly interpolating the meteorological information from data points prior and post the missing data. Finally, we excluded sites with less than 15 years of data to insure sufficient sampling to assess inter-annual climate variability (Soltani and Hoogenboom, 2003; Van Wart et al., 2013). With this method, we compiled 1160 site-years of meteorological data spanning a total of 60 sites, each site with available weather data ranging from 15-27 years. See Fig. C.1 for the final simulation sites.

4.3.3 Parameter selection and sensitivity analysis

We selected several key model parameters that represent physiological, phenological, and morphological aspects of maize plant traits, as well as management practices known to affect growth and yield (Table 4.1). The traits selected here are not meant to be exhaustive, but rather to cover a range of processes within the model. We set biologically reasonable ranges for our selected parameters that are based in literature when possible (Table 4.1 – perturbation range) and assigned a uniform parameter distribution within these boundaries since we do not have robust observation-supported knowledge on distributions for most of these parameters. We assumed all parameters to be non-correlated and sampled within the boundaries following a Latin hypercube sampling method to create ensemble simulations of 100 different parameter combinations (McKay et al., 1979), which we refer to as trait $\times$ management (T $\times$ M) combinations throughout the study.

Our parameter perturbations led to a range of emergent properties, including leaf-level properties such as photosynthetic rate and stomatal conductance, whole-plant properties such as total leaf area, water usage properties such as water deficit, and phenological properties such as plant emergent time, grain-filling start time, and grain-filling duration (Table 4.2). We used a sensitivity analysis framework to identify emergent properties critical for high performance by calculating the partial correlation coefficient between emergent properties and yield and yield stability, respectively (see supplement section C.1).

4.3.4 Idealized climate treatment

To investigate how top performing T $\times$ M combinations differ under future climate, we assembled monthly maps of expected anomalies in temperature and relative humidity, as well as uniformly reducing precipitation levels and increasing CO_2 by the end of the century, and applied these changes directly to our observed meteorology data. By applying these changes in climate to our meteorological dataset rather than using modeled output directly, we can preserve short timescale correlations between variables (i.e. between solar radiation, temperature and humidity) and limit known biases in modeled variability (Vargas Zeppetello et al., 2019; Donat et al., 2017).

Table 4.1: MAIZSIM parameters tested for yield optimization

Processes	Params	Description	Default (Range)	Citation
Physiology	g_1	Ball-Berry g_s model slope	4 (2∼6)	Miner et al. (2017); Shekoofa et al. (2016)
	V_{cmax}	Max RUBISCO capacity	65 (65∼80)	Kim et al. (2006); Wu et al. (2019)
	J_{max}	Max electron transport rate	350 (350∼420)	Kim et al. (2006); Wu et al. (2019)
	phyf	Reference leaf water potential (MPa) used to describe stomata sensitivity to leaf water potential	-1.9 (-3∼-1)	Tuzet et al. (2003); Yang et al. (2009a); Shekoofa et al. (2016)
Phenology	sg	Duration that leaves maintain active function (stay-green) after reaching maturity	3 (2∼6)	Zhang et al. (2019); Gregersen et al. (2013); Timlin et al. (2019)
	leaf	Total leaf number	19 (11∼25)	Parent et al. (2018); Padilla and Otegui (2005)
	ltar	Max leaf tip appearance rate (leaves/day)	0.5 (0.4∼0.8)	Kim et al. (2012); Padilla and Otegui (2005)
Morphology	len	Length of the longest leaf (cm)	115 (80∼120)	
	laf	Leaf angle factor	1.37 (0.9∼1.4)	Campbell (1986); Dzievit et al. (2019)
Management	gdd	Growing degree days accumulated by sowing	100 (80∼160)	Sacks and Kucharik (2011); Timlin et al. (2019)
	pop	Density (plants/m^2)	8 (6∼10)	Timlin et al. (2019); Stone et al. (2000)

Table 4.2: Description of emergent properties

Output	Description	Unit
Photosynthesis	Average net photosynthetic rate during the grain-filling period	µmol CO_2 m^{-2} sec^{-1}
Stomatal conductance	Mean stomatal conductance during the grain-filling period	g H_2O m^{-2} sec^{-1}
Leaf area	Maximum leaf area throughout growing season	cm^2
Water deficit	Evaporative demand - Evaporative supply during the grain-filing period	g H_2O
Emergence time	Timing of emergence of the first leaf	day of year
Grain-filling start time	Timing of the start of the grain-filling phenological stage	day of year
Grain-filling duration	Total length of the grain-filling period	days

We used simulation outputs from the Coupled Model Intercomparison Project version 6 (CMIP6) to create these anomaly maps. Specifically, we used the monthly multimodel mean of the spatial pattern scaled by the average magnitude of change expected for temperature and relative humidity from a scenario of future human activities which includes substantial but not extreme emissions of greenhouse gasses (SSP3-7.0, Riahi et al., 2017), which project global mean warming of 3.1°C for year 2100 under atmospheric CO_2 concentration of roughly 850 ppm. Since both magnitude and pattern of future precipitation projections are highly uncertain, we applied a general 30% trend of precipitation decline in accordance to the SSP3-7.0 scenario.

4.3.5 Experiment setup and model simulation

We carried out a site-level ensemble simulation in which we used past meteorology data (see section 4.3.2) to run an ensemble model simulation of 100 trait-management parameter

combinations for each of our 1160 site–years and identified top performing (high yield and high yield stability) trait-management combinations. Finally, we repeated the site-specific trait and management ensemble simulations with idealized future climate (see section 4.3.4) to understand how high performing trait and management combinations under current climate conditions fared under future climate (for additional detail see supplement section C.2).

4.3.6 Determine performance of G × M combinations

We developed a cost function (see supplement section C.3) to identify top-performing T × M combinations for each simulation site that show high yield (i.e. yield mean across years within a simulation site) and high yield stability (i.e. low yield dispersion across years within a simulation site); the former provides information on high performing genetic and management combinations that mitigate climate risk by generally performing well on an average year, while the latter identifies combinations that contribute to more stable yield given natural climate variability. We ranked the top 20 performing T × M combinations for all simulation sites (Fig 4.1a) and determined overall performance for each T × M combination by their performance across all simulation sites. Combinations with high rankings across few sites versus combinations with medium rankings across many sites could all result in overall high performance, while combinations that do not rank within the top 20 performers at any site will not receive a ranking (open circles in Fig 4.1b). We used this ranking system to understand trait and management combinations that lead to high performance under current versus future climate conditions. Further analysis on spatial difference of performance across simulation sites can be found in Hsiao et al. (2022a, preprint).

4.3.7 Identify top-performing strategies

In order to identify strategies for high performance under present and future climate conditions, we clustered all T × M combinations that ranked within top 20 at least at one simulation site (Fig. 4.1a) based on high impact emergent properties (i.e. grain-filling start time, grain-filling duration, total leaf area, Fig. 4.2a) through K-means clustering. We

selected cluster groups with at least 50 % of T × M combinations that ranked within the top-20 performers (Fig. 4.2b, T × M combinations in large gray circles) and averaged their emergent properties to describe a summarized strategy for high performance within that cluster group. However, not all high-performing T × M combinations were well-captured through the clustering method, so we handpicked a few additional combinations and described their strategies manually.

4.4 Results

4.4.1 Mechanisms for high performance under current climate

Ensemble simulations under current climate conditions showed a range of final yield and yield stability levels across T × M combinations and simulation sites; some top performing combinations showed relatively lower yield and higher yield stability, while others had relatively higher yield and lower yield stability, highlighting a trade-off between yield and yield stability among top-performing T × M combinations (Fig. 4.1b, C.6). Multiple combinations achieved high performance under current climate (Fig. 4.2); we investigated potential mechanisms that led to these differences in performance (Fig. 4.3).

A range of parameter combinations made up top-performing T × M combinations (Fig. C.3), leading to a number of emergent properties that affect final performance through impacts on yield and yield stability in a synergistic or antagonistic fashion (Fig. 4.2). Specifically, we identified key phenological (grain-filling start time and duration) and morphological (total leaf area) emergent properties as key factors to achieve high performance (Fig. 4.2a). For example, a combination of higher leaf numbers ($leaf$) and greater leaf length (len) can lead to greater total leaf area (Fig. 4.2b); the emergent property of greater leaf area partially correlates with high yield but also with low yield stability, thus having an antagonistic impact on final performance (Fig. 4.2a, antagonistic). Both leaf number ($leaf$) and leaf developmental rate ($ltar$) influence grain-filling start time (Fig. 4.2b), in which an earlier reproductive start time partially correlates with higher yield and higher yield stability (Fig. 4.2a, synergistic). Staygreen values (sg) that determine the heritable delayed leaf senescence character (Thomas and Ougham, 2014) have the strongest impact on grain-

filling duration (Fig. 4.2b), which shows an antagonistic impact on achieving high yield and high yield stability (Fig. 4.2a, antagonistic). These compensating mechanisms within traits and emergent properties highlight the complexity within the trait-management landscape, and create multiple avenues that balance between yield and yield stability to achieve high performance.

4.4.2 Pathways for high performance under current climate

We categorized a few pathways towards high performance under current climate conditions grouped based on the three most impactful emergent properties on yield and yield stability - grain-filling start time, grain-filling duration, and total leaf area (Fig. 4.2a) using a clustering approach (see section 4.3.7). For example, we described T × M combinations with a small canopy size, an early grain-filling start time, and a short grain-filling duration as *Stress Averting*, combinations with similar characteristics but with a long grain-filling duration as *Slow Aging*, and combinations with the earliest start dates, medium grain-filling durations, and small canopy sizes as *Early Starting* (Fig. 4.3).

Stress Averting, *Slow Aging*, and *Early Starting* strategies tend to have fewer number of leaves and faster leaf developmental rates (Fig. 4.3a, whole-plant photosynthesis). This leads to early reproduction with a smaller canopy size, and lower whole-plant-level photosynthesis during the vegetative stage (Fig. C.2a). This trade-off between canopy size and phenology can be partially offset by increasing leaf area through greater leaf size while maintaining lower leaf numbers – we see high-performing T × M in regions with low leaf numbers ($leaf$) combined with high leaf length (len) (Fig. C.4). Plants may also compensate lower yields that come with smaller canopies through a prolonged reproductive stage (Fig. 4.3a, *Slow Aging*), in which total carbon gain picks up in later reproductive stages due to long leaf longevity (Fig. C.2b, photosynthesis through time). T × M combinations with smaller canopy sizes that lack this feature tend to have lower yield, but can partially make up in performance through higher yield stability (Fig. C.6; Fig. 4.3, *Stress Averting*).

On the flip side, strategies such as *High Yielding* tend to be larger in canopy size with a delayed reproductive start time (Fig. 4.3a). Ample leaf area and time available to pho-

tosynthesize allows for high yield, but comes with the trade-off of lower yield stability due to a delayed reproductive start (Fig. C.6). The trade-off between canopy size and phenology can be compensated through faster leaf developmental rates; high performing T × M combinations with high leaf numbers often also show fast leaf developmental rates (Fig. C.4).

4.4.3 G × M combination performance under changing climate

We show a change in performance ranking among T × M combinations by the end of the century (Fig. 4.4a). Several top ranking combinations dropped significantly in performance ranking (e.g. 44, 57, 58, 59), while others progressed further in ranking within top-tiered T × M combinations (e.g. 5, 9, 81, 88) or advanced into it (e.g. 7, 12, 18, 30, 89) (Fig. 4.4). However, note that performance ranking is relative among all T × M combinations – as the climate becomes progressively warmer and drier, all combinations suffered from yield loss, but those with improved performance rankings buffered the loss better than those that declined in performance ranking (Fig. 4.4b). Yield sensitivity (% yield loss per degree C warming) for T × M combinations with improved performance rankings averaged at -4%, while combinations with declined performance rankings averaged at -7% (Fig. 4.4b).

Changes in yield and yield stability both contributed to final shifts in performance ranking among T × M combinations – combinations with most improved performance rankings benefited greatly from improved yield stability, while combinations with the most declined performance rankings suffered mainly through loss in yield (Fig. C.7). These shifts led to changes in top-performing strategies by the end of the century. *Slow Aging* and *Stress Averting* T × M combinations maintained similar overall performance rankings (Fig. 4.3b), while *Early Starting* combinations suffered the most and dropped out as one of the top-performing strategies (Fig. 4.3b, faded dotted orange line, 4.4). *High Yielding* T × M combinations progressed further in performance rankings (Fig. 4.3b, solid forest green line), and new strategies such as *Compensating*, *Middle Ground* and *Large Canopy* advanced in performance rankings, entering the ranks of top performers by the end of the century (Fig. 4.3b, solid dark green, lime green, and sky blue line, respectively). In general, strategies

with larger canopies and a later grain-filling start time showed the greatest improvement in performance ranking relative to others (Fig. 4.3b).

A weakened trade-off between achieving an early reproductive start versus achieving greater leaf area for carbon gain largely contributed to shifts in the performance of T × M combinations (Fig. 4.4). Under present-day climate conditions, T × M combinations with an early grain-filling start time tend to rank higher in performance due to synergistic benefits in achieving both high yield and high yield stability (Fig. 4.2a). Avenues to achieve an early grain-filling start under our parameter perturbations include possessing fewer leaves and/or displaying faster developmental rates (Fig. 4.2b). Among these features, lower number of leaves generally results in a smaller canopy (Fig. C.5a), such that strategies with an early reproductive start tend to also have a smaller canopy size (Fig. 4.3). Faster developmental rates under warmer future temperatures weaken this trade-off, buffering the negative impacts T × M combinations with larger canopies tend to have from delayed reproductive start time, and improve their relative competitiveness.

Strategies with improved performance ranking under future climate (Fig. 4.3b) tend to show a later grain-filling start and larger canopy size compared to top performers under present-day climate conditions (Fig. 4.3a). On the other hand, a wide range of grain-filling durations existed among top-performing strategies under future conditions (Fig. 4.3b). Among strategies that remained high-performing or improved in performance rankings under future climate conditions (Fig. 4.3b, dashed lines and solid lines, respectively), certain strategies still ranked higher in performance compared to others. For example, *Slow Aging* strategies remained as one of the highest performers, both under present-day climate and under future climate conditions, whereas strategies such as *Middle Ground* advances a lot in performance rankings, but still remained on the lower end of overall performance ranking (Fig. 4.4a).

4.5 Discussion

In this work, we construct a modeling framework to probe and evaluate maize performance across a trait-management-environment landscape, and further investigate how performance within this landscape shifts under a changing climate. We show that multiple trait and

management combinations exist to confer high performance under current climate; general trait combinations exist within emergent properties that allow for high performance either through high yield or high yield stability, yet trade-offs exist between these two features. While we observed overall yield loss across all T × M combinations by the end of the century, shifts in performance under future climate allow for new high-performing pathways to emerge, partially buffering loss.

Multiple pathways confer high performance

Timing of grain-filling start, grain-filling duration, and total leaf area are critical for final yield as well as yield stability, yet timing of reproduction and canopy size often compromise one another for achieving high performance (Fig. 4.2). The complexity within the trait-management landscape and their links to various emergent properties allow for multiple avenues to achieve high performance (Fig. 4.3). Some traits may be easier to select and breed for within the existing germplasm, while others may be less straightforward or may currently be coupled with other less desirable traits. The idealized approach within our modeling framework alleviates these constraints, allowing us to consider crop performance through a theoretical lens. While many T × M combinations and strategies presented in this work may not currently exist or may be challenging to breed for, general trends identified through these modeling exercises can still hold valuable information to help identify breeding targets specific for climate adaptation.

Several key traits in maize hybrids have changed due to active breeding efforts in the past few decades (Duvick, 2005; Fischer and Edmeades, 2010), including noticeable increases in the staygreen values, longer grain-filling durations, and more erect canopy structures, to name a few. Along with these shifts though, certain traits such as days to flowering (largely controlled through total leaf number) and maximum leaf area index remained relatively unchanged (Duvick, 2005; Fischer and Edmeades, 2010). In addition to general trends in breeding directions, breeding of new cultivars typically requires defined target environments within a geographical scope for which the target traits are developed (Cooper et al., 2016). This breeding strategy allows for designing different hybrids to perform favorably

and withstand stresses in their target environments, and growers throughout the US plant different commercial hybrids most suitable for their targeted growth environment. However, comprehensive mapping of existing target traits of commercial maize hybrids across the environmental gradients within the country remains scarce. Privatized trait data of modern maize hybrids within the US make direct comparisons between our modeled T × M combinations and existing cultivars a tricky task. Regardless, we see alignment between our model results for high performance and certain breeding trends such as longer grain-filling duration and increased staygreen values. Divergences in other areas such as the lack of change in flowering time, leaf number, and canopy size in modern hybrids suggest potential new directions to explore.

In our analyses, we assigned equal weight of importance to yield and yield stability when determining the performance of our simulated T × M combinations, and presented high-performing strategies identified under such assumptions. However, we acknowledge that what growers may consider as high performing will likely depend on risk tolerance; large-scale producers may have buffer and leverage to aim for high yield low yield stability T × M combinations, while smaller-scale producers may need to opt for a mix or aim towards lower-risk combinations with a trade-off in yield. Top performing strategies differed slightly when we assigned more importance to yield or yield stability in our analyses (Fig. C.3). Specifically, *Slow Aging* remained as a top performing strategy under current climate conditions across all scenarios, whereas *High Yielding* and *Large Canopy* strategies were identified as top-performing when imposing a higher importance on yield (Fig. C.3b), and *Early Starting* and *Stress Averting* strategies were identified as top performing when more emphasis was placed on yield stability (Fig. C.3c).

Performance of G × M combinations shift with changing climate

High performing T × M combinations under current climate conditions does not guarantee high performance under future climate. Several high performing combinations identified under current climate conditions experienced steep declines in their performance when evaluated under future climate simulations, while several lower-performing combinations under

present-day climate became more competitive relative to others under future climate (Fig. 4.4).

In our work, we identified high importance in emergent properties (Fig. 4.2a) and plant traits (Fig. 4.2b) associated with phenology and morphology, and demonstrated how a relaxed trade-off between these two features shifted performance rankings among T × M combinations under a warmer and drier future climate (Fig. 4.3b). Specifically, traits that influenced transition time from vegetative stage into reproductive stage (e.g., leaf number, leaf appearance rate) greatly impacted the trade-off between phenology and morphology; T × M combinations with early transitions into reproductive stages suffered more from hastened development and senescence rates under a warmer future climate, while T × M combinations with later transitions (i.e., greater heat requirements) maintained longer crop cycle durations at a given location (total days from planting to maturity and harvest), partially buffering performance loss (Fig. 4.3b).

Literature in maize flowering time provides a reasonable comparison to grain-filling start time identified in our simulations, both representing to some degree the timing of transition from vegetative stage into reproductive stages within a crop. Flowering time within a crop demonstrates the optimization of the timing and duration between vegetative and reproductive stages, and serves as an emergent property of how crops have adopted to local growing environment (Buckler et al., 2009). Flowering time and crop cycle duration varies greatly among maize landraces (Bolaños and Edmeades, 1996), and genetic resources relating to maize flowering time have since been identified (Buckler et al., 2009). Existing cultivar differences between maize crops planted in cooler corn belt regions in the U.S. versus those planted in warmer southern locations reflect the temperature dependence of developmental and senescence rates, with crops in the south planted and harvested earlier in the season (USDA- NASS, Crop Progress and Conditions, `https://www.nass.usda.gov/Charts_and_Maps/Crop_Progress_&_Condition/`). Parent et al. (2018) demonstrated that utilizing currently existing genetic variability within maize flowering time can be sufficient in creating optimal cropping duration and sustaining yield within various European climate conditions under a changing climate. Despite limited evidence that growers in the U.S. Midwest are currently shifting to longer maturity cultivars in accor-

dance with changes in climate in the past two decades (Abendroth et al., 2021), switching varieties in the future remains a highly responsive strategy for growers.

While we identified relatively later transition to reproductive stages and larger canopies as favorable features under future climate perturbations, we also note potential limitations in the model's ability to capture late-stage water stress and heat stress impacts. Growth duration for rain-fed maize is tightly associated with water stress, and while longer season varieties could buffer yield losses from accelerated development and senescence rates under warmer temperatures, it may also lead to greater water demand and water stress in later developmental stages. MAIZSIM differs from several widely used crop simulation models in its dynamic approach when describing water relations and gas exchange in response to temperature, relative humidity, and CO_2 concentrations throughout the growing season (Yang et al., 2009a). However, the model has limited ability in capturing heat and water stress impacts on reproductive processes such as flowering, pollination, and grain-filling. In addition, process-based models in general struggle to represent the process of plant death under unfavorable climate conditions. It is important to note that such caveats could potentially lead to dampened benefits that come from T $\times$ M combinations with longer growth durations (Lobell, 2014).

Implications for climate adaptation

Up to 39% of global crop land may require new cultivars to avoid yield loss by the end of the century under a SSP5-8.5 climate change scenario (Zabel et al., 2021), yet a typical breeding cycle can take up to a decade or two (Voss-Fels et al., 2019), or even longer when considering the complete cycle of breeding, delivery, and adoption (Challinor et al., 2017). The lag between development of new cultivars and when those new cultivars actually become available along with the concurrent rate of climate change poses a challenge to develop cultivars targeted towards climate adaptation. Current advances in modern breeding techniques have increased the rate of crop improvement, but more efficient strategies are still needed when addressing food security issues with a changing climate (Voss-Fels et al., 2019).

Growers in North America have been adapting varieties and management practices dating back to the 19th and 20th centuries (Olmstead and Rhode, 2011). In addition to breeding efforts in the private and public sector, a recent survey showed a third to half of farmers in the U.S. Corn Belt are willing to make adjustments in management practices in response to changing climate (Roesch-McNally et al., 2017). Switching cultivars, if more suitable options are available, are dynamic adaptation strategies that can be updated each season and do not necessarily require long-term investments. Current trends and magnitudes in climate change may not be large enough to serve as a major driver for growers when selecting cultivars, but a future tipping point may exist. The time and resources required to develop and adopt new cultivars strongly advocates for climate-ready cultivars as adaptation options moving forward.

A vast body of recent work and discussion has surrounded the topic of using process-based models to aid breeding practices (model-assisted breeding, ideotype design, predictive breeding, etc.), better capture G $\times$ E $\times$ M interactions, and serve as key tools for predictive agriculture (Martre et al., 2015; Rötter et al., 2015; Muller and Martre, 2019). Process-based crop models can serve as powerful tools, but also come with built-in assumptions and limitations. Scaling models spatially and temporally is challenging, especially when integrating information at the scale useful for plant breeders and agronomists at the genetic, whole-plant, and field scale, with broader implications of food security and climate adaptation at a regional to global scale. There is a growing awareness within the community to consider modeling as a multi-scale system that spans the genetics, organ, regional, and global scale that incorporates various streams of data sources and modeling tool to better understand processes, further develop and evaluate models, and collect and integrate data products with models (Peng et al., 2020). Communication and collaboration across fields is even more critical when working across scales. Our findings serve as a starting point for more integrated conversations between modelers, breeders, agronomists, and growers, in order to advance current adaptation efforts to increase agriculture resilience.

4.6 Acknowledgements

We thank Lucas Vargas Zeppetello for providing CMIP6 temperature and relative humidity projection scaling patterns. We also thank Carlos Messina for helpful comments. JH acknowledges support from the AFRI NIFA Fellowships Grant Program: Predoctoral Fellowships [grant no. 2020-67034-31736] from the USDA National Institute of Food and Agriculture. ALSS acknowledges support from NSF AGS-1553715

4.7 Figures and tables

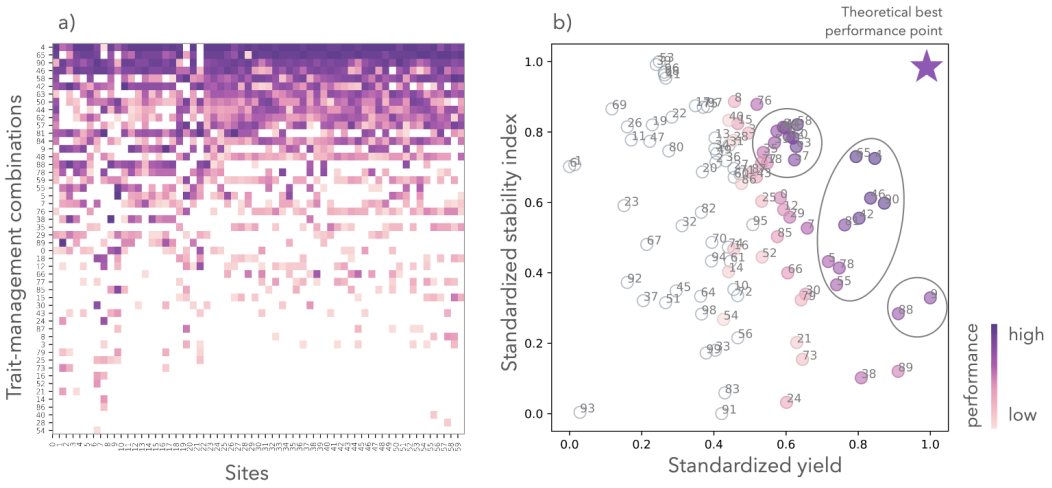

Figure 4.1: a) Performance of all T × M combinations across all simulation sites, ordered top to bottom from the highest performer to lowest. Only T × M combinations that rank top 20 in at least one location are shown. b) Standardized mean yield across all site-years and standardized yield stability across simulation years averaged across all sites for all T × M combinations. Top performing combinations have filled in colors that indicate performance based on ranking methods described in section C.3. Top 20 performers are circled in open gray circles.

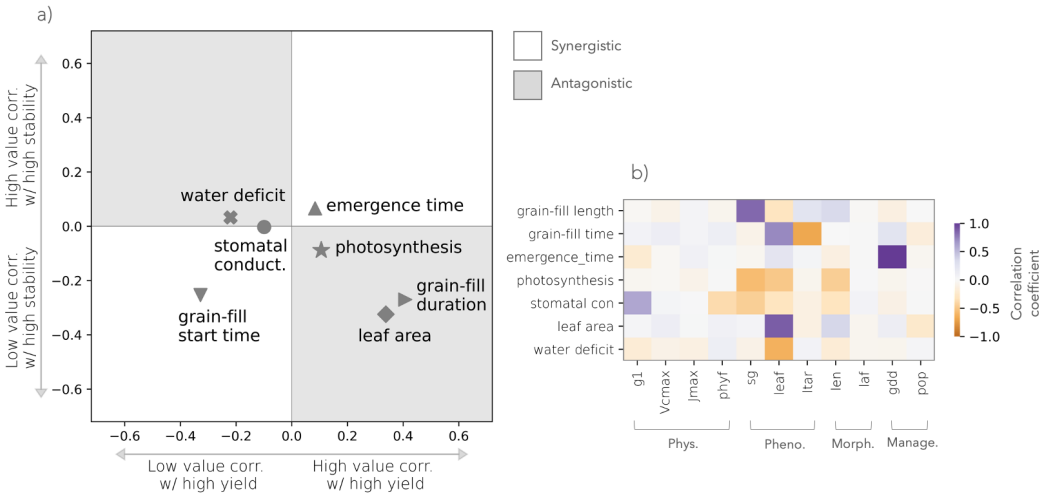

Figure 4.2: a) Partial correlation coefficient (PCC) between emergent properties (Table 4.2) and high yield (x-axis) and high stability (y-axis). b) Correlation coefficient between perturbed parameters (Table 4.1) and emergent properties (Table 4.2).

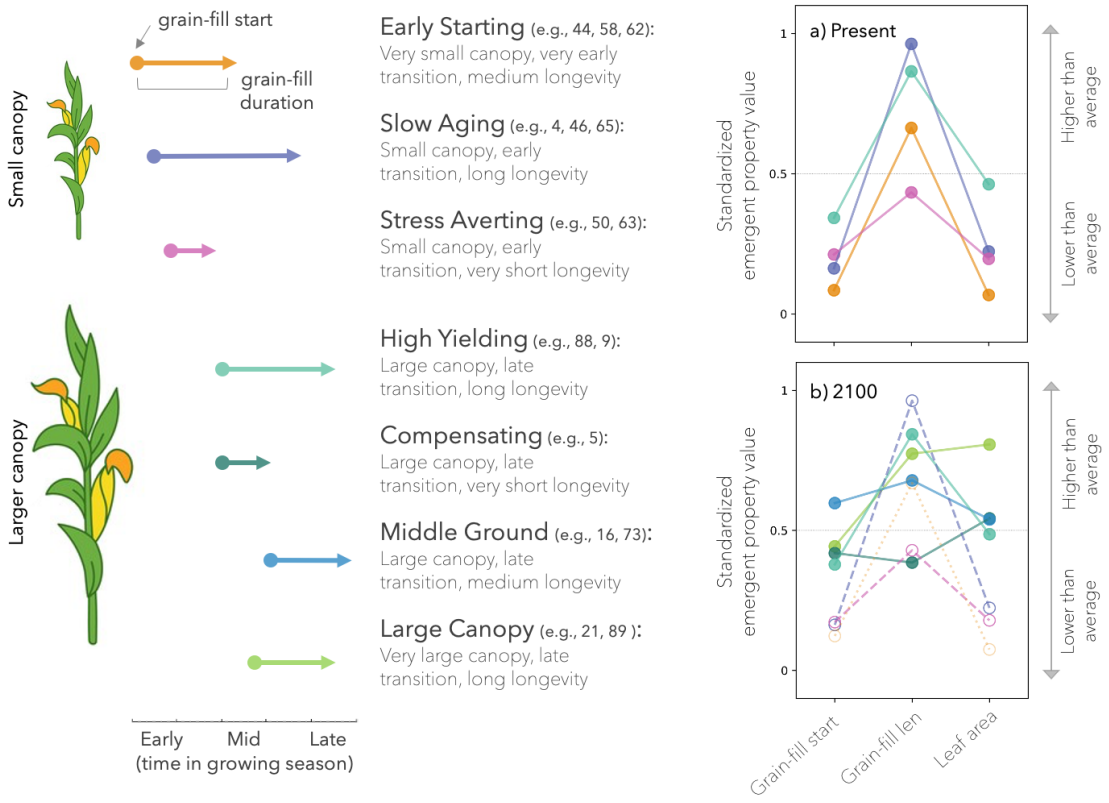

Figure 4.3: Selected strategies among top performing T × M combinations under present-day climate, grouped based on phenological and morphological properties. a) Standardized grain-filling start time, grain-filing duration, and total leaf area for the select few T × M combinations listed on the left. Values are standardized among all 100 T × M combinations. Values greater than 0.5 indicate higher-than-average values when compared to all other T × M combinations, and vice versa. b) Top-performing strategies by the end of the century with reference to strategies identified under current climate conditions. Solid lines show top-performing strategies that improved in performance ranking, dashed lines indicate strategies that remained similar in performance rankings, and faded lines show strategies that dropped out as top performing by the end of the century.

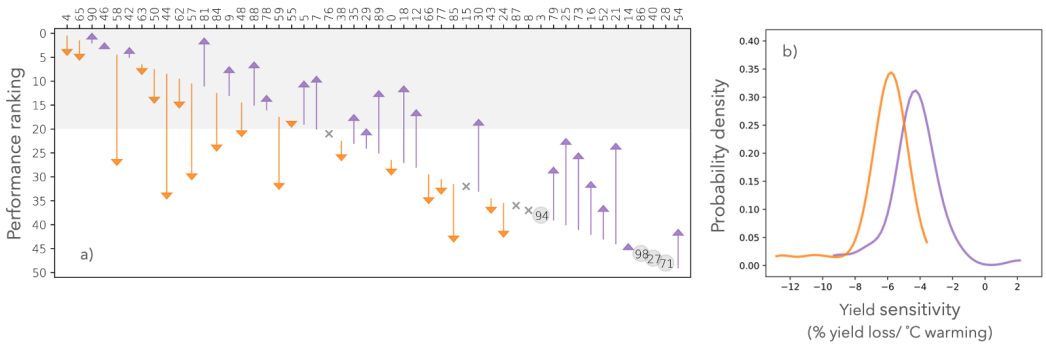

Figure 4.4: a) Change in performance ranking among T × M combinations across simulation sites under future climate conditions at 2100. T × M combinations are ranked based on their performances under current climate conditions on the x-axis, with lower ranking values denoting higher performance. Improvement in rankings are shown with purple upward pointing arrows, while decrease in performances are shown with orange downward pointing arrows. The shaded box describes area for top 20 T × M combinations. b) Probability density function of yield sensitivity (percent yield loss per degree warming) across all simulation sites for most improved (purple) versus most declined (orange) T × M combinations.

Appendix A

CHAPTER 2 SUPPLEMENTARY INFORMATION

Disentangling Temperature and VPD

We followed the Clausius-Clapeyron equation (Eqn. A.1) to make independent adjustments to temperature and VPD. The equation uses the saturation vapor pressure (E_{sref}, 6.11mb) at a reference temperature (T_{ref}, 273.15 K), the vaporization latent heat (L_v, 2.5*106 J/kg), and the gas constant (R_v, 461 J/K*kg) to calculate the saturated water vapor pressure (E_s) at air temperature (T):

$$E_s = E_{sref} \cdot e^{\frac{L_v}{R_v} \cdot (\frac{1}{T_{ref}} - \frac{1}{T_{air}})} \tag{A.1}$$

With relative humidity (RH, %) available from our weather data, we can further calculate the actual water vapor pressure within the atmosphere (E, mb) through Equation A.2, and VPD (mb) through Equation A.3:

$$E = \frac{E_s \cdot RH}{100} \tag{A.2}$$

$$VPD = E_s - E \tag{A.3}$$

Under our 2°C elevated temperature treatment, E_s simultaneously increases with temperature following equation A.1. Normally, this would also cause an increase in VPD with an assumption that E remains constant throughout warming (Eqn. A.3). To tease these two factors apart, we artificially increased RH levels such that VPD would remain constant (Eqn. A.2, A.3). Similarly, under our elevated VPD treatment, we calculated the VPD increase that would have occurred along with a 2°C warming (Eqn. A.1, A.3) and increased the VPD values within our weather data based on these calculations while holding temperature constant.

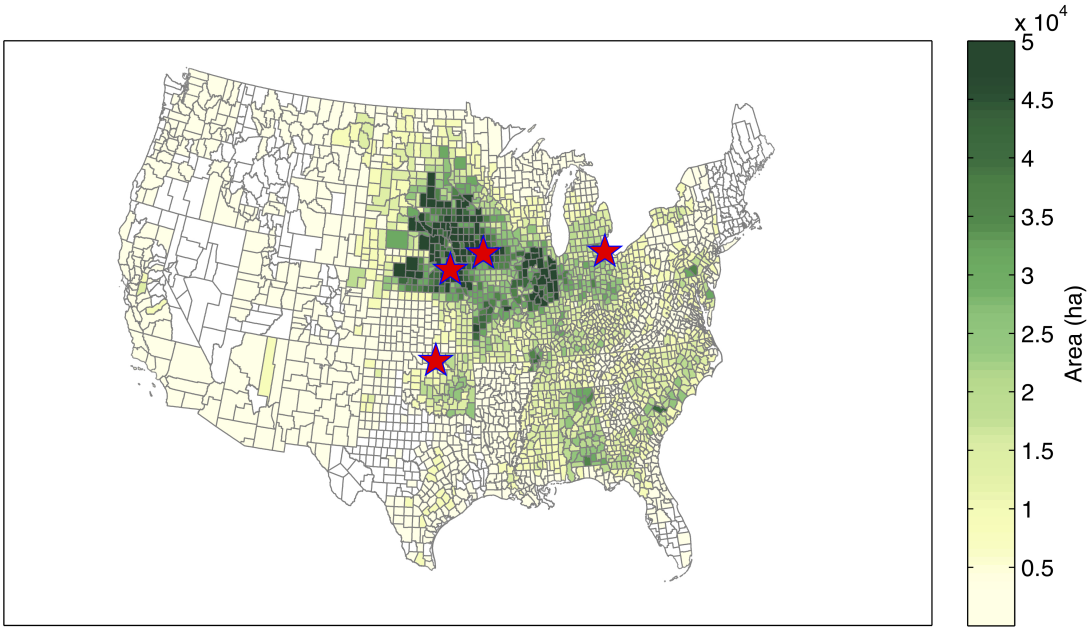

Figure A.1: Area planted in maize for all purpose production averaged across the most recent five years at the U.S. county-level, with the most recent year being 2014 (data from U.S. Department for Agriculture, National Agriculture Statistical Service). Red stars show the location of simulation sites.

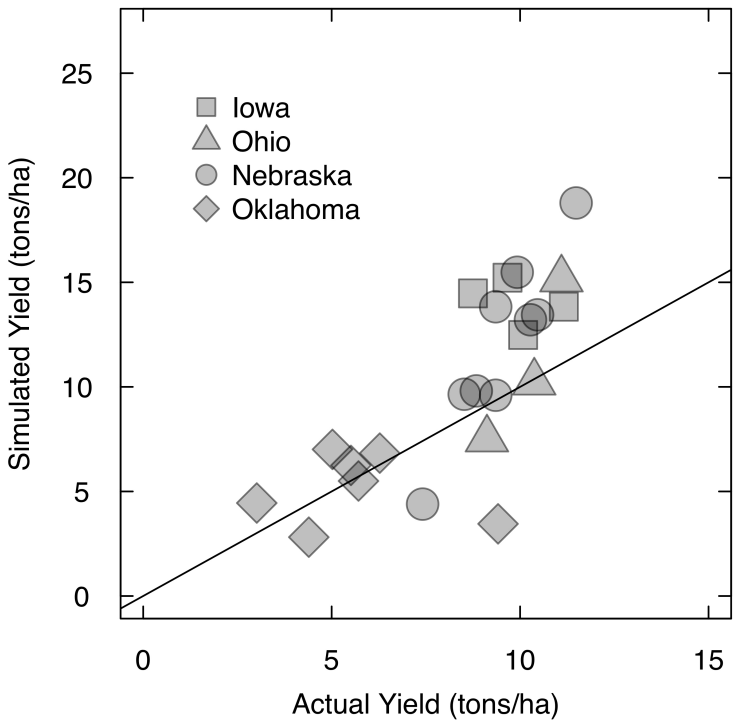

Figure A.2: Comparison between model simulation of final maize yield and actual yield observations across the study site and years (USDA NASS National Agricultural Statistics Service).

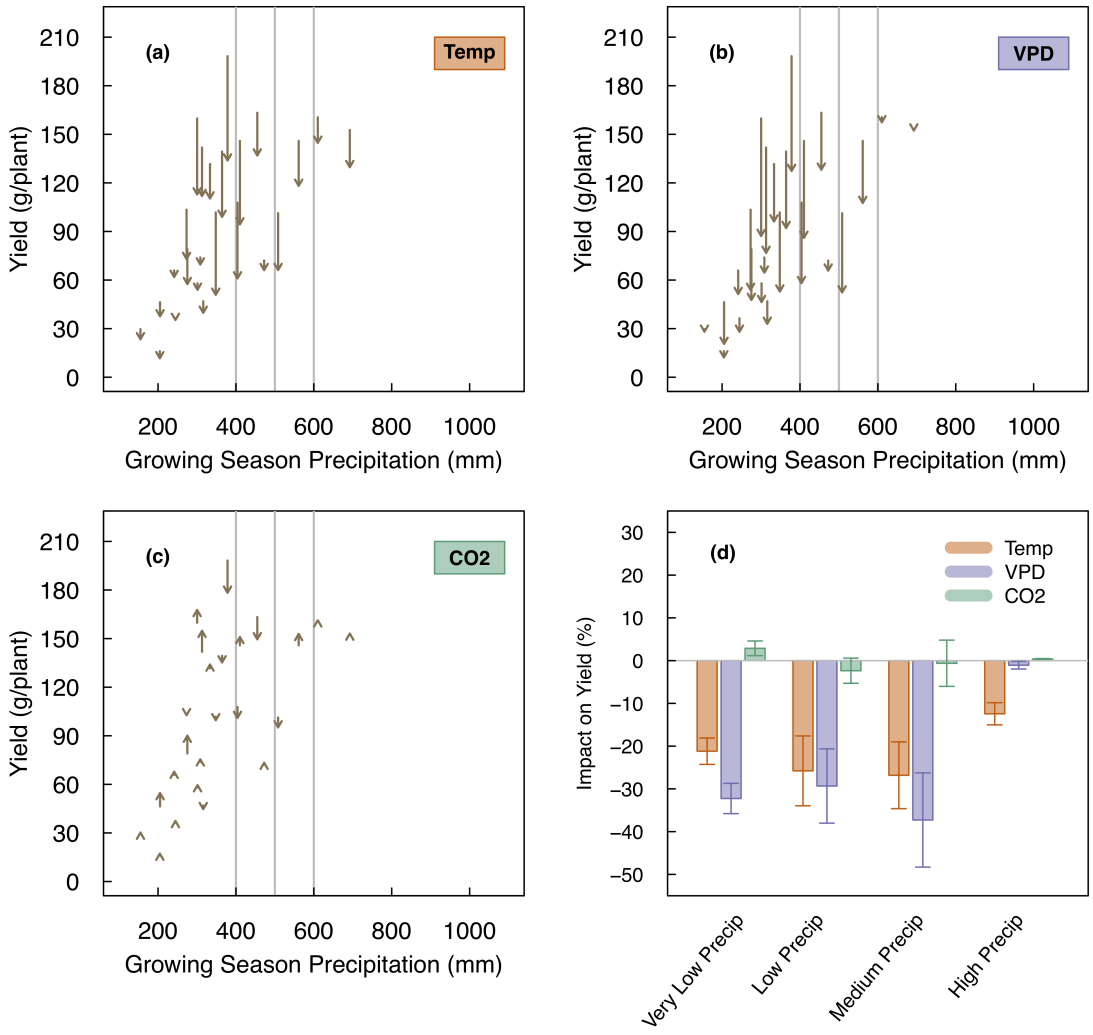

Figure A.3: Direction and magnitude of yield change between treatment and control yield under an additional 30% rainfall cut, across precipitation range within simulated sites and years for a) temperature, b) VPD, and c) CO_2. The vertical grey lines categorize the precipitation range into very low (<400 mm growing season precipitation), low (400-500 mm), medium (500-600 mm), and high (>600 mm) precipitation levels. d) Percent yield impact from 2°C warming (orange), increased VPD that accompanies 2°C warming (purple), and doubling CO_2 levels from 400-800 ppm (green) under different precipitation ranges. Error bars denote standard error calculated across simulation sites and years.

Table A.1: Description of Ameriflux tower data used for MAIZSIM weather input, and their mean growing season climate conditions and the standard deviation during simulation years.

Location	Site Name	Lat/Lon	Site Description	Mean Growing Season Temp. (°C)	Total Growing Season Precip. (mm)	Mean Growing Season VPD (kPa)	Data Years Used
Iowa	US-Br1: Brooks Filed Site 10-Ames [1]	41.69/ -93.69	Corn/soybean rotation cropland	18.81 ± 6.03	730.76 ± 207.57	0.58 ± 0.31	2007-2008, 2010-2011
Nebraska	US-Ne3: Mead [2]	41.19/-96.44	Rain-fed maize-soybean rotation site	19.42 ± 6.03	540.71 ± 152.53	0.72 ± 0.38	2004-2012
Ohio	US-CRT: Curtice Walter-Berger Cropland [3]	41.63/-83.35	Soybean/winter wheat rotation	18.93 ± 5.82	466.43 ± 79.60	0.64 ± 0.38	2011-2013
Oklahoma	US-ARM: Southern Great Plains - Lamont [4]	36.60/-97.49	Winter wheat, corn, soybean, alfalfa	23.53 ± 5.91	400.68 ± 127.48	1.18 ± 0.73	2003-2007, 2009-2011

[1] Prueger and Parkin, doi:10.17190/AMF/1246038, [2] Suyker, doi:10.17190/AMF/1246086, [3] Chen, doi:10.17190/AMF/1246156, [4] Biraud, doi:10.17190/AMF/1246027

Appendix B

CHAPTER 3 SUPPLEMENTARY INFORMATION

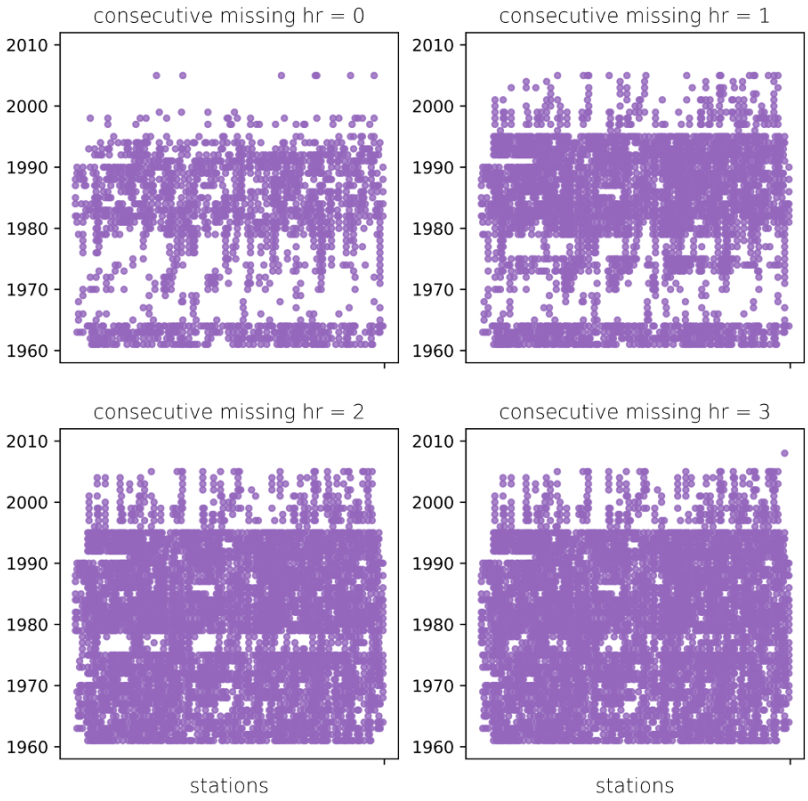

Figure B.1: Available weather data based on different gap-filling intervals. For example, if consecutive missing hours equals 0, then only site-years with complete hourly weather data records will be included for weather data. If consecutive missing hour equals 1, site-years with gaps no greater than one hour consecutively will be included and gap-filled linearly.

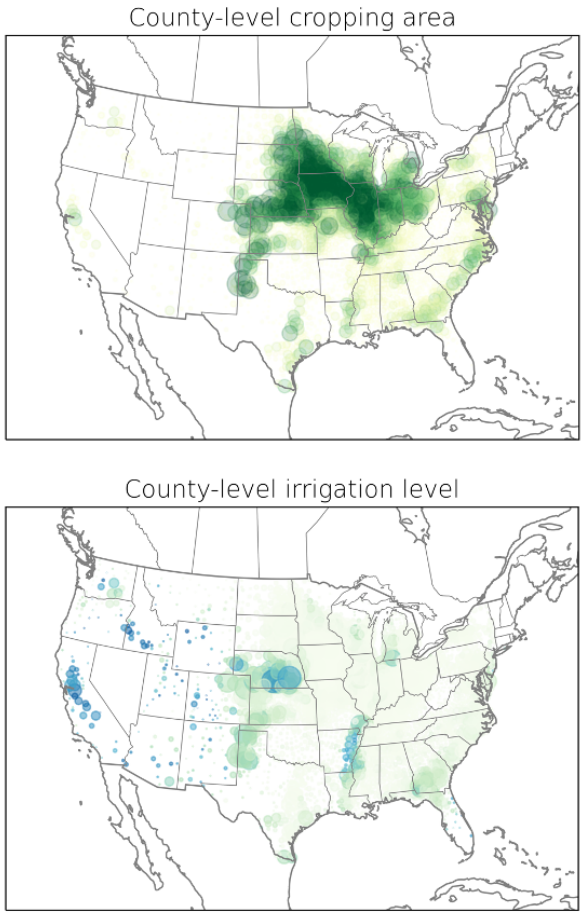

Figure B.2: Maize planting area (top) and irrigation levels (bottom) across continental U.S.

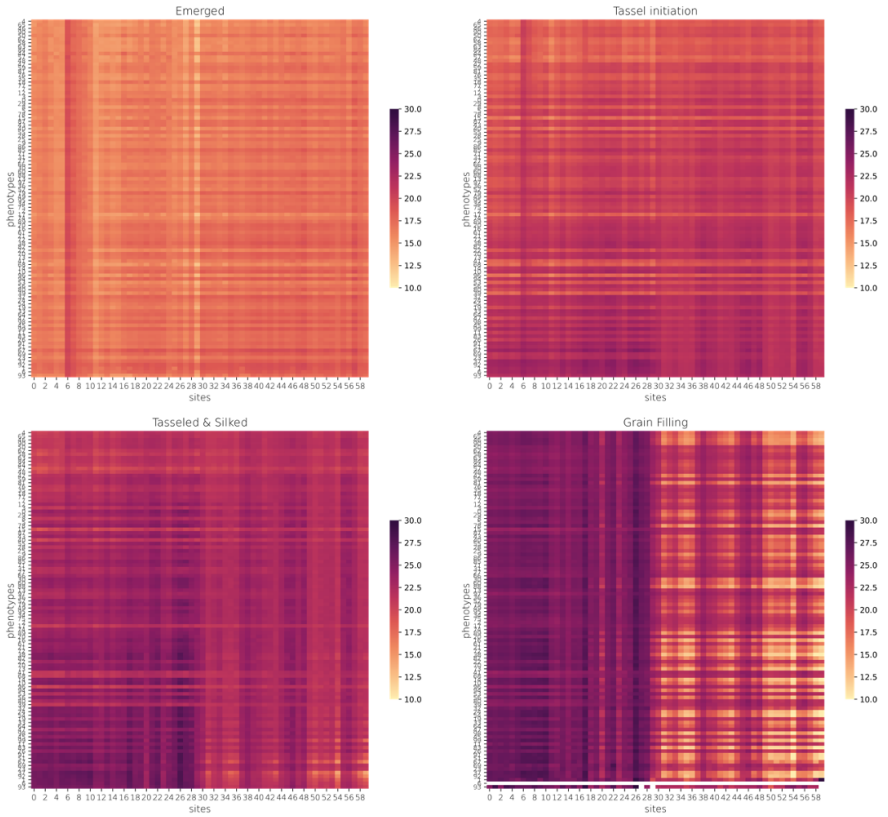

Figure B.3: Mean air temperature (°C) across phenological stages for top phenotypes across all sites, ranked by performance of G × M combinations, and averaged within phenological stages.

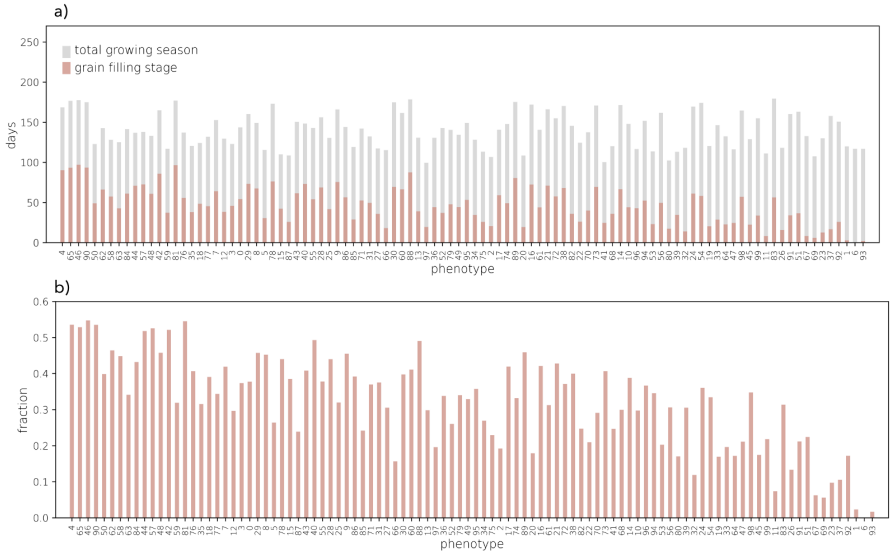

Figure B.4: a) Total growing season length (gray, days) and grain-filling length (pink, days) for all phenotypes, ranked by performance, starting with the highest performers towards the left, and b) the fraction of grain-filling over total growing season.

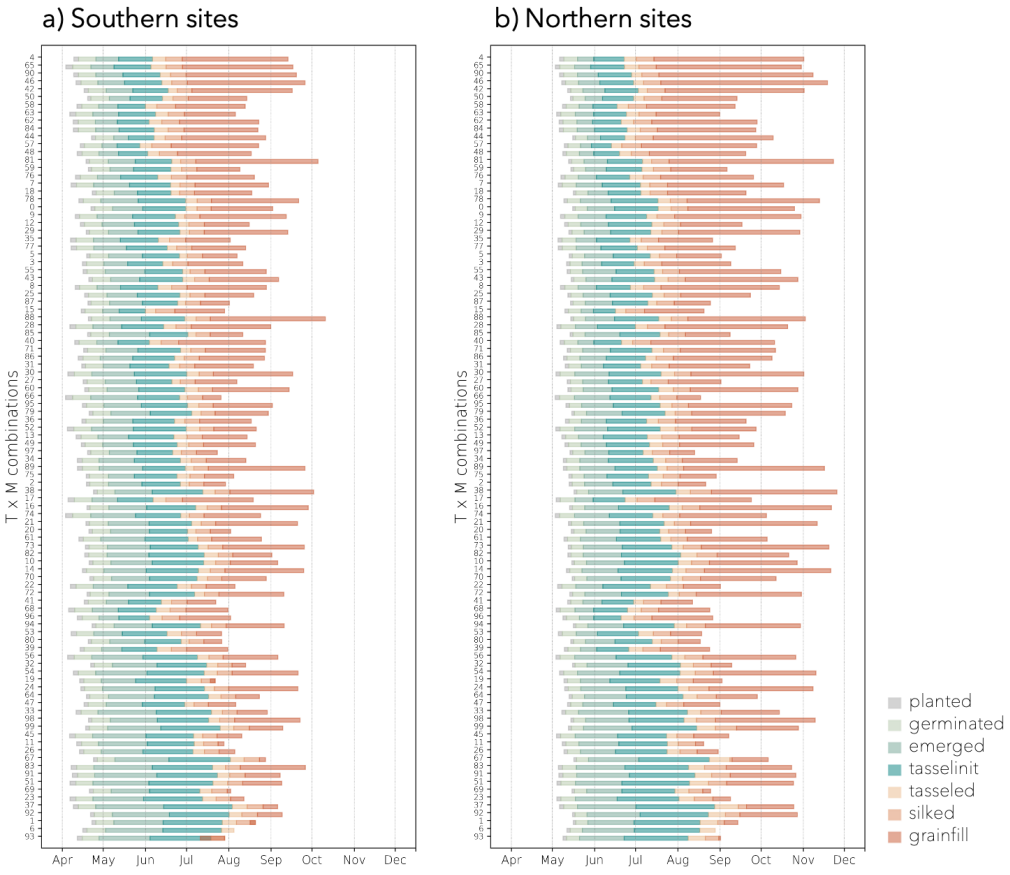

Figure B.5: Start time and duration of each phenological stage across T × M combinations, averaged across all simulation sites for a) southern sites versus b) northern sites, ranked by overall performance, with the highest performers listed towards the top.

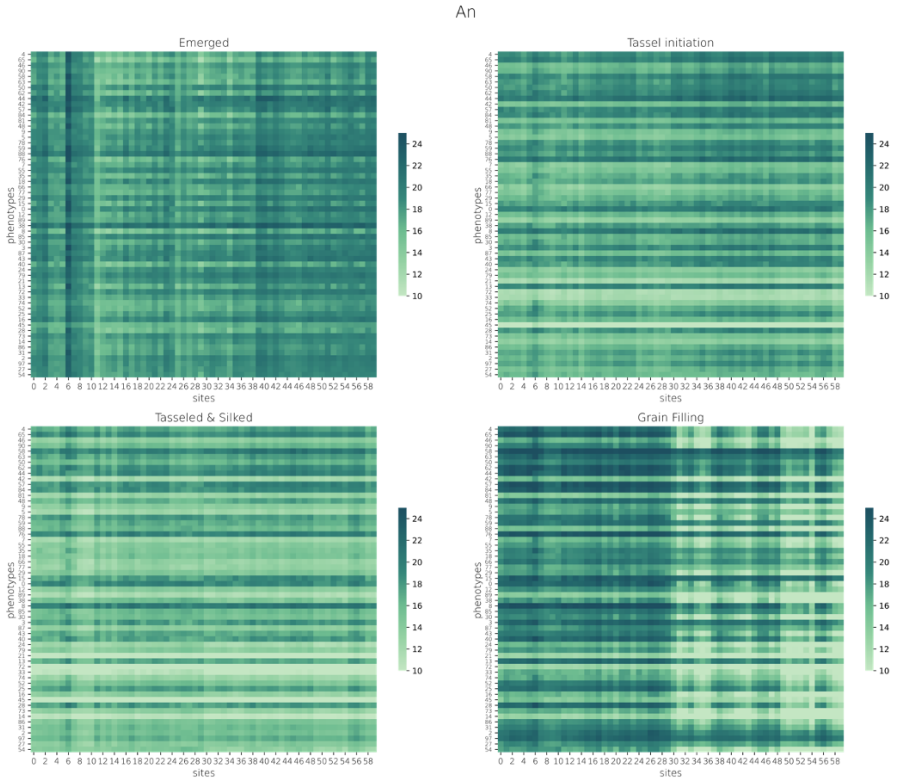

Figure B.6: Net photosynthetic rate (µmol CO_2 m^{-2} sec^{-1}) across phenotypes and sites, ranked by phenotype performance, and averaged within each developmental stage.

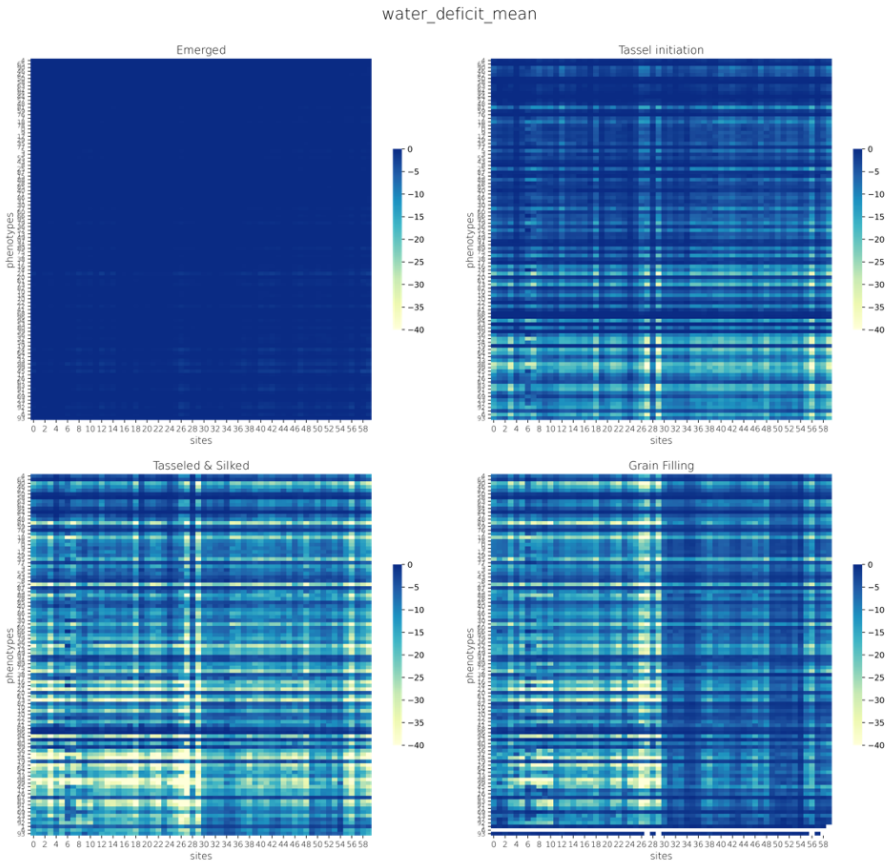

Figure B.7: Mean water deficit (g H_2O) across phenotypes and sites, ranked by phenotype performance, and averaged within each developmental stage.

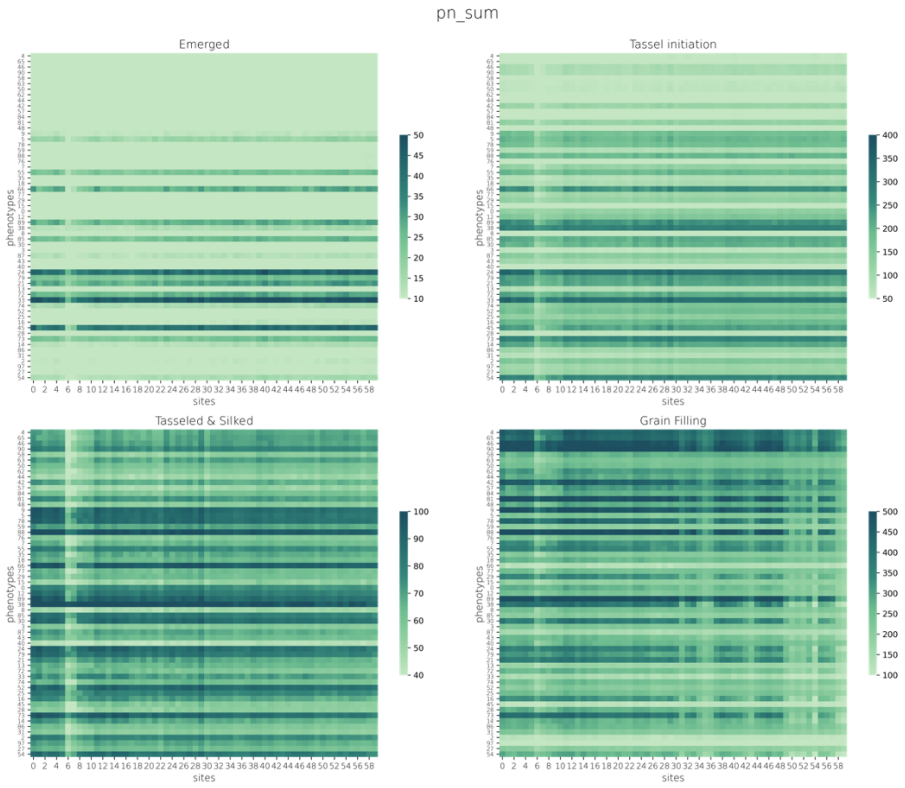

Figure B.8: Net carbon gain throughout phenological stage (g C) across phenotypes and sites, ranked by phenotype performance, and averaged within each developmental stage.

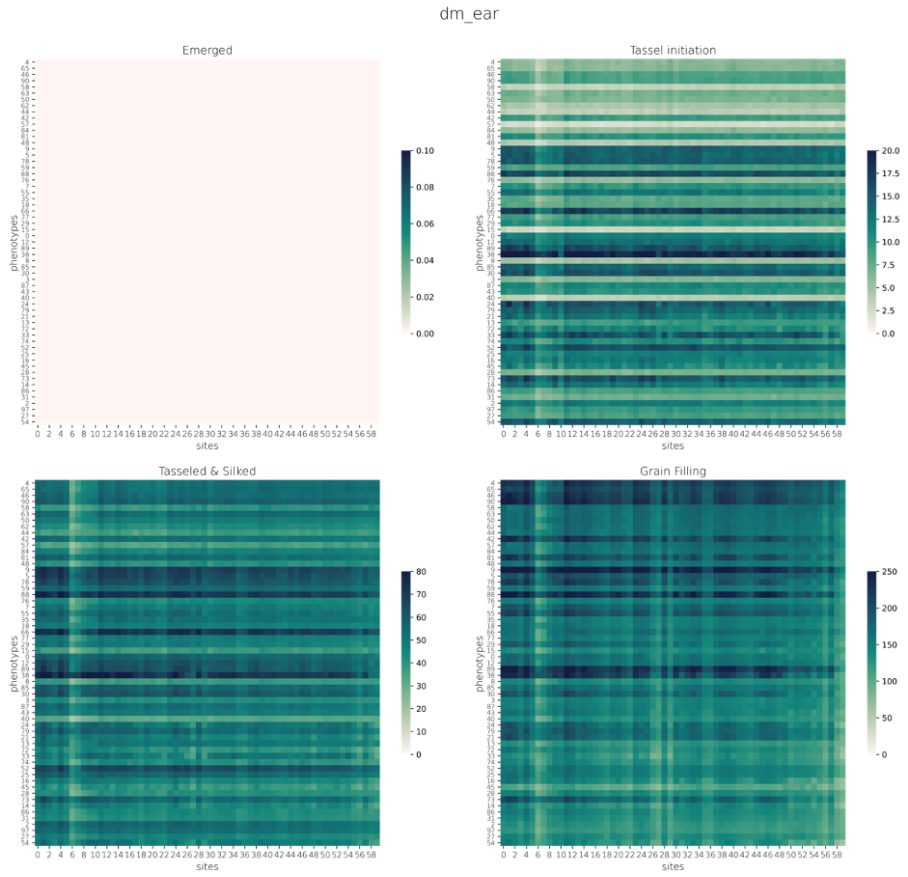

Figure B.9: Ear biomass (g/plant) across phenotypes and sites, ranked by phenotype performance, and averaged within each developmental stage.

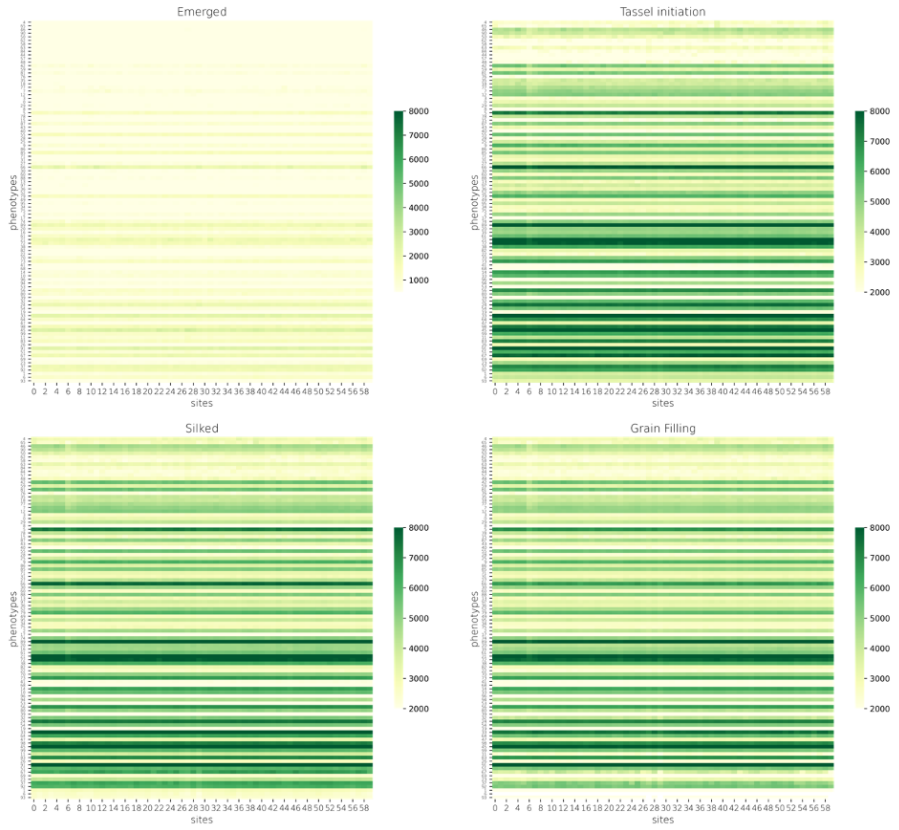

Figure B.10: Total leaf area (cm^2) across phenotypes and sites, ranked by phenotype performance, and averaged within phenological stages..

Appendix C

CHAPTER 4 SUPPLEMENTARY INFORMATION

C.1 Sensitivity analysis - partial correlation coefficient

Partial correlation coefficient (PCC) is a sampling-based method that measures the linear relationship between an individual parameter (x_p) and a specified model output (y) after removing the linear effects that remaining parameters ($x_j, j = 1, 2, ..., k, j \neq p$) have on y. To calculate the PCC between parameter x_j (in our case, a specific emergent property) and y, one would calculate the correlation coefficient between residuals $x_j - \hat{x}_j$ and $y - \hat{y}$, in which $\hat{x}_j$ and $\hat{y}$ represent the associated linear regression models (Eqn. C.1-C.2):

$$\hat{x}_j = c_0 + \sum_{p=1, p\neq j}^{k} c_p x_p \tag{C.1}$$

$$\hat{y} = b_0 + \sum_{p=1, p\neq j}^{k} b_p x_p \tag{C.2}$$

C.2 Experiment setup and model simulation

We set up the MAIZSIM model with sampled planting density (Table 4.1) for each ensemble member and prescribed a total of 200 kg ha^{-1} of nitrogen throughout the growing season, applying half as base fertilizer prior to planting and the rest top-dressed one month post planting to simulate non-nutrient-limited growth conditions. Next, we estimated planting dates for each simulation site by calculating the accumulated growing degree days (GDD) with a base temperature of 8°C (Kim et al., 2012) and started GDD accumulation calculations from February 1st and assigned the planting date once GDD values surpassed values determined through the parameter sampling process for each ensemble member (Table 4.1).

Soil properties are highly heterogeneous. To create site-specific soil input files for each of our simulation sites, we queried soil information from the National Resources of Conservation Services (NRCS) SSURGO soil database (Soil Survey Staff) for nearby NASS sites

with maize planting area greater than 10000 acres and irrigation levels less than 25%. Since our simulation sites are determined through weather station locations, this method allows us to broadly represent average soil properties of agricultural lands nearby our simulation sites. Specifically, we queried sand–silt–clay–organic matter composition, soil bulk density (the oven dry weight of less than 2 mm soil material per unit volume of soil at a water tension of 1/3 bar), and the volumetric content of soil water retained at a tension of 1/3 bar (33 kPa) expressed as a percentage of the whole soil at five depth categories (surface, 50, 100, 150, and 200 cm). We used the sand–silt–clay composition to categorize soils into 12 texture groups following the USDA Textural Soil Classification (Staff, 1999) and excluded sites classified as Sandy or Clay due to their lack of representation in agricultural fields. We averaged soil properties within each soil category from all filtered NASS sites, assigned each simulation site the most dominant soil class from 11 nearest NASS sites calculated through Euclidean distance, and estimated soil hydraulic properties of each soil type through a water release curve predicted by the van Genuchten equation (van Genuchten, 1980).

C.3 Identifying top performing T × M combinations

We calculated the D_{score} for each T × M combination at each simulation site:

$$D_{score} = \sqrt{w_{yield} * (y_{mean} - y_{max})^2 + w_{disp} * (y_{disp} - d_{min})^2} \tag{C.3}$$

The score quantifies the performance of a T × M combination at a specific location by calculating its distance to a theoretical best-performing T × M combination within the yield and yield stability space. y_{mean} represents the mean simulated yield of a specific T × M combination at a specific simulation site, whereas y_{disp} denotes the simulated yield dispersion (variance/mean) across the simulation years. y_{max} and d_{min} denote the maximum mean yield and minimum yield dispersion (i.e. maximum yield stability) achieved within all T × M combinations at a specific simulation site, respectively. We standardized yield and dispersion values to between 0 and 1 to avoid skewed contribution due to difference in scale. We determined stability index values by calculating the difference between standardized dispersion and 1, such that low dispersion levels would equate high yield stability, and vice

versa. w_{yield} and w_{disp} are empirical coefficients that assign weighted importance to yield mean and yield dispersion, respectively.

We assumed equal importance between yield and yield stability for our main analyses ($w_{yield} = w_{disp} = 0.5$), but tested two additional assumptions that either weighed high yielding with greater importance ($w_{yield} = 0.7$, $w_{disp} = 0.3$), or weighed high yield stability with greater importance ($w_{yield} = 0.3$, $w_{disp} = 0.7$).

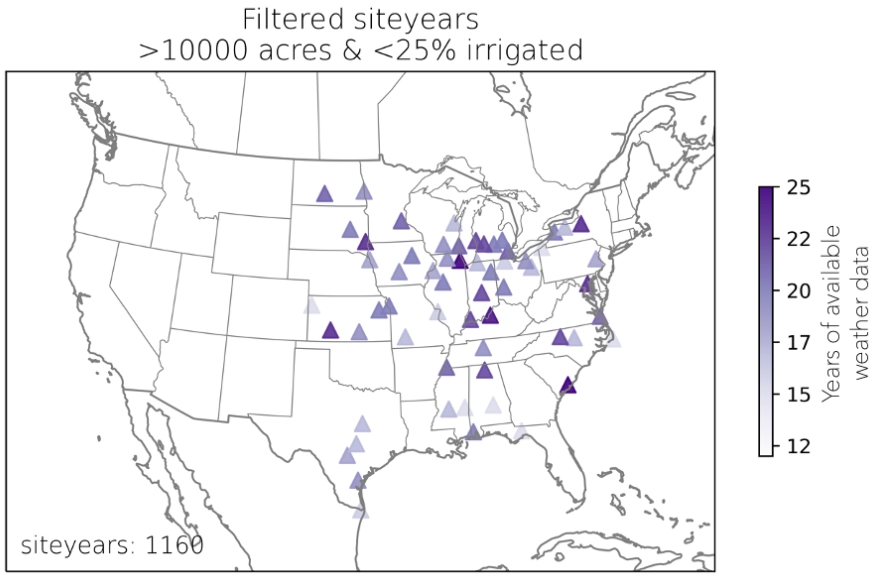

Figure C.1: Simulation sites and number of years simulated with available weather station data.

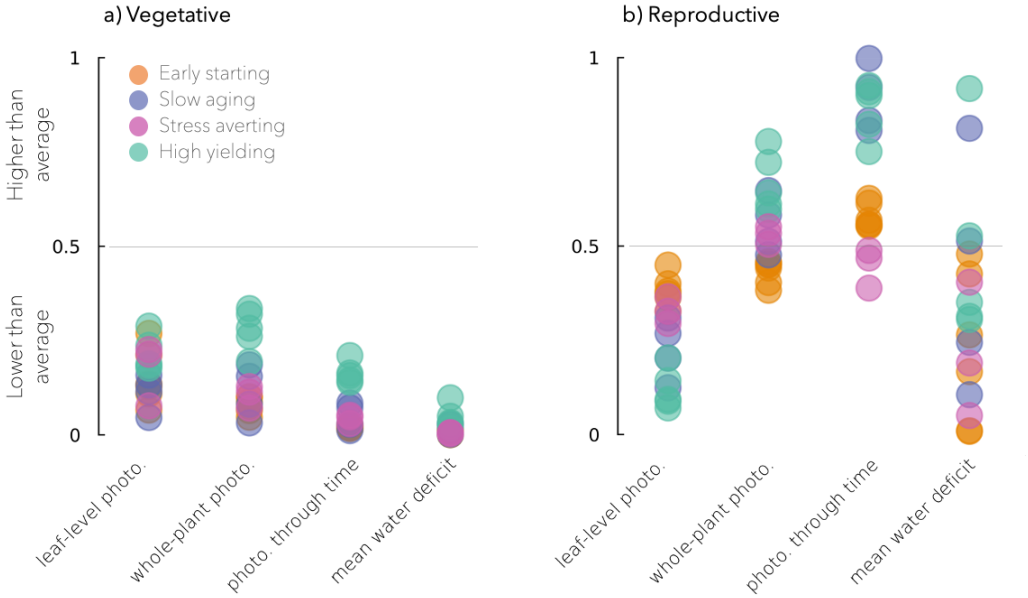

Figure C.2: Mechanisms. Leaf-level photosynthetic rate, whole-plant level photosynthetic rate, whole plant level accumulated carbon through time, mean water deficit.

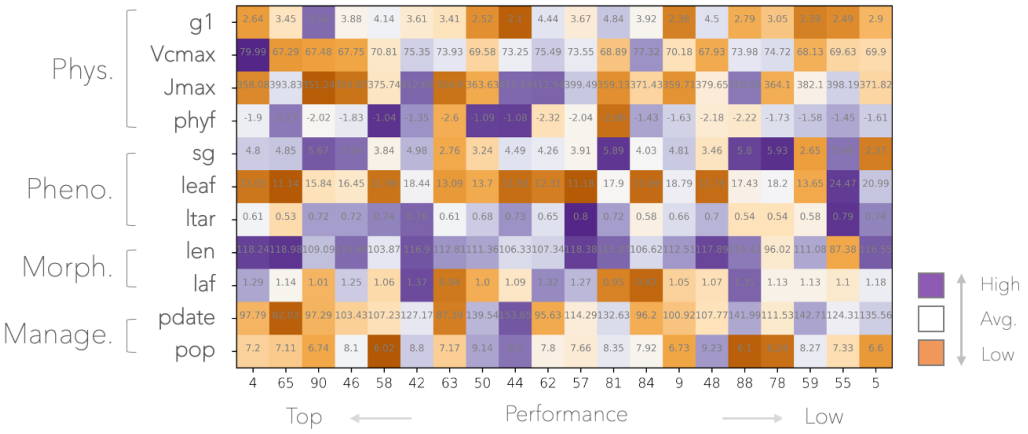

Figure C.3: Parameter values of top 20 performing T × M combinations. Colors show standardized parameter value among all T × M combinations, in which purple indicates higher-than average parameter values and orange for lower-than average parameter values when compared to all other T × M combinations. Gray values within each cell shows the raw parameter value.

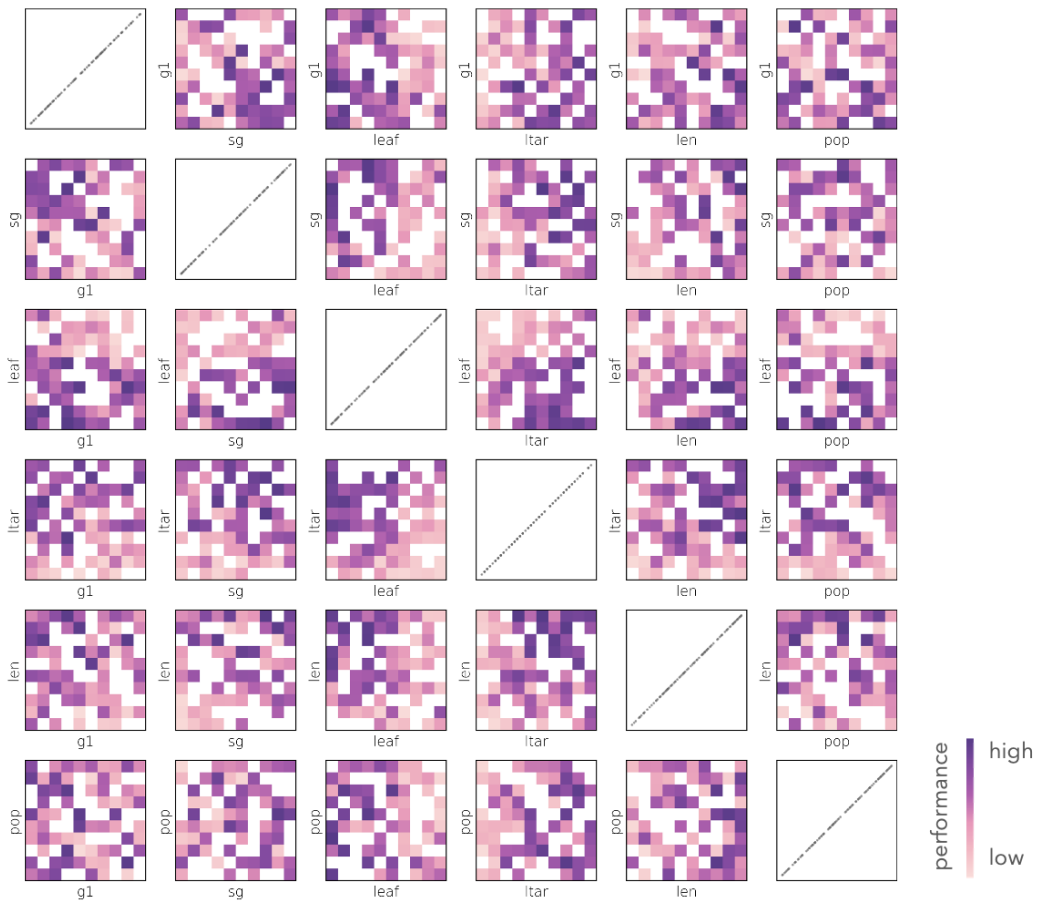

Figure C.4: Performance of T × M combinations within parameter space for key parameters.

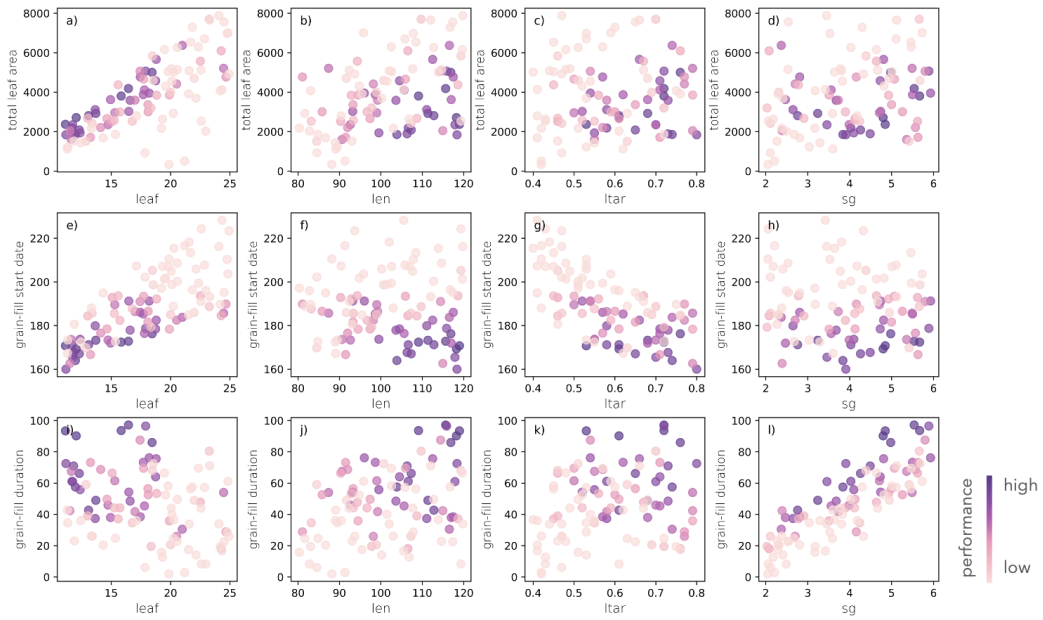

Figure C.5: Correlation between key parameters (*juv_leaves*, *lm_min*, *rmax_ltar*, *staygreen*) and emergent properties (total leaf area, grain-filling duration, grain-filling start date) for all T × M combinations. Filled colors indicate performance of T × M combinations.

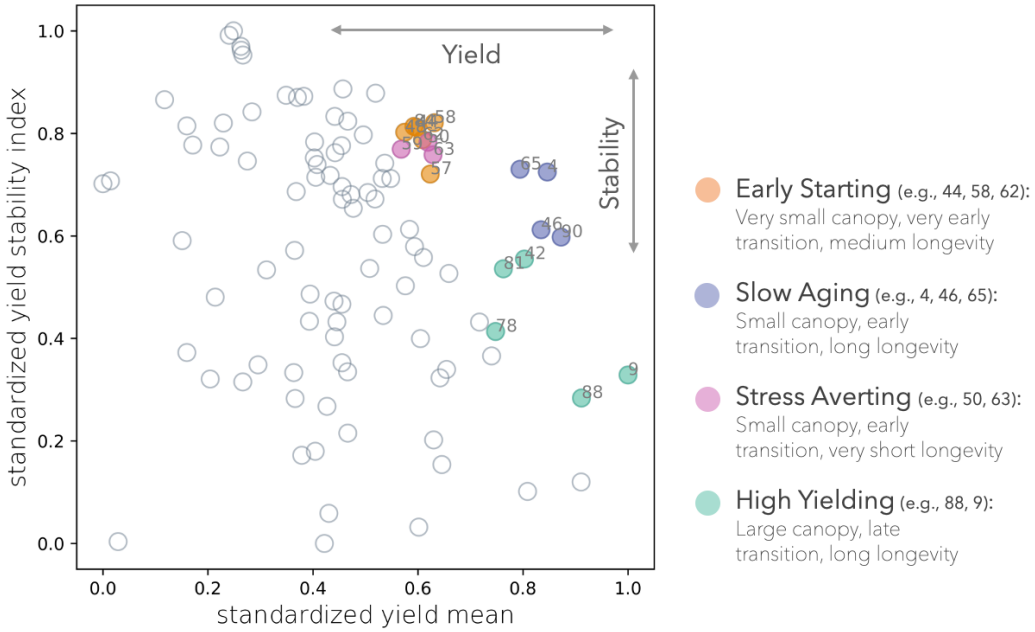

Figure C.6: Standardized mean yield across all site-years and standardized yield stability across simulation years averaged across all sites for all T × M combinations. Top performing combinations have filled in colors that indicate performance based on ranking methods described in section C.3. Select top performing strategies among T × M combinations are shown in large colored circles that correspond to descriptions on the right.

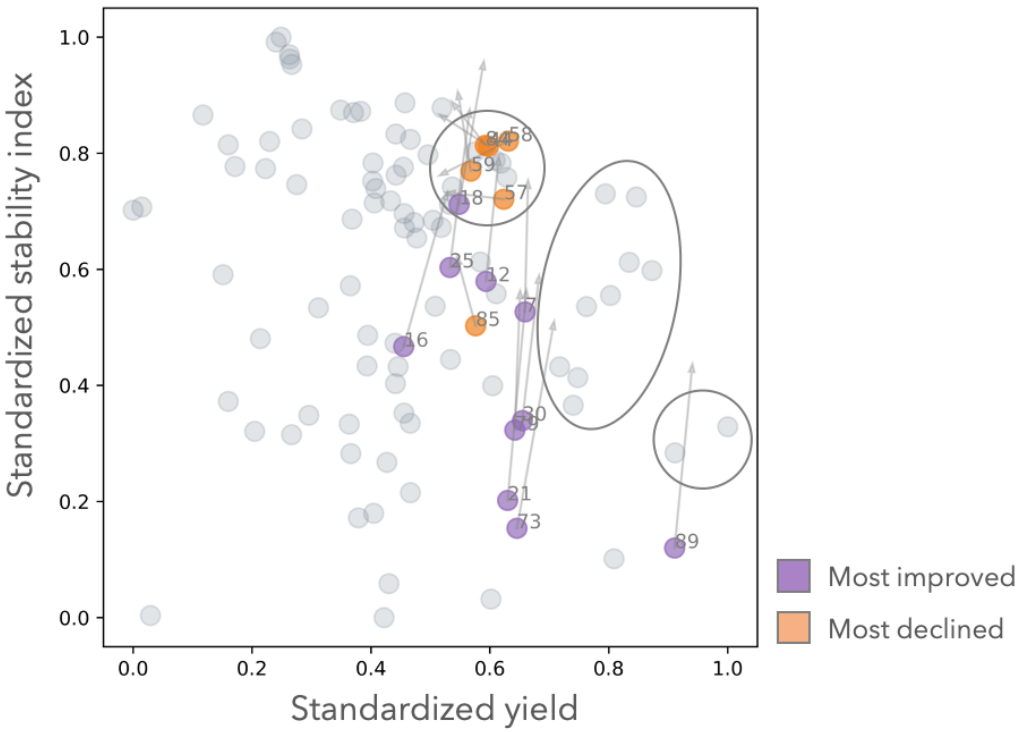

Figure C.7: Most improved (purple) and declined (orange) T × M combinations under year 2100 future simulations (greater than 10% change in rank). Scatter points show present-day yield and yield dispersion values for all T × M combinations while the arrows show shifts in yield and yield dispersion space under 2100 future climate simulations for the most improved and declined T × M combinations. Top 20 performers under present-day climate are circled in solid gray outlines.

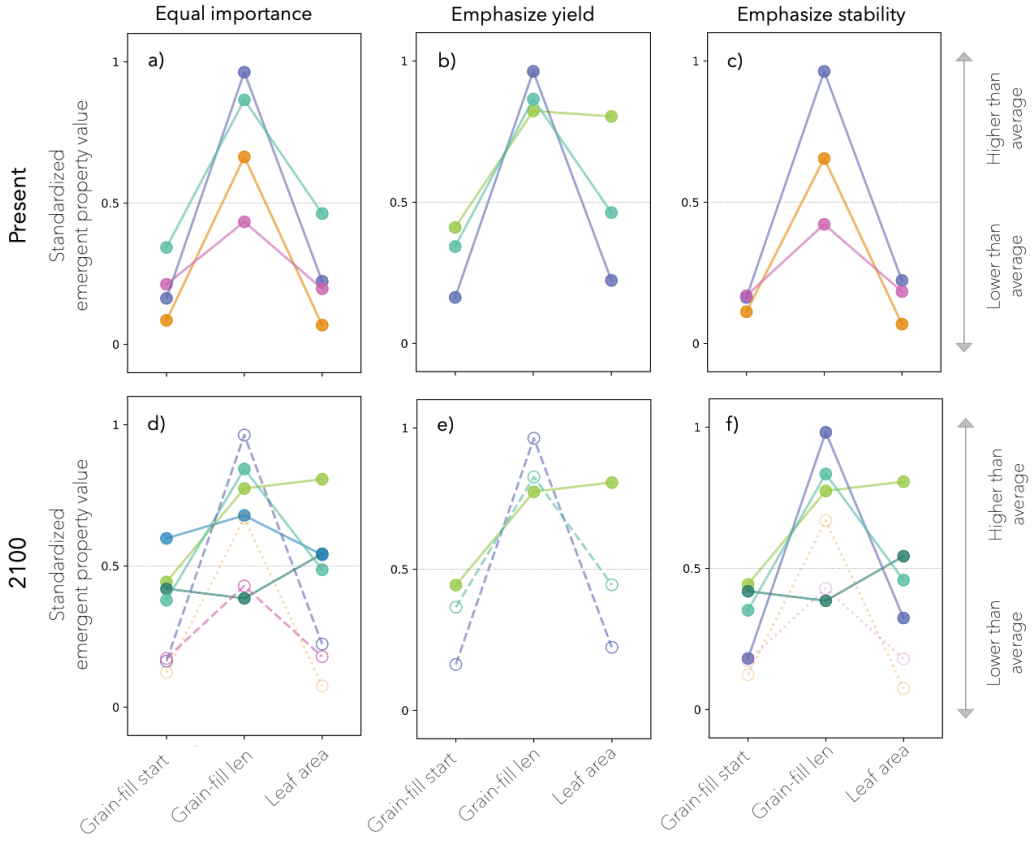

Figure C.8: Selected strategies among top performing T × M combinations under present-day climate (a-c) and their performance shifts by 2100 (d-f), under assumptions of equal importance of yield and yield stability (a, d), greater importance of yield (b, e), and greater importance of yield stability (c, f). Solid lines show top-performing strategies that improved in performance ranking, dashed lines indicate strategies that remained similar in performance rankings, and faded lines show strategies that dropped out as top performing by the end of the century.

BIBLIOGRAPHY

M. Abberton, J. Batley, A. Bentley, J. Bryant, H. Cai, J. Cockram, A. Costa de Oliveira, L. J. Cseke, H. Dempewolf, C. De Pace, D. Edwards, P. Gepts, A. Greenland, A. E. Hall, R. Henry, K. Hori, G. T. Howe, S. Hughes, M. Humphreys, D. Lightfoot, A. Marshall, S. Mayes, H. T. Nguyen, F. C. Ogbonnaya, R. Ortiz, A. H. Paterson, R. Tuberosa, B. Valliyodan, R. K. Varshney, and M. Yano. Global agricultural intensification during climate change: A role for genomics. *Plant Biotechnology Journal*, 14(4):1095–1098, 2016. ISSN 14677652. doi: 10.1111/pbi.12467.

L. J. Abendroth, F. E. Miguez, M. J. Castellano, P. R. Carter, C. D. Messina, P. M. Dixon, and J. L. Hatfield. Lengthening of maize maturity time is not a widespread climate change adaptation strategy in the US Midwest. *Global Change Biology*, 27(11):2426–2440, 2021. ISSN 13652486. doi: 10.1111/gcb.15565.

R. P. Allan, M. Barlow, M. P. Byrne, A. Cherchi, H. Douville, H. J. Fowler, T. Y. Gan, A. G. Pendergrass, D. Rosenfeld, A. L. Swann, L. J. Wilcox, and O. Zolina. Advances in understanding large-scale responses of the water cycle to climate change. *Annals of the New York Academy of Sciences*, 1472(1):49–75, 2020. ISSN 17496632. doi: 10.1111/nyas.14337.

D. Andrivon, C. Giorgetti, A. Baranger, A. Calonnec, P. Cartolaro, R. Faivre, S. Guyader, P. E. Lauri, F. Lescourret, L. Parisi, B. Ney, B. Tivoli, and I. Sache. Defining and designing plant architectural ideotypes to control epidemics ? *Eur J Plant Patol*, 2012. doi: 10.1007/s10658-012-0126-y.

L. Arve, S. Torre, J. Olsen, and K. Tanino. Stomatal Responses to Drought Stress and Air Humidity. In A. Shanker and B. Venkateswarlu, editors, *Abiotic Stress in Plants - Mechanisms and Adaptation*, chapter 12. IntechOpen, Rijeka, 2011. doi: 10.5772/24661.

S. Asseng, F. Ewert, P. Martre, and R. P. Rötter. Rising temperatures reduce global wheat production. *Nature Climate Change*, 5(2):143–147, 2015. doi: 10.1038/nclimate2470.

J. T. Ball, I. E. Woodrow, and J. A. Berry. A model predicting stomatal conductance and its contribution to the control of photosynthesis under different environmental conditions. *Progress in photosynthesis research*, 4(5):221–224, 1987. doi: 10.1007/978-94-017-0519-6_48.

T. Barker, H. Campos, M. Cooper, D. Dolan, G. Edmeades, J. Habben, J. Schussler, D. Wright, and C. Zinselmeier. Improving Drought Tolerance in Maize. In J. Janick, editor, *Plant Breeding Reviewers*, volume 25. 2005. ISBN 9780471666936.

G. A. Barron-Gafford, K. A. Grieve, and R. Murthy. Leaf- and stand-level responses of a forested mesocosm to independent manipulations of temperature and vapor pressure deficit. *New Phytologist*, 174(3):614–625, 2007. doi: 10.1111/j.1469-8137.2007.02035.x.

B. Basso and J. Antle. Digital agriculture to design sustainable agricultural systems. *Nature Sustainability*, 3(4):254–256, 2020. ISSN 23989629. doi: 10.1038/s41893-020-0510-0.

S. Bassu, N. Brisson, J.-L. Durand, K. Boote, J. Lizaso, J. W. Jones, C. Rosenzweig, A. C. Ruane, M. Adam, C. Baron, B. Basso, C. Biernath, H. Boogaard, S. Conijn, M. Corbeels, D. Deryng, G. D. Sanctis, S. Gayler, P. Grassini, J. Hatfield, S. Hoek, C. Izaurralde, R. Jongschaap, A. R. Kemanian, K. C. Kersebaum, S.-H. Kim, N. S. Kumar, D. Makowski, C. Müller, C. Nendel, E. Priesack, M. V. Pravia, F. Sau, I. Shcherbak, F. Tao, E. Teixeira, D. Timlin, and K. Waha. How do various maize crop models vary in their responses to climate change factors? *Global Change Biology*, 20(7):2301–2320, 2014.

D. S. Battisti and R. L. Naylor. Historical warnings of future food insecurity with unprecedented seasonal heat. *Science*, 323(5911):240–244, 2009. doi: 10.1126/science.1164363.

A. Berg, K. Findell, B. Lintner, A. Giannini, S. I. Seneviratne, B. van den Hurk, R. Lorenz, A. Pitman, S. Hagemann, A. Meier, F. Cheruy, A. Ducharne, S. Malyshev, and P. C. D.

Milly. Land-atmosphere feedbacks amplify aridity increase over land under global warming. *Nature Climate Change*, 6(9):869–874, 2016. doi: 10.1038/nclimate3029.

J. Bolaños and G. O. Edmeades. The importance of the anthesis-silking interval in breeding for drought tolerance in tropical maize. *Field Crops Research*, 48(1):65–80, 1996. ISSN 03784290. doi: 10.1016/0378-4290(96)00036-6.

K. J. Boote, J. W. Jones, J. W. White, S. Asseng, and J. I. Lizaso. Putting mechanisms into crop production models. *Plant, Cell and Environment*, 36(9):1658–1672, 2013. ISSN 01407791. doi: 10.1111/pce.12119.

K. J. Boote, J. W. Jones, and G. Hoogenboom. Incorporating realistic trait physiology into crop growth models to support genetic improvement. *In Silico Plants*, 3(1):1–19, 2021. ISSN 25175025. doi: 10.1093/insilicoplants/diab002.

D. D. Breshears, H. D. Adams, D. Eamus, N. G. McDowell, D. J. Law, R. E. Will, A. P. Williams, and C. B. Zou. The critical amplifying role of increasing atmospheric moisture demand on tree mortality and associated regional die-off. *Frontiers in Plant Science*, 4 (266), 2013. doi: 10.3389/fpls.2013.00266.

E. S. Buckler, J. B. Holland, P. J. Bradbury, C. B. Acharya, P. J. Brown, C. Browne, E. Ersoz, S. Flint-Garcia, A. Garcia, J. C. Glaubitz, M. M. Goodman, C. Harjes, K. Guill, D. E. Kroon, S. Larsson, N. K. Lepak, H. Li, S. E. Mitchell, G. Pressoir, J. A. Peiffer, M. O. Rosas, T. R. Rocheford, M. C. Romay, S. Romero, S. Salvo, H. S. Villeda, H. S. da Silva, Q. Sun, F. Tian, N. Upadyayula, D. Ware, H. Yates, J. Yu, Z. Zhang, S. Kresovich, and M. D. McMullen. The genetic architecture of maize flowering time. *Science*, 325(5941):714–718, 2009. doi: 10.1126/science.1174276.

J. A. Bunce. How do leaf hydraulics limit stomatal conductance at high water vapour pressure deficits? *Plant, Cell & Environment*, 29(8):1644–1650, 2006. ISSN 1365-3040. doi: 10.1111/j.1365-3040.2006.01541.x.

M. B. Burke, D. B. Lobell, and L. Guarino. Shifts in African crop climates by 2050 ,

and the implications for crop improvement and genetic resources conservation. *Global Environmetnal Change*, 19:317–325, 2009. doi: 10.1016/j.gloenvcha.2009.04.003.

E. E. Butler and P. Huybers. Adaptation of US maize to temperature variations. *Nature Climate Change*, 3(1):68–72, 2013. ISSN 1758678X. doi: 10.1038/nclimate1585.

E. E. Butler, N. D. Mueller, and P. Huybers. Peculiarly pleasant weather for US maize. *PNAS*, 115(47), 2018. doi: 10.1073/pnas.1808035115.

M. P. Byrne and P. A. O'Gorman. Understanding decreases in land relative humidity with global warming: Conceptual model and GCM simulations. *Journal of Climate*, 29(24): 9045–9061, 2016. ISSN 08948755. doi: 10.1175/JCLI-D-16-0351.1.

R. Çakir. Effect of water stress at different development stages on vegetative and reproductive growth of corn. *Field Crops Res.*, 89(1):1–16, 2004. ISSN 03784290. doi: 10.1016/j.fcr.2004.01.005.

G. S. Campbell. Extinction coefficients for radiation in plant canopies calculated using an ellipsoidal inclination angle distribution. Technical report, 1986.

V. B. Cardwell. Fifty Years of Minnesota Corn Production: Sources of Yield Increase1. *Agronomy Journal*, 74(6):984, 1982. doi: 10.2134/agronj1982.00021962007400060013x.

S. Ceccarelli. Plant breeding and climate changes. (148):627–637, 2010. doi: 10.1017/S0021859610000651.

A. J. Challinor, J. Watson, D. B. Lobell, S. M. Howden, D. R. Smith, and N. Chhetri. A meta-analysis of crop yield under climate change and adaptation. *Nature Climate Change*, 4(4):287–291, 2014. doi: 10.1038/nclimate2153.

A. J. Challinor, C. Müller, S. Asseng, C. Deva, K. J. Nicklin, D. Wallach, E. Vanuytrecht, S. Whitfield, J. Ramirez-Villegas, and A. K. Koehler. Improving the use of crop models for risk assessment and climate change adaptation. *Agricultural Systems*, 159:296–306, 2017. doi: 10.1016/j.agsy.2017.07.010.

J. A. Chun, Q. Wang, D. Timlin, D. Fleisher, and V. R. Reddy. Effect of elevated carbon dioxide and water stress on gas exchange and water use efficiency in corn. *Agricultural and Forest Meteorology*, 151(3):378–384, 2011. ISSN 01681923. doi: 10.1016/j.agrformet.2010.11.015.

G. J. Collatz, M. Ribas-Carbo, and J. A. Berry. Coupled Photosynthesis-Stomatal Conductance Model for Leaves of C4 Plants. *Australian Journal of Plant Physiology*, 19(5):519–538, 1992. doi: 10.1071/PP9920519.

M. Collins, R. Knutti, J. Arblaster, J.-L. Dufresne, T. Fichefet, P. Friedlingstein, X. Gao, W. Gutowski, T. Johns, G. Krinner, M. Shongwe., C. Tebaldi, A. Weaver, and M. Mehner. Long-term Climate Change: Projections, Com- mitments and Irreversibility. *Climate Change 2013: The Physical Science Basis. Contribution of Working Group I to the Fifth Assessment Report of the Intergovernmental Panel on Climate Change*, pages 1–108, 2013.

M. Cooper, C. Gho, R. Leafgren, T. Tang, and C. Messina. Breeding drought-tolerant maize hybrids for the US corn-belt: Discovery to product. *Journal of Experimental Botany*, 65(21):6191–6194, 2014a. ISSN 14602431. doi: 10.1093/jxb/eru064.

M. Cooper, C. D. Messina, D. Podlich, L. R. Totir, A. Baumgarten, N. J. Hausmann, D. Wright, and G. Graham. Predicting the future of plant breeding: Complementing empirical evaluation with genetic prediction. *Crop and Pasture Science*, 65(4):311–336, 2014b. ISSN 18365795. doi: 10.1071/CP14007.

M. Cooper, F. Technow, C. Messina, C. Gho, and L. Radu Totir. Use of crop growth models with whole-genome prediction: Application to a maize multienvironment trial. *Crop Science*, 56(5):2141–2156, 2016. ISSN 14350653. doi: 10.2135/cropsci2015.08.0512.

M. Cooper, T. Tang, C. Gho, T. Hart, G. Hammer, and C. Messina. Integrating genetic gain and gap analysis to predict improvements in crop productivity. *Crop Science*, 60(2):582–604, 2020. ISSN 14350653. doi: 10.1002/csc2.20109.

P. Q. Craufurd and T. R. Wheeler. Climate change and the flowering time of annual crops. *J. Exp. Bot.*, 60(9):2529–2539, 2009. ISSN 0022-0957. doi: 10.1093/jxb/erp196.

R. I. Cukier, C. M. Fortuin, K. E. Shuler, A. G. Petschek, and J. H. Schaibly. Study of the sensitivity of coupled reaction systems to uncertainties in rate coefficients. I Theory. *Journal of Chemical Physics*, 59(8):3873–3878, 1973. ISSN 10897690. doi: 10.1063/1.1680571.

M. E. Day. Influence of temperature and leaf-to-air vapor pressure deficit on net photosynthesis and stomatal conductance in red spruce {(Picea} rubens). *Tree Physiology*, 20(1): 57–63, 2000. ISSN 0829-318X. doi: 10.1093/treephys/20.1.57.

D. G. G. de Pury and G. D. Farquhar. Simple scaling of photosynthesis from leaves to canopies without the errors of big-leaf models. *Plant, Cell & Environment*, 20:537–557, 1997.

D. Deryng, W. J. Sacks, C. C. Barford, and N. Ramankutty. Simulating the effects of climate and agricultural management practices on global crop yield. *Global Biogeochemical Cycles*, 25(2):n/a–n/a, 2011. ISSN 0886-6236. doi: 10.1029/2009gb003765.

C. M. Donald. The breeding of crop ideotypes. *Euphytica*, 17:385–403, 1968.

M. G. Donat, A. J. Pitman, and S. I. Seneviratne. Regional warming of hot extremes accelerated by surface energy fluxes. *Geophysical Research Letters*, 44(13):7011–7019, 2017. ISSN 19448007. doi: 10.1002/2017GL073733.

J.-L. Durand, K. Delusca, K. Boote, J. Lizaso, R. Manderscheid, H. J. Weigel, A. C. Ruane, C. Rosenzweig, J. Jones, L. Ahuja, S. Anapalli, B. Basso, C. Baron, P. Bertuzzi, C. Biernath, D. Deryng, F. Ewert, T. Gaiser, S. Gayler, F. Heinlein, K. C. Kersebaum, S.-H. Kim, C. Müller, C. Nendel, A. Olioso, E. Priesack, J. R. Villegas, D. Ripoche, R. P. Rötter, S. I. Seidel, A. Srivastava, F. Tao, D. Timlin, T. Twine, E. Wang, H. Webber, and Z. Zhao. How accurately do maize crop models simulate the interactions of atmospheric CO2 concentration levels with limited water supply on water use and yield? *Eur J Agron*, 100:67–75, 2018.

D. N. Duvick. The Contribution of Breeding to Yield Advances in maize (Zea mays L.), 2005. ISSN 00652113.

D. N. Duvick and K. G. Cassman. Post–Green Revolution Trends in Yield Potential of Temperate Maize in the North-Central United States. pages 1622–1630, 1999. doi: 10.2135/cropsci1999.3961622x.

M. J. Dzievit, X. Li, and J. Yu. Dissection of Leaf Angle Variation in Maize through Genetic Mapping and Meta-Analysis. *The Plant Genome*, 12(1):180024, 2019. ISSN 1940-3372. doi: 10.3835/plantgenome2018.05.0024.

D. Eamus, N. Boulain, J. Cleverly, and D. D. Breshears. Global change-type drought-induced tree mortality: vapor pressure deficit is more important than temperature per se in causing decline in tree health. *Ecology and Evolution*, 3(8):2711–2729, 2013. ISSN 20457758. doi: 10.1002/ece3.664.

F. Ewert, R. P. Rötter, M. Bindi, H. Webber, M. Trnka, K. C. Kersebaum, J. E. Olesen, M. K. van Ittersum, S. Janssen, M. Rivington, M. A. Semenov, D. Wallach, J. R. Porter, D. Stewart, J. Verhagen, T. Gaiser, T. Palosuo, F. Tao, C. Nendel, P. P. Roggero, L. Bartošová, and S. Asseng. Crop modelling for integrated assessment of risk to food production from climate change. *Environmental Modelling and Software*, 72(C):287–303, 2015. doi: 10.1016/j.envsoft.2014.12.003.

M. Farooq, A. Wahid, N. Kobayashi, D. Fujita, and S. M. A. Basra. Plant drought stress: effects, mechanisms and management. *Agronomy for Sustainable Development*, 29(1): 185–212, 2009. doi: 10.1051/agro:2008021.

R. A. Fischer and G. O. Edmeades. Breeding and cereal yield progress. *Crop Science*, 50: S–85–S–98, 2010. ISSN 14350653. doi: 10.2135/cropsci2009.10.0564.

T. Fischer, D. Byerlee, and G. Edmeades. *Crop yields and global food security: will yield increase continue to feed the world?* Australian Center for International Agricultural Research, Canberra, 2014.

A. Fita, A. Rodríguez-Burruezo, M. Boscaiu, J. Prohens, and O. Vicente. Breeding and domesticating crops adapted to drought and salinity: A new paradigm for increasing food

production. *Frontiers in Plant Science*, 6:1–14, 2015. ISSN 1664462X. doi: 10.3389/fpls.2015.00978.

P. J. Franks, J. A. Berry, D. L. Lombardozzi, and G. B. Bonan. Stomatal Function across Temporal and Spatial Scales: Deep-Time Trends, Land-Atmosphere Coupling and Global Models. *Plant Physiology*, 174(2):583–602, 2017. doi: 10.1104/pp.17.00287.

Q. Fu and S. Feng. Response of terrestrial aridity to global warming. *Journal of Geophysical Research-Atmospheres*, 119:7863–7875, 2014. ISSN 00280836. doi: 10.1038/175238c0.

J. Gaffney, J. Schussler, C. Löffler, W. Cai, S. Paszkiewicz, C. Messina, J. Groeteke, J. Keaschall, and M. Cooper. Industry-scale evaluation of maize hybrids selected for increased yield in drought-stress conditions of the US corn belt. *Crop Science*, 55(4):1608–1618, 2015. ISSN 14350653. doi: 10.2135/cropsci2014.09.0654.

O. Ghannoum. C4 photosynthesis and water stress. *Annals of Botany*, 103(4):635–644, 2009. doi: 10.1093/aob/mcn093.

O. Ghannoum, S. V. Caemmerer, L. H. Ziska, and J. P. Conroy. The growth response of C4 plants to rising atmospheric CO2 partial pressure: a reassessment. *Plant, Cell & Environment*, 23(9):931–942, 2000. doi: 10.1046/j.1365-3040.2000.00609.x.

H. C. J. Godfray, J. R. Beddington, I. R. Crute, L. Haddad, D. Lawrence, J. F. Muir, J. Pretty, S. Robinson, S. M. Thomas, and C. Toulmin. Food Security: The Challenge of Feeding 9 Billion People. *Science*, 327(5967):812–818, 2010. doi: 10.1126/science.1185383.

P. L. Gregersen, A. Culetic, L. Boschian, and K. Krupinska. Plant senescence and crop productivity. *Plant Molecular Biology*, 82(6):603–622, 2013. ISSN 01674412. doi: 10.1007/s11103-013-0013-8.

G. Hammer, M. Cooper, F. Tardieu, S. Welch, B. Walsh, F. van Eeuwijk, S. Chapman, and D. Podlich. Models for navigating biological complexity in breeding improved crop plants. *Trends in Plant Science*, 11(12):587–593, 2006. ISSN 13601385. doi: 10.1016/j.tplants.2006.10.006.

G. Hammer, G. McLean, E. Oosterom, S. Chapman, B. Zheng, A. Wu, A. Doherty, and D. Jordan. Designing crops for adaptation to the drought and high temperature risks anticipated in future climates. *Crop Science*, pages 1–17, 2020. ISSN 0011-183X. doi: 10.1002/csc2.20110.

G. L. Hammer, Z. Dong, G. McLean, A. Doherty, C. Messina, J. Schussler, C. Zinselmeier, S. Paszkiewicz, and M. Cooper. Can changes in canopy and/or root system architecture explain historical maize yield trends in the U.S. corn belt? *Crop Science*, 49(1):299–312, 2009. ISSN 0011183X. doi: 10.2135/cropsci2008.03.0152.

M. T. Harrison, F. Tardieu, Z. Dong, C. D. Messina, and G. L. Hammer. Characterizing drought stress and trait influence on maize yield under current and future conditions. *Global Change Biology*, 20(3):867–878, 2014. ISSN 13541013. doi: 10.1111/gcb.12381.

J. L. Hatfield and C. L. Walthall. Meeting Global Food Needs : Realizing the Potential via Genetics × Environment × Management Interactions. pages 1215–1226, 2015. doi: 10.2134/agronj15.0076.

J. Hsiao, A. L. S. Swann, and S.-H. Kim. Maize yield under a changing climate: The hidden role of vapor pressure deficit. *Agricultural and Forest Meteorology*, 279:107692, 2019. ISSN 01681923. doi: 10.1016/j.agrformet.2019.107692.

J. Hsiao, S.-H. Kim, D. J. Timlin, N. D. Mueller, and A. L. S. Swann. A framework for model-assisted t × e × m exploration in maize. *arXiv*, 2022a. doi: https://doi.org/10.48550/arXiv.2206.02793.

J. Hsiao, S.-H. Kim, D. J. Timlin, N. D. Mueller, and A. L. S. Swann. Model-aided climate adaptation for future maize in the u.s. *submitted*, 2022b.

M. C. Hunter, R. G. Smith, M. E. Schipanski, L. W. Atwood, and D. A. Mortensen. Agriculture in 2050: Recalibrating targets for sustainable intensification. *BioScience*, 67(4):386–391, 2017. ISSN 15253244. doi: 10.1093/biosci/bix010.

IPCC. Summary for Policymakers. 2013.

P. Jennings. Plant Type as a Rice Breeding Objective. *Crop Science*, 4:13–15, 1964.

J. W. Jones, J. M. Antle, B. Basso, K. J. Boote, R. T. Conant, I. Foster, H. C. J. Godfray, M. Herrero, R. E. Howitt, S. Janssen, B. A. Keating, R. Munoz-Carpena, C. H. Porter, C. Rosenzweig, and T. R. Wheeler. Brief history of agricultural systems modeling. *Agricultural Systems*, 155:240–254, 2017. ISSN 0308521X. doi: 10.1016/j.agsy.2016.05.014.

S.-H. Kim and J. H. Lieth. A coupled model of photosynthesis, stomatal conductance and transpiration for a rose leaf (Rosa hybrida L.). *Annals of Botany*, 91(7):771–781, 2003. ISSN 0305-7364. doi: 10.1093/aob/mcg080.

S.-H. Kim, R. C. Sicher, H. Bae, D. C. Gitz, J. T. Baker, D. J. Timlin, and V. R. Reddy. Canopy photosynthesis, evapotranspiration, leaf nitrogen, and transcription profiles of maize in response to CO2 enrichment. *Global Change Biology*, 12(3):588–600, 2006. doi: 10.1111/j.1365-2486.2006.01110.x.

S.-H. Kim, D. C. Gitz, R. C. Sicher, J. T. Baker, D. J. Timlin, and V. R. Reddy. Temperature dependence of growth, development, and photosynthesis in maize under elevated {CO2}. *Environ Exp Bot*, 61(3):224–236, 2007. ISSN 0098-8472. doi: 10.1016/j.envexpbot.2007.06.005.

S.-H. Kim, Y. Yang, D. J. Timlin, D. H. Fleisher, A. Dathe, V. R. Reddy, and K. Staver. Modeling temperature responses of leaf growth, development, and biomass in maize with MAIZSIM. *Agronomy Journal*, 104(6):1523–1537, 2012. doi: 10.2134/agronj2011.0321.

B. A. Kimball, K. J. Boote, J. L. Hatfield, L. R. Ahuja, C. Stockle, S. Archontoulis, C. Baron, B. Basso, P. Bertuzzi, J. Constantin, D. Deryng, B. Dumont, J. L. Durand, F. Ewert, T. Gaiser, S. Gayler, M. P. Hoffmann, Q. Jiang, S. H. Kim, J. Lizaso, S. Moulin, C. Nendel, P. Parker, T. Palosuo, E. Priesack, Z. Qi, A. Srivastava, T. Stella, F. Tao, K. R. Thorp, D. Timlin, T. E. Twine, H. Webber, M. Willaume, and K. Williams. Simulation of maize evapotranspiration: An inter-comparison among 29 maize models. *Agricultural and Forest Meteorology*, 271:264–284, 2019. ISSN 01681923. doi: 10.1016/j.agrformet.2019.02.037.

C. J. Kucharik. Contribution of planting date trends to increased maize yields in the central United States. *Agronomy Journal*, 100(2):328–336, 2008. ISSN 00021962. doi: 10.2134/agronj2007.0145.

A. D. Leakey, M. Uribelarreà, E. A. Ainsworth, S. L. Naidu, A. Rogers, D. R. Ort, and S. P. Long. Photosynthesis, productivity, and yield of maize are not affected by open-air elevation of CO2 concentration in the absence of drought. *Plant Physiology*, 140(2): 779–790, 2006. ISSN 00320889. doi: 10.1104/pp.105.073957.

A. D. B. Leakey, E. A. Ainsworth, C. J. Bernacchi, A. Rogers, S. P. Long, and D. R. Ort. Elevated CO2 effects on plant carbon, nitrogen, and water relations: six important lessons from FACE. *Journal of Experimental Botany*, 60(10):2859–2876, 2009. doi: 10.1093/jxb/erp096.

J. I. Lizaso, W. D. Batchelor, and M. E. Westgate. A leaf area model to simulate cultivar-specific expansion and senescence of maize leaves. *Field Crops Research*, 80(1):1–17, 2003. ISSN 03784290. doi: 10.1016/S0378-4290(02)00151-X.

D. B. Lobell. Climate change adaptation in crop production: Beware of illusions. *Global Food Security*, 3(2):72–76, 2014. ISSN 22119124. doi: 10.1016/j.gfs.2014.05.002.

D. B. Lobell, M. B. Burke, C. Tebaldi, M. D. Mastrandrea, W. P. Falcon, and R. L. Naylor. Prioritizing climate change adaptation needs for food security in 2030. *Science*, 319(5863): 607–610, 2008. doi: 10.1126/science.1152339.

D. B. Lobell, M. Bänziger, C. Magorokosho, and B. Vivek. Nonlinear heat effects on African maize as evidenced by historical yield trials. *Nature Climate Change*, 1(1):42–45, 2011a. doi: 10.1038/nclimate1043.

D. B. Lobell, W. Schlenker, and J. Costa-Roberts. Climate trends and global crop production since 1980. *Science*, 333(6042):616–620, 2011b. doi: 10.1126/science.1206376.

D. B. Lobell, G. L. Hammer, G. McLean, C. Messina, M. J. Roberts, and W. Schlenker. The critical role of extreme heat for maize production in the United States. *Nature Climate Change*, 3(5):497–501, 2013. ISSN 1758-678X. doi: 10.1038/nclimate1832.

R. Manderscheid, M. Erbs, and H.-J. Weigel. Interactive effects of free-air CO2 enrichment and drought stress on maize growth. *European Journal of Agronomy*, 52:11–21, 2014. doi: 10.1016/j.eja.2011.12.007.

P. Martre, B. Quilot-Turion, D. Luquet, M. M. O. S. Memmah, K. Chenu, and P. Debaeke. Model-assisted phenotyping and ideotype design. *Crop Physiology: Applications for Genetic Improvement and Agronomy: Second Edition*, (Chapter 1):349–373, 2015. doi: 10.1016/B978-0-12-417104-6.00014-5.

S. McCouch, G. J. Baute, J. Bradeen, P. Bramel, P. K. Bretting, E. Buckler, J. M. Burke, D. Charest, S. Cloutier, G. Cole, H. Dempewolf, M. Dingkuhn, C. Feuillet, P. Gepts, D. Grattapaglia, L. Guarino, S. Jackson, S. Knapp, P. Langridge, A. Lawton-Rauh, Q. Lijua, C. Lusty, T. Michael, S. Myles, K. Naito, R. L. Nelson, R. Pontarollo, C. M. Richards, L. Rieseberg, J. Ross-Ibarra, S. Rounsley, R. S. Hamilton, U. Schurr, N. Stein, N. Tomooka, E. van der Knaap, D. van Tassel, J. Toll, J. Valls, R. K. Varshney, J. Ward, R. Waugh, P. Wenzl, and D. Zamir. Feeding the future. *Nature*, 499(7456):23–24, 2013. ISSN 1476-4687. doi: 10.1038/499023a.

M. D. McKay, R. J. Beckman, and W. J. Conover. A comparison of three methods for selecting values of input variables in the analysis of output from a computer code. *Technometrics*, 21(2):239–245, 1979. ISSN 15372723. doi: 10.1080/00401706.2000.10485979.

G. S. McMaster, W. W. Wilhelm, and A. B. Frank. Developmental sequences for simulating crop phenology for water-limiting conditions. *Australian Journal of Agricultural Research*, 56(11):1277–1288, 2005. ISSN 00049409. doi: 10.1071/AR05068.

B. E. Medlyn, R. A. Duursma, D. Eamus, D. S. Ellsworth, I. C. Prentice, C. V. M. Barton, K. Y. Crous, P. De Angelis, M. Freeman, and L. Wingate. Reconciling the optimal and empirical approaches to modelling stomatal conductance. *Global Change Biology*, 17(6): 2134–2144, 2011. doi: 10.1111/j.1365-2486.2010.02375.x.

C. D. Messina, D. Podlich, Z. Dong, M. Samples, and M. Cooper. Yield-trait performance

landscapes: From theory to application in breeding maize for drought tolerance. *Journal of Experimental Botany*, 62(3):855–868, 2011. ISSN 00220957. doi: 10.1093/jxb/erq329.

C. D. Messina, T. R. Sinclair, G. L. Hammer, D. Curan, J. Thompson, Z. Oler, C. Gho, and M. Cooper. Limited-transpiration trait may increase maize drought tolerance in the US corn belt. *Agronomy Journal*, 107(6):1978–1986, 2015. ISSN 14350645. doi: 10.2134/agronj15.0016.

C. D. Messina, M. Cooper, G. L. Hammer, D. Berning, I. Ciampitti, R. Clark, C. Diepenbrock, C. Gho, M. Jines, T. Lee, R. McCormick, E. Mihura, D. Podlich, J. Rotundo, M. Smalley, T. Tang, S. Truong, and F. van Eeuwijk. Two decades of creating drought tolerant maize and underpinning prediction technologies in the US corn-belt: Review and perspectives on the future of crop design. *bioRxiv*, 2020a. ISSN 26928205. doi: 10.1101/2020.10.29.361337.

C. D. Messina, M. Cooper, M. Reynolds, and G. L. Hammer. Crop science: A foundation for advancing predictive agriculture. *Crop Science*, 60(2):544–546, 2020b. ISSN 14350653. doi: 10.1002/csc2.20116.

M. V. Mickelbart, P. M. Hasegawa, and J. Bailey-Serres. Genetic mechanisms of abiotic stress tolerance that translate to crop yield stability. *Nature Reviews Genetics*, 16(4): 237–251, 2015. ISSN 14710064. doi: 10.1038/nrg3901.

G. L. Miner, W. L. Bauerle, and D. D. Baldocchi. Estimating the sensitivity of stomatal conductance to photosynthesis: a review. *Plant Cell and Environment*, 40(7):1214–1238, 2017. ISSN 13653040. doi: 10.1111/pce.12871.

J. L. Monteith. A Reinterpretation of Stomatal Responses to Humidity. *Plant Cell Environ.*, 18(4):357–364, 1995. ISSN 1365-3040. doi: 10.1111/j.1365-3040.1995.tb00371.x.

K. A. Mott. Leaf hydraulic conductivity and stomatal responses to humidity in amphistomatous leaves. *Plant, Cell & Environment*, 30(11):1444–1449, 2007. ISSN 1365-3040. doi: 10.1111/j.1365-3040.2007.01720.x.

K. A. Mott and D. F. Parkhurst. Stomatal responses to humidity in air and helox. *Plant, Cell & Environment*, 14(5):509–515, 1991. ISSN 1365-3040. doi: 10.1111/j.1365-3040.1991.tb01521.x.

N. D. Mueller, E. E. Butler, K. A. McKinnon, and A. Rhines. Cooling of US Midwest summer temperature extremes from cropland intensification. *Nature Climate Change*, 6 (3), 2016. doi: 10.1038/nclimate2825.

B. Muller and P. Martre. Plant and crop simulation models: Powerful tools to link physiology, genetics, and phenomics. *Journal of Experimental Botany*, 70(9):2339–2344, 2019. ISSN 14602431. doi: 10.1093/jxb/erz175.

H. Nonami. Plant water relations and control of cell elongation at low water potentials. *Journal of Plant Research*, 111(3):373–382, 1998. ISSN 0918-9440. doi: 10.1007/BF02507801.

K. A. Novick, D. L. Ficklin, P. C. Stoy, C. A. Williams, G. Bohrer, A. Oishi, S. A. Papuga, P. D. Blanken, A. Noormets, B. N. Sulman, R. L. Scott, L. Wang, and R. P. Phillips. The increasing importance of atmospheric demand for ecosystem water and carbon fluxes. *Nature Climate Change*, 6(11):1023–1027, 2016. ISSN 1758-678X. doi: 10.1038/nclimate3114.

J. E. Olesen, M. Trnka, K. C. Kersebaum, S. ag, B. Seguin, P.-S. P, F. Rossi, J. Kozyra, and F. Micale. Impacts and adaptation of European crop production systems to climate change. *Eur J Agron*, 34(2):96–112, 2011. ISSN 1161-0301. doi: 10.1016/j.eja.2010.11.003.

A. L. Olmstead and P. W. Rhode. Adapting North American wheat production to climatic challenges, 1839-2009. *Proceedings of the National Academy of Sciences of the United States of America*, 108(2):480–485, 2011. ISSN 10916490. doi: 10.1073/pnas.1008279108.

B. C. O'Neill, C. Tebaldi, D. P. Van Vuuren, V. Eyring, P. Friedlingstein, G. Hurtt, R. Knutti, E. Kriegler, J. F. Lamarque, J. Lowe, G. A. Meehl, R. Moss, K. Riahi, and B. M. Sanderson. The Scenario Model Intercomparison Project (ScenarioMIP) for CMIP6. *Geoscientific Model Development*, 9(9):3461–3482, 2016. ISSN 19919603. doi: 10.5194/gmd-9-3461-2016.

D. R. Ort and S. P. Long. Limits on yields in the corn belt. *Science*, 344(6183):484–485, 2014. ISSN 0036-8075. doi: 10.1126/science.1253884.

T. Osborne, G. Rose, and T. Wheeler. Variation in the global-scale impacts of climate change on crop productivity due to climate model uncertainty and adaptation. *Agricultural and Forest Meteorology*, 170:183–194, 2013. doi: 10.1016/j.agrformet.2012.07.006.

J. M. Padilla and M. E. Otegui. Co-ordination between leaf initiation and leaf appearance in field-grown maize (Zea mays): Genotypic differences in response of rates to temperature. *Annals of Botany*, 96(6):997–1007, nov 2005. ISSN 03057364. doi: 10.1093/aob/mci251.

B. Parent, M. Leclere, S. Lacube, M. A. Semenov, C. Welcker, P. Martre, and F. Tardieu. Maize yields over Europe may increase in spite of climate change, with an appropriate use of the genetic variability of flowering time. *Proceedings of the National Academy of Sciences of the United States of America*, 115(42):10642–10647, 2018. ISSN 10916490. doi: 10.1073/pnas.1720716115.

B. Peng, K. Guan, J. Tang, E. A. Ainsworth, S. Asseng, C. J. Bernacchi, M. Cooper, E. H. Delucia, J. W. Elliott, F. Ewert, R. F. Grant, D. I. Gustafson, G. L. Hammer, Z. Jin, J. W. Jones, H. Kimm, D. M. Lawrence, Y. Li, D. L. Lombardozzi, A. Marshall-colon, C. D. Messina, D. R. Ort, J. C. Schnable, C. E. Vallejos, A. Wu, X. Yin, and W. Zhou. Towards a multiscale crop modeling framework for climate change adaptation assessment. *Nature Plants*, 6(April), 2020. ISSN 2055-0278. doi: 10.1038/s41477-020-0625-3.

S. Peng, J. Huang, J. E. Sheehy, R. C. Laza, R. M. Visperas, X. Zhong, G. S. Centeno, G. S. Khush, and K. G. Cassman. Rice yields decline with higher night temperature from global warming. *Proceedings of the National Academy of Sciences*, 101(27):9971–9975, 2004. doi: 10.1073/pnas.0403720101.

S. Peng, G. S. Khush, P. Virk, Q. Tang, and Y. Zou. Progress in ideotype breeding to increase rice yield potential. *Field Crops Research*, 108(1):32–38, 2008. ISSN 03784290. doi: 10.1016/j.fcr.2008.04.001.

E. Plischke. An effective algorithm for computing global sensitivity indices (EASI). *Reliability Engineering and System Safety*, 95(4):354–360, 2010. ISSN 09518320. doi: 10.1016/j.ress.2009.11.005.

J. Ramirez-Villegas, J. Watson, and A. J. Challinor. Identifying traits for genotypic adaptation using crop models. *Journal of Experimental Botany*, 66(12):3451–3462, 2015. doi: 10.1093/jxb/erv014.

J. D. Ray, R. W. Gesch, T. R. Sinclair, and L. H. Allen. The effect of vapor pressure deficit on maize transpiration response to a drying soil. *Plant and Soil*, 239(1):113–121, 2002. doi: 10.1023/A:1014947422468.

R. Redden. New approaches for crop genetic adaptation to the abiotic stresses predicted with climate change. *Agronomy*, 3(2):419–432, 2013. ISSN 20734395. doi: 10.3390/agronomy3020419.

J. P. Resop, D. H. Fleisher, D. J. Timlin, D. Mutiibwa, and V. R. Reddy. Climate, water management, and land use: Estimating potential potato and corn production in the U.S. northeastern seaboard region. *Transactions of the ASABE*, 59(6):1539–1553, 2016. ISSN 21510032. doi: 10.13031/trans.59.11748.

M. Reynolds and P. Langridge. Physiological breeding. *Current Opinion in Plant Biology*, 31:162–171, 2016. ISSN 13695266. doi: 10.1016/j.pbi.2016.04.005.

K. Riahi, D. P. van Vuuren, E. Kriegler, J. Edmonds, B. C. O'Neill, S. Fujimori, N. Bauer, K. Calvin, R. Dellink, O. Fricko, W. Lutz, A. Popp, J. C. Cuaresma, S. KC, M. Leimbach, L. Jiang, T. Kram, S. Rao, J. Emmerling, K. Ebi, T. Hasegawa, P. Havlik, F. Humpenöder, L. A. Da Silva, S. Smith, E. Stehfest, V. Bosetti, J. Eom, D. Gernaat, T. Masui, J. Rogelj, J. Strefler, L. Drouet, V. Krey, G. Luderer, M. Harmsen, K. Takahashi, L. Baumstark, J. C. Doelman, M. Kainuma, Z. Klimont, G. Marangoni, H. Lotze-Campen, M. Obersteiner, A. Tabeau, and M. Tavoni. The Shared Socioeconomic Pathways and their energy, land use, and greenhouse gas emissions implications:

An overview. *Global Environmental Change*, 42:153–168, 2017. ISSN 09593780. doi: 10.1016/j.gloenvcha.2016.05.009.

A. J. Rigden, N. D. Mueller, N. M. Holbrook, N. Pillai, and P. Huybers. Combined influence of soil moisture and atmospheric evaporative demand is important for accurately predicting US maize yields. *Nature Food*, 1(2):127–133, 2020. ISSN 2662-1355. doi: 10.1038/s43016-020-0028-7.

G. E. Roesch-McNally, J. Gordon Arbuckle, and J. C. Tyndall. What would farmers do? Adaptation intentions under a Corn Belt climate change scenario. *Agriculture and Human Values*, 34(2):333–346, 2017. ISSN 15728366. doi: 10.1007/s10460-016-9719-y.

R. P. Rötter, F. Tao, J. G. Höhn, and T. Palosuo. Use of crop simulation modelling to aid ideotype design of future cereal cultivars. *Journal of Experimental Botany*, 66(12): 3463–3476, 2015. ISSN 14602431. doi: 10.1093/jxb/erv098.

W. J. Sacks and C. J. Kucharik. Crop management and phenology trends in the U.S. Corn Belt: Impacts on yields, evapotranspiration and energy balance. *Agric. For. Meteorol*, 151(7):882–894, 2011. ISSN 0168-1923. doi: 10.1016/j.agrformet.2011.02.010.

R. F. Sage and D. S. Kubien. The temperature response of C3 and C4 photosynthesis. *Plant, Cell & Environment*, 30(9):1086–1106, 2007. doi: 10.1111/j.1365-3040.2007.01682.x.

H. B. H. Salah and F. Tardieu. Quantitative analysis of the combined effects of temperature, evaporative demand and light on leaf elongation rate in well-watered field and laboratory-grown maize plants. *Journal of Experimental Botany*, 47(11):1689–1698, 1996. doi: 10.1093/jxb/47.11.1689.

P. Sanginés de Cárcer, Y. Vitasse, J. Peñuelas, V. E. Jassey, A. Buttler, and C. Signarbieux. Vapor–pressure deficit and extreme climatic variables limit tree growth. *Global Change Biology*, 24(3):1108–1122, 2018. ISSN 13652486. doi: 10.1111/gcb.13973.

F. E. Satterthwaite. Random Balance Experimentation. *Technometrics*, 1(2):111–137, may 1959. ISSN 0040-1706. doi: 10.1080/00401706.1959.10489853.

J. Schaibly and K. E. Shuler. Study of the sensitivity of coupled reaction systems to uncertainties in rate coefficients. II Applications. *Journal of Chemical Physics*, 59(8): 3873–3878, 1973. ISSN 10897690. doi: 10.1063/1.1680571.

W. Schlenker and M. J. Roberts. Nonlinear temperature effects indicate severe damages to U.S. crop yields under climate change. *Proceedings of the National Academy of Sciences*, 106(37):15594–15598, 2009. ISSN 0027-8424. doi: 10.1073/pnas.0906865106.

M. A. Semenov, P. Stratonovitch, F. Alghabari, and M. J. Gooding. Adapting wheat in Europe for climate change. *Journal of Cereal Science*, 59(3):245–256, 2014. ISSN 10959963. doi: 10.1016/j.jcs.2014.01.006.

A. Shekoofa, T. R. Sinclair, C. D. Messina, and M. Cooper. Variation among maize hybrids in response to high vapor pressure deficit at high temperatures. *Crop Science*, 56(1): 392–396, 2016. ISSN 14350653. doi: 10.2135/cropsci2015.02.0134.

P. A. Shirke and U. V. Pathre. Influence of leaf-to-air vapour pressure deficit (VPD) on the biochemistry and physiology of photosynthesis in Prosopis juliflora. *Journal of Experimental Botany*, 55(405):2111–2120, 2004. doi: 10.1093/jxb/erh229.

L. L. Sloat, S. J. Davis, J. S. Gerber, P. C. West, N. D. Mueller, F. C. Moore, and D. K. Ray. Climate adaptation by crop migration. *Nature Communications*, 11(1243):1–9, 2020. ISSN 2041-1723. doi: 10.1038/s41467-020-15076-4.

Soil Survey Division Staff. Soil Survey Manual - Chapter 3 Examination and description of soils. *Soil Survey Manual*, 18:46–155, 1993.

U. S. D. A. Soil Survey Staff, Natural Resources Conservation Service. Soil Survey Geographic (SSURGO) Database. Available online. Accessed [09/15/2019].

A. Soltani and G. Hoogenboom. Minimum data requirements for parameter estimation of stochastic weather generators. *Climate Research*, 25(2):109–119, 2003. ISSN 0936577X. doi: 10.3354/cr025109.

S. S. Staff. *Soil taxonomy: A basic system of soil classification for making and interpreting soil surveys. 2nd edition. Natural Resources Conservation Service. U.S. Department of Agriculture Handbook 436.* 1999.

C. O. Stockle and J. R. Kiniry. Variability in crop radiation-use efficiency associated with vapor-pressure deficit. *Field Crops Research*, 25(3-4):171–181, 1990. ISSN 03784290. doi: 10.1016/0378-4290(90)90001-R.

C. O. Stöckle, M. Donatelli, and R. Nelson. CropSyst, a cropping systems simulation model. *European Journal of Agronomy*, 18(3-4):289–307, 2003. ISSN 11610301. doi: 10.1016/S1161-0301(02)00109-0.

P. J. Stone, A. J. Pearson, I. B. Sorensen, and B. T. Rogers. Effect of row spacing and plant population on maize yield and quality. *Agronomy New Zealand*, 30:67–75, 2000.

A. L. S. Swann, F. M. Hoffman, C. D. Koven, and J. T. Randerson. Plant responses to increasing CO2 reduce estimates of climate impacts on drought severity. *Proceedings of the National Academy of Sciences*, 113(36):10019–10024, 2016. doi: 10.1073/pnas.1604581113.

V. Tanguilig, E. B. Yambao, J. C. O'Toole, and S. K. De Datta. Water stress effects on leaf elongation, leaf water potential, transpiration, and nutrient uptake of rice, maize, and soybean. *Plant and Soil*, 103:155–168, 1987. ISSN 0032079X. doi: 10.1007/BF02370385.

S. Tarantola, D. Gatelli, and T. A. Mara. Random balance designs for the estimation of first order global sensitivity indices. *Reliability Engineering and System Safety*, 91(6):717–727, 2006. ISSN 09518320. doi: 10.1016/j.ress.2005.06.003.

H. Thomas and H. Ougham. The stay-green trait. *Journal of Experimental Botany*, 65(14):3889–3900, 2014. ISSN 14602431. doi: 10.1093/jxb/eru037.

D. Tilman, C. Balzer, J. Hill, and B. L. Befort. Global food demand and the sustainable intensification of agriculture. *Proceedings of the National Academy of Sciences of the United States of America*, 108(50):20260–20264, 2011. ISSN 00278424. doi: 10.1073/pnas.1116437108.

D. Timlin, Y. A. Pachepsky, and B. Acock. A design for a modular, generic soil simulator to interface with plant models. *Agronomy Journal*, 88(2):162–169, 1996. doi: 10.2134/agronj1996.00021962008800020008x.

D. Timlin, S.-H. Kim, D. Fleisher, Z. Wang, and V. R. Reddy. Chapter 3 - Maize water use and yield in the solar corridor system: a simulation study. In C. L. Deichman and R. J. Kremer, editors, *The Solar Corridor Crop System*, pages 57–78. Academic Press, 2019. ISBN 978-0-12-814792-4. doi: https://doi.org/10.1016/B978-0-12-814792-4.00003-6.

D. J. Timlin, Y. A. Pachepsky, B. A. Acock, and J. Šimunek. {2DSOIL} - A Modular Simulator of Soil and Root Processes. *Agricultural Systems*, 88(2):162–169, 2002. doi: 10.2134/agronj1996.00021962008800020008x.

J. Y. Tissot and C. Prieur. Bias correction for the estimation of sensitivity indices based on random balance designs. *Reliability Engineering and System Safety*, 107:205–213, 2012. ISSN 09518320. doi: 10.1016/j.ress.2012.06.010.

A. Tuzet, A. Perrier, and R. Leuning. A coupled model of stomatal conductance, photosynthesis and transpiration. *Plant, Cell & Environment*, 26(7):1097–1116, 2003.

M. T. van Genuchten. A Closed-form Equation for Predicting the Hydraulic Conductivity of Unsaturated Soils. *Soil Science Society of America Journal*, 44(5):892–898, 1980. doi: https://doi.org/10.2136/sssaj1980.03615995004400050002x.

J. Van Wart, P. Grassini, and K. G. Cassman. Impact of derived global weather data on simulated crop yields. *Global Change Biology*, 19(12):3822–3834, 2013. ISSN 13541013. doi: 10.1111/gcb.12302.

L. R. Vargas Zeppetello, D. S. Battisti, and M. B. Baker. The origin of soil moisture evaporation "regimes". *Journal of Climate*, 32(20):6939–6960, 2019. ISSN 08948755. doi: 10.1175/JCLI-D-19-0209.1.

S. von Caemmerer. *Biochemical Models of Leaf Photosynthesis*. CSIRO Publishing, Collingwood, Victoria, Australia, 2000.

K. P. Voss-Fels, A. Stahl, and L. T. Hickey. Q&A: Modern crop breeding for future food security 07 Agricultural and Veterinary Sciences 0703 Crop and Pasture Production 06 Biological Sciences 0607 Plant Biology 06 Biological Sciences 0604 Genetics. *BMC Biology*, 17(1):1–7, 2019. ISSN 17417007.

J. D. Washburn, M. B. Burch, and J. A. Franco. Predictive breeding for maize: Making use of molecular phenotypes, machine learning, and physiological crop models. *Crop Science*, 60(2):622–638, 2020. ISSN 14350653. doi: 10.1002/csc2.20052.

A. Wu, G. L. Hammer, A. Doherty, S. von Caemmerer, and G. D. Farquhar. Quantifying impacts of enhancing photosynthesis on crop yield. *Nature plants*, 5(4):380–388, 2019. ISSN 20550278. doi: 10.1038/s41477-019-0398-8.

Y. Yang, S.-H. Kim, D. J. Timlin, D. H. Fleisher, B. Quebedeaux, and V. R. Reddy. Simulating canopy transpiration and photosynthesis of corn plants under contrasting water regimes using a coupled model. *Transactions of the ASABE*, 52(3):1011–1024, 2009a. doi: 10.13031/2013.27370.

Y. Yang, D. J. Timlin, D. H. Fleisher, S. H. Kim, B. Quebedeaux, and V. R. Reddy. Simulating leaf area of corn plants at contrasting water status. *Agricultural and Forest Meteorology*, 149(6-7):1161–1167, jun 2009b. doi: 10.1016/j.agrformet.2009.02.005.

X. Yin, M. J. Kropff, G. McLaren, and R. M. Visperas. A nonlinear model for crop development as a function of temperature. *Agricultural and Forest Meteorology*, 77(1-2):1–16, 1995. ISSN 01681923. doi: 10.1016/0168-1923(95)02236-Q.

F. Zabel, C. Müller, J. Elliott, S. Minoli, J. Jägermeyr, J. M. Schneider, J. A. Franke, E. Moyer, M. Dury, L. Francois, C. Folberth, W. Liu, T. A. Pugh, S. Olin, S. S. Rabin, W. Mauser, T. Hank, A. C. Ruane, and S. Asseng. Large potential for crop production adaptation depends on available future varieties. *Global Change Biology*, 27(16):3870–3882, 2021. ISSN 13652486. doi: 10.1111/gcb.15649.

J. Zhang, K. A. Fengler, J. L. Van Hemert, R. Gupta, N. Mongar, J. Sun, W. B. Allen, Y. Wang, B. Weers, H. Mo, R. Lafitte, Z. Hou, A. Bryant, F. Ibraheem, J. Arp, K. Swami-

nathan, S. P. Moose, B. Li, and B. Shen. Identification and characterization of a novel stay-green QTL that increases yield in maize. *Plant Biotechnology Journal*, 17(12):2272–2285, dec 2019. ISSN 14677652. doi: 10.1111/pbi.13139.

S. Zhang, F. Tao, and Z. Zhang. Spatial and temporal changes in vapor pressure deficit and their impacts on crop yields in China during 1980 – 2008. *Journal of Meteorological Research*, 31(4):800–808, 2017. doi: 10.1007/s13351-017-6137-z.1.Introduction.

P. Zhu, Z. Jin, Q. Zhuang, P. Ciais, C. Bernacchi, X. Wang, D. Makowski, and D. Lobell. The important but weakening maize yield benefit of grain filling prolongation in the US Midwest. pages 4718–4730, 2018. doi: 10.1111/gcb.14356.